

Chief

College Station, Texas

Chief

Pasadena, Calif.

Houston, Tex.

Uppsala

Frankfurt

Los Angeles, Calif.

Palisades

Palisades, N.Y.

Durham

Houston, Tex.

Salt Lake City, Utah

Rennes

Edinburgh

Durham

Uppsala

North Ryde, N.S.W.

Los Angeles, Calif.

Canberra City

Paris

Massagno

Paris

Tuscaloosa, Ala.

Santa Barbara, Calif.

College Station, Tex.

Oslo

Ney, B.C.

Ottawa, Ont.

Cincinnati, Ohio

Edinburgh

Pasadena, Calif.

Los Angeles, Calif.

Andoëuvre-lès-Nancy

Paris

Uppsala

Durban

Cambridge, Mass.

S. Uyeda, Tokyo

W.D. Means, Albany, N.Y.

R.O. Meissner, Kiel

H.W. Menard, La Jolla, Calif.

S. Mueller, Zurich

K. Nakamura, Tokyo

T.H. Nelson, The Woodlands, Tex.

A. Nicolas, Nantes

A. Nur, Stanford, Calif.

R.J. O'Connell, Cambridge, Mass.

G.F. Oertel, Los Angeles, Calif.

H.R. Pollack, Ann Arbor, Mich.

N.J. Price, London

H. Ramberg, Uppsala

J.G. Ramsay, Zurich

N. Rast, Lexington, Ky.

T. Rikitake, Tokyo

S.K. Runcorn, Newcastle upon Tyne

M.P. Ryan, Reston, Va.

W.M. Schwerdtner, Toronto, Ont.

J.G. Sclater, Austin, Tex.

A.M.C. Sengör, Istanbul

N. Sleep, Stanford, Calif.

A.G. Smith, Cambridge

P. Tapponnier, Paris

M.N. Toksöz, Cambridge, Mass.

J. Tullis, Providence, R.I.

D.L. Turcotte, Ithaca, N.Y.

R. Van der Voo, Ann Arbor, Mich.

P. Vyskočil, Zdrby

R. Wang, Beijing

A.B. Watts, Palisades, N.Y.

L.E. Weiss, Berkeley, Calif.

B.F. Windley, Leicester

P.J. Wyllie, Pasadena, Calif.

H.J. Zwart, Utrecht

## THE STREAM FUNCTION AND GAUSS' PRINCIPLE OF LEAST CONSTRAINT: TWO USEFUL CONCEPTS FOR STRUCTURAL GEOLOGY

HANS RAMBERG

Department of Mineralogy and Petrology, Institute of Geology, University of Uppsala, Box 555, S-75122 Uppsala (Sweden)

(Received January 14, 1986; revised version accepted April 16, 1986)

### ABSTRACT

Ramberg, H., 1986. The stream function and Gauss' principle of least constraint: two useful concepts for structural geology. *Tectonophysics*, 131: 205–246.

To the extent that rock deformation can be approximated by a two-dimensional Newtonian model, a powerful stream-function simulation method is applicable. The significance of stream functions is that velocity, strain, stress and energy derived from the same stream function satisfy automatically three basic conditions of dynamics: (1) the condition of continuity, (2) the Navier-Stokes equations, and (3) conservation of energy. Hence we state with Jaeger: "If a stream function can be found which satisfies the boundary conditions of a dynamic model the complete solution follows." All pertinent bits of dynamic information are implied in the stream function from which they can be directly derived, guaranteed—so to speak—not to violate the basic conditions of dynamics. Stream functions useful in structural geology are solutions of:

$$\nabla^4 \psi = \frac{\partial^4 \psi}{\partial x^4} + 2 \frac{\partial^4 \psi}{\partial x^2 \partial y^2} + \frac{\partial^4 \psi}{\partial y^4} = 0$$

A double-polynomial solution of max. degree 14 is developed, in which the coefficients are related controlled by the  $\nabla^4 \psi = 0$  constraint, and their absolute values are determined by the boundary conditions of specific models and by the condition of maximum rate of energy dissipation or maximum rate of decline of potential energy. The polynomial stream function is applied to a collapsing viscous "nappe" consisting of a thin basal layer with low viscosity on which a thicker layer with high viscosity slides due to gravitational spreading. The velocity of forward movement depends upon absolute and relative values of the following parameters: viscosity, thickness, the aspect ratio and density. The velocity of a variety of nappes with different thicknesses, aspect ratios, viscosities and densities is determined.

### INTRODUCTION

It is known that the mechanical behaviour of crystalline rocks is infinitely more complex than that of Newtonian fluids; nevertheless, much insight into the evolution of deformation structures of rocks exposed to dynamothermal metamorphism

(Text continued on inside back cover)

### Journal

*Tectonophysics* is an international medium for the publication of original studies and comprehensive reviews in the field of geotectonics and the geology and physics of the earth's crust and interior. The journal endeavours to maintain a high scientific level and it is hoped that with its international character it will contribute to the sound development of this field.

The journal is provided as a publication outlet for short papers which require rapid publication.

### Subscription and circulation information

Check cover.

### Subscription Center

For those in the U.S. and Canada wishing information on this and other Elsevier journals, please contact the Subscription Center, Elsevier Science Publishing Co. Inc., 52 Vanderbilt Avenue, New York, N.Y. 10017, Telephone: (212) 916 1250.

may be gained from theoretical models in which rocks are treated as just Newtonian fluids, albeit with an extremely high effective viscosity. I believe analyses based on Newtonian models have considerably deepened our understanding of the dynamics of folds and boudinage (Biot, 1959, 1961, 1963; Ramberg, 1968, 1981; Johnson, 1970; Fletcher, 1977; Smith, 1975), of salt- and gneiss domes (Biot and Ode, 1965; Ramberg, op. cit.), of mantle diapirism and of thrust sheets (Elliott, 1976; Price, 1973; Ramberg, 1981) and not least of isostatic adjustment (Haskel, 1935; Crittenden, 1963; Cathles, 1975; Ramberg, 1968; Artyushkov, 1971).

In this paper we shall continue to treat rocks as Newtonian bodies with high effective viscosity when exposed to deviatoric stress and the force of gravity in and on the Earth's crust.

The aim of the paper is to demonstrate how a well-known concept in fluid dynamics—the Stream Function—can be combined with another well-known physical principle—Gauss' Principle of Least Constraint—to give information on the evolution of rock structures, including the velocity at which deformation structures develop.

The special structure treated in the paper is a set of composite nappes with dissimilar geometric dimensions and viscosities.

To apply the Stream Function Method it is first necessary to develop a general solution of the biharmonic equation:

$$\partial^4\psi/\partial x^4 + 2\partial^4\psi/\partial x^2\partial y^2 + \partial^4\psi/\partial y^4 = 0$$

This is done in the section "A useful double-polynomial stream function", p. 210. It is further necessary to develop special solutions valid for the particular models considered; in our case composite nappes. The development of special solutions is treated in the section "Coefficient determination by the method of extremizing the rate of energy change", p. 216. Here it is shown how Gauss' classic Principle of Least Constraint (recast in the form of the Principle of Extreme Rate of Energy Change) is used to determine arbitrary coefficients in the polynomial stream function. Coefficients in the stream function valid for the double-layer nappe are determined in the section "Simulation of a spreading composite nappe", p. 218.

The most significant results from the numerical simulation of composite nappes are the velocities and their relation to layer-thickness and length (aspect ratio), to viscosity and viscosity ratio of the two layers as well as to their density. These relationships are presented in the illustrations in Figs. 4–15, which actually contain all pertinent information obtained by the simulation procedure. Readers not interested in the theoretical part of the paper may therefore find useful data concerning nappe motion by studying the illustrations and their text.

#### THE STREAM FUNCTION METHOD

The assumption that rocks behave during regional metamorphism as extremely viscous Newtonian fluids, combined with the knowledge that inertia is insignificant

for slow tectonic processes, enables us to apply a powerful stream-function to the evolution of a number of deformation structures encountered in

Any two-dimensional motion can be described by a stream function (Lamb, 1781; Rankin, 1864; Lamb, 1932),  $\psi$ , which for non-inertial Newtonian creeping motion—is defined as a solution of the biharmonic equation:

$$\nabla^4\psi = \partial^4\psi/\partial x^4 + 2\partial^4\psi/\partial x^2\partial y^2 + \partial^4\psi/\partial y^4 = 0$$

The stream function is related to the velocity components by the expressions

$$u = -\partial\psi/\partial y$$

and:

$$v = \partial\psi/\partial x$$

Here  $u$  is the velocity component in the horizontal direction  $x$ , and  $v$  is the velocity component in the vertical direction  $y$ .

The significance of the stream-function method is based on the fact that solutions of the biharmonic equation are functions (by definition stream functions) whose derived velocity, strains and stresses automatically satisfy three dynamic relationships, viz. (1) the condition of continuity, (2) the equation of motion, and (3) conservation of energy.

For two-dimensional flow of incompressible fluids the relation:

$$\partial u/\partial x + \partial v/\partial y = 0$$

expresses the condition of continuity. From the definition  $u = -\partial\psi/\partial y$  and  $v = \partial\psi/\partial x$  follow  $\partial u/\partial x = -\partial^2\psi/\partial y\partial x$  and  $\partial v/\partial y = \partial^2\psi/\partial x\partial y$ , and immediately that continuity is automatically satisfied in models defined by a stream function.

For non-inertial viscous flow in two dimensions the Navier-Stokes equations of motion take the form:

$$\partial P/\partial x - \eta(\partial^2 u/\partial x^2 + \partial^2 u/\partial y^2) = 0$$

$$\partial P/\partial y - \eta(\partial^2 v/\partial x^2 + \partial^2 v/\partial y^2) + \rho g = 0$$

Since  $v$  is the velocity component in the vertical direction  $y$ , the gravity force is included in eqn. (6).

Differentiation of all terms in eqn. (5) with respect to  $y$  and all terms in eqn. (6) with respect to  $x$  yields:

$$\partial^2 P/\partial x\partial y - \eta(\partial^3 u/\partial x^2\partial y + \partial^3 u/\partial y^3) = 0$$

$$\partial^2 P/\partial y\partial x - \eta(\partial^3 v/\partial x^3 + \partial^3 v/\partial y^2\partial x) = 0$$

Subtracting eqn. (8) from (7) and applying expressions  $\partial\psi/\partial y = -u$  and  $\partial\psi/\partial x = v$  one obtains:

$$\partial^4\psi/\partial x^4 + 2\partial^4\psi/\partial x^2\partial y^2 + \partial^4\psi/\partial y^4 = 0$$

IS THIS A SLOW TECTONIC PROCESS?  
WHAT IS A SLOW TECTONIC PROCESS?  
EXAMPLE OF SETTING WHERE REGIONAL METAMORPHISM TAKES PLACE

ned from theoretical models in which rocks are treated as just Newtonian it with an extremely high effective viscosity. I believe analyses based on models have considerably deepened our understanding of the dynamics id boudinage (Biot, 1959, 1961, 1963; Ramberg, 1968, 1981; Johnson, her, 1977; Smith, 1975), of salt- and gneiss domes (Biot and Ode, 1965; op. cit.), of mantle diapirism and of thrust sheets (Elliott, 1976; Price, berg, 1981) and not least of isostatic adjustment (Haskel, 1935; Critten-Cathles, 1975; Ramberg, 1968; Artyushkov, 1971).

paper we shall continue to treat rocks as Newtonian bodies with high viscosity when exposed to deviatoric stress and the force of gravity in and h's crust.

of the paper is to demonstrate how a well-known concept in fluid the Stream Function—can be combined with another well-known physi-e—Gauss' Principle of Least Constraint—to give information on the f rock structures, including the velocity at which deformation structures

ial structure treated in the paper is a set of composite nappes with eometric dimensions and viscosities.

the Stream Function Method it is first necessary to develop a general the biharmonic equation:

$$\nabla^4 \psi = \partial^4 \psi / \partial x^2 \partial y^2 + \partial^4 \psi / \partial y^4 = 0$$

in the section "A useful double-polynomial stream function", p. 210. It necessary to develop special solutions valid for the particular models in our case composite nappes. The development of special solutions is ie section "Coefficient determination by the method of extremizing the gy change", p. 216. Here it is shown how Gauss' classic Principle of raint (recast in the form of the Principle of Extreme Rate of Energy used to determine arbitrary coefficients in the polynomial stream eefficients in the stream function valid for the double-layer nappe are in the section "Simulation of a spreading composite nappe", p. 218.

significant results from the numerical simulation of composite nappes cities and their relation to layer-thickness and length (aspect ratio), to d viscosity ratio of the two layers as well as to their density. These are presented in the illustrations in Figs. 4-15, which actually contain information obtained by the simulation procedure. Readers not inter-theoretical part of the paper may therefore find useful data concerning n by studying the illustrations and their text.

### FUNCTION METHOD

ption that rocks behave during regional metamorphism as extremely tonian fluids, combined with the knowledge that inertia is insignificant

for slow tectonic processes, enables us to apply a powerful stream-function method to the evolution of a number of deformation structures encountered in the field.

Any two-dimensional motion can be described by a stream function (Lagrange, 1781; Rankin, 1864; Lamb, 1932),  $\psi$ , which for non-inertial Newtonian flow—so-called creeping motion—is defined as a solution of the biharmonic differential equation:

$$\nabla^4 \psi = \partial^4 \psi / \partial x^4 + 2\partial^4 \psi / \partial x^2 \partial y^2 + \partial^4 \psi / \partial y^4 = 0 \tag{1}$$

The stream function is related to the velocity components by the expressions:

$$u = -\partial \psi / \partial y \tag{2}$$

and:

$$v = \partial \psi / \partial x \tag{3}$$

Here  $u$  is the velocity component in the horizontal direction  $x$ , and  $v$  the velocity component in the vertical direction  $y$ .

The significance of the stream-function method is based on the condition that solutions of the biharmonic equation are functions (by definition stream functions), whose derived velocity, strains and stresses automatically satisfy three crucial fluid dynamic relationships, viz. (1) the condition of continuity, (2) the Navier-Stokes equation of motion, and (3) conservation of energy.

For two-dimensional flow of incompressible fluids the relation:

$$\partial u / \partial x + \partial v / \partial y = 0 \tag{4}$$

expresses the condition of continuity. From the definition  $u = -\partial \psi / \partial y$  and  $v = \partial \psi / \partial x$  follow  $\partial u / \partial x = -\partial^2 \psi / \partial y \partial x$  and  $\partial v / \partial y = \partial^2 \psi / \partial x \partial y$ , and one sees immediately that continuity is automatically satisfied in models defined by a stream function.

For non-inertial viscous flow in two dimensions the Navier-Stokes equations of motion take the form:

$$\partial P / \partial x - \eta (\partial^2 u / \partial x^2 + \partial^2 u / \partial y^2) = 0 \tag{5}$$

$$\partial P / \partial y - \eta (\partial^2 v / \partial x^2 + \partial^2 v / \partial y^2) + \rho g = 0 \tag{6}$$

Since  $v$  is the velocity component in the vertical direction  $y$ , the gravity term  $\rho g$  is included in eqn. (6).

Differentiation of all terms in eqn. (5) with respect to  $y$  and all terms in eqn. (6) with respect to  $x$  yields:

$$\partial^2 P / \partial x \partial y - \eta (\partial^3 u / \partial x^2 \partial y + \partial^3 u / \partial y^3) = 0 \tag{7}$$

$$\partial^2 P / \partial y \partial x - \eta (\partial^3 v / \partial x^3 + \partial^3 v / \partial y^2 \partial x) = 0 \tag{8}$$

Subtracting eqn. (8) from (7) and applying expressions  $\partial \psi / \partial y = -u$  and  $\partial \psi / \partial x = v$  one obtains:

$$\partial^4 \psi / \partial x^4 + 2\partial^4 \psi / \partial x^2 \partial y^2 + \partial^4 \psi / \partial y^4 = 0$$

which is the biharmonic base for stream functions. Hence the equations of motion are automatically satisfied in models defined by stream functions.

It is particularly important to realize that energy is also automatically conserved when expressed by formulas derived from one and the same stream function. This gives crucial support to the validity of the energy-extremizing method of determining coefficients in a polynomial stream function (p. 216).

To demonstrate that energy is automatically conserved when derived from a stream function requires quite a lengthy mathematical procedure, so let it suffice here to merely indicate how the demonstration may be performed.

For a deforming viscous model described by a stream function there are several categories of mechanical energy to consider, and all are derivable from the stream function used. Expressed in terms of rate of change of energy per unit volume (for strain energy and potential energy) or per unit surface area (for energy due to stress at the boundary), the different categories are:

$$\dot{e}_\epsilon = 4\eta\dot{\epsilon}_\phi^2, \quad \text{the rate of change of normal-strain energy per unit volume;} \quad (9)$$

$$\dot{e}_\gamma = \eta\dot{\gamma}_\phi^2, \quad \text{the rate of change of shear-strain energy per unit volume;} \quad (10)$$

$$\dot{e}_{\text{pot}} = \rho g v, \quad \text{the rate of change of gravitational energy per unit volume;} \quad (11)$$

$$\dot{e}_\tau = \tau_t v_t, \quad \text{the rate of energy input or output per unit area due to shear stress at the boundary; and finally} \quad (12)$$

$$\dot{e}_\sigma = \sigma_n u_n, \quad \text{the rate of energy input or output per unit area due to normal stress at the boundary.} \quad (13)$$

In these expressions subscript  $\phi$  indicates direction in space,  $v$  is the velocity component in the vertical direction,  $\tau_t$  is shear stress parallel to the boundary,  $v_t$  is the velocity at the boundary parallel to the shear stress,  $\sigma_n$  is normal stress at the boundary and  $u_n$  is the velocity component normal to the boundary.

To obtain the energy changes for the whole model the quantities  $\dot{e}_\epsilon$ ,  $\dot{e}_\gamma$  and  $\dot{e}_{\text{pot}}$  must be integrated over the volume occupied by the model and  $\dot{e}_\tau$  and  $\dot{e}_\sigma$  must be integrated over the boundary. Using capital letters for the integrated energies we combine some of the energies specified above:

$$\dot{E}_{\epsilon\gamma} = \dot{E}_\epsilon + \dot{E}_\gamma \quad (14)$$

$$\dot{E}_{\sigma\tau} = \dot{E}_\sigma + \dot{E}_\tau \quad (15)$$

The crucial point is that when  $\dot{E}_{\epsilon\gamma}$ ,  $\dot{E}_{\sigma\tau}$  and  $\dot{E}_{\text{pot}}$  are derived from one and the same stream function, we find that the condition of conservation is automatically satisfied, viz:

$$\dot{E}_{\epsilon\gamma} + \dot{E}_{\sigma\tau} + \dot{E}_{\text{pot}} = 0 \quad (16)$$

In other words, energy—as expressed by formulas derived from a stream function—is being conserved during the strain and motion which occur in the model.

In order to derive the energies the following formulas are used:

$$\dot{\epsilon}_x^2 = \left(\frac{\partial u}{\partial x}\right)^2 = \left(-\frac{\partial^2 \psi}{\partial x \partial y}\right)^2, \quad \dot{\epsilon}_y^2 = \left(\frac{\partial v}{\partial y}\right)^2 = \left(\frac{\partial^2 \psi}{\partial x \partial y}\right)^2$$

$$\dot{\gamma}_{xy}^2 = \left(\frac{\partial u}{\partial y} + \frac{\partial v}{\partial x}\right)^2 = \left(-\frac{\partial^2 \psi}{\partial y^2} + \frac{\partial^2 \psi}{\partial x^2}\right)^2$$

$$\tau_{xy} = \eta \dot{\gamma}_{xy} \quad \text{and} \quad \sigma_x = 2\eta \dot{\epsilon}_x - P$$

together with the derived velocity components.

To form  $P$ , the general formula:

$$dP = \frac{\partial P}{\partial x} dx + \frac{\partial P}{\partial y} dy$$

is applicable. Here we introduce:

$$\frac{\partial P}{\partial x} = \eta \left( \frac{\partial^2 u}{\partial x^2} + \frac{\partial^2 u}{\partial y^2} \right) = -\eta \left( \frac{\partial^3 \psi}{\partial x^2 \partial y} + \frac{\partial^3 \psi}{\partial y^3} \right)$$

and:

$$\frac{\partial P}{\partial y} = \eta \left( \frac{\partial^2 v}{\partial x^2} + \frac{\partial^2 v}{\partial y^2} \right) - \rho g = \eta \left( \frac{\partial^3 \psi}{\partial x^3} + \frac{\partial^3 \psi}{\partial x \partial y^2} \right) - \rho g$$

Again, the last two equations are directly derived from the stream function.

In order to obtain  $P$  (and thus also  $\sigma$ ) by integration of eqn. (20) realize that  $dP$  is an exact differential. This can be shown when the

$$\partial \left( \frac{\partial P}{\partial x} \right) / \partial y = \partial \left( \frac{\partial P}{\partial y} \right) / \partial x$$

is applied in combination with the biharmonic  $\nabla^4 \psi = 0$ .

When the above formulas are applied to a stream function describing model of Newtonian material the condition of conservation energy expressed in eqn. (16) follows.

In accordance with the explanation above, we conclude with J 140): "If a stream function can be found which satisfies the boundary conditions of a dynamic model the complete solution follows." The stream function, which in turn implies the strain rate and accordingly the coefficient and density—also implies the stress distribution and the dissipation due to viscous strain, as well as the rate of change of  $P$ . Also the rate of energy input/output due to stress acting on moving boundaries is implied in the stream function when viscosity and density are given. *the real problem is to find the appropriate stream function; to extract the pertinent information is mostly routine use of standard fluid dynamic.*

We note that stream functions give the instantaneous velocities, the instantaneous strain rates, the instantaneous stress distribution etc. The ev

e biharmonic base for stream functions. Hence the equations of motion are automatically satisfied in models defined by stream functions.

It is particularly important to realize that energy is also automatically conserved as expressed by formulas derived from one and the same stream function. This provides support to the validity of the energy-extremizing method of determinants in a polynomial stream function (p. 216).

It can be demonstrated that energy is automatically conserved when derived from a stream function. This demonstration requires quite a lengthy mathematical procedure, so let it suffice to merely indicate how the demonstration may be performed.

In forming a viscous model described by a stream function there are several categories of mechanical energy to consider, and all are derivable from the stream function. Expressed in terms of rate of change of energy per unit volume (for kinetic energy) or per unit surface area (for energy due to stress and potential energy), the different categories are:

the rate of change of normal-strain energy per unit volume; (9)

the rate of change of shear-strain energy per unit volume; (10)

the rate of change of gravitational energy per unit volume; (11)

the rate of energy input or output per unit area due to shear stress at the boundary; and finally (12)

the rate of energy input or output per unit area due to normal stress at the boundary. (13)

where the subscript  $\phi$  indicates direction in space,  $v$  is the velocity in the vertical direction,  $\tau_t$  is shear stress parallel to the boundary,  $v_t$  is the velocity parallel to the shear stress,  $\sigma_n$  is normal stress at the boundary and  $u_n$  is the velocity component normal to the boundary.

For the energy changes for the whole model the quantities  $\dot{e}_e$ ,  $\dot{e}_v$  and  $\dot{e}_{pot}$  are integrated over the volume occupied by the model and  $\dot{e}_\tau$  and  $\dot{e}_\sigma$  must be integrated over the boundary. Using capital letters for the integrated energies we have:

$$\dot{E}_e = 0 \quad (14)$$

$$\dot{E}_v = 0 \quad (15)$$

It is evident that when  $\dot{E}_{e_v}$ ,  $\dot{E}_{\sigma_\tau}$  and  $\dot{E}_{pot}$  are derived from one and the same stream function, we find that the condition of conservation is automatically satisfied.

$$\dot{E}_{pot} = 0 \quad (16)$$

It is evident that energy—as expressed by formulas derived from a stream function—is being conserved during the strain and motion which occur in the

In order to derive the energies the following formulas are used:

$$\dot{\epsilon}_x^2 = \left( \frac{\partial u}{\partial x} \right)^2 = \left( - \frac{\partial^2 \psi}{\partial x \partial y} \right)^2, \quad \dot{\epsilon}_y^2 = \left( \frac{\partial v}{\partial y} \right)^2 = \left( \frac{\partial^2 \psi}{\partial x \partial y} \right)^2 \quad (17)$$

$$\dot{\gamma}_{xy}^2 = \left( \frac{\partial u}{\partial y} + \frac{\partial v}{\partial x} \right)^2 = \left( - \frac{\partial^2 \psi}{\partial y^2} + \frac{\partial^2 \psi}{\partial x^2} \right)^2 \quad (18)$$

$$\tau_{xy} = \eta \dot{\gamma}_{xy} \text{ and } \sigma_x = 2\eta \dot{\epsilon}_x - P \quad (19)$$

together with the derived velocity components.

To form  $P$ , the general formula:

$$dP = \frac{\partial P}{\partial x} dx + \frac{\partial P}{\partial y} dy \quad (20)$$

is applicable. Here we introduce:

$$\frac{\partial P}{\partial x} = \eta \left( \frac{\partial^2 u}{\partial x^2} + \frac{\partial^2 u}{\partial y^2} \right) = -\eta \left( \frac{\partial^3 \psi}{\partial x^2 \partial y} + \frac{\partial^3 \psi}{\partial y^3} \right) \quad (21)$$

and:

$$\frac{\partial P}{\partial y} = \eta \left( \frac{\partial^2 v}{\partial x^2} + \frac{\partial^2 v}{\partial y^2} \right) - \rho g = \eta \left( \frac{\partial^3 \psi}{\partial x^3} + \frac{\partial^3 \psi}{\partial x \partial y^2} \right) - \rho g \quad (22)$$

Again, the last two equations are directly derived from the stream function.

In order to obtain  $P$  (and thus also  $\sigma$ ) by integration of eqn. (20) it is useful to realize that  $dP$  is an exact differential. This can be shown when the criterium:

$$\partial \left( \frac{\partial P}{\partial x} \right) / \partial y = \partial \left( \frac{\partial P}{\partial y} \right) / \partial x$$

is applied in combination with the biharmonic  $\nabla^4 \psi = 0$ .

When the above formulas are applied to a stream function describing a deforming model of Newtonian material the condition of conservation of mechanical energy expressed in eqn. (16) follows.

In accordance with the explanation above, we conclude with Jaeger (1956, p. 140): "If a stream function can be found which satisfies the boundary conditions of a dynamic model the complete solution follows." The stream function implies the velocity field, which in turn implies the strain rate and accordingly—via viscosity coefficient and density—also implies the stress distribution and the rate of energy dissipation due to viscous strain, as well as the rate of change of potential energy. Also the rate of energy input/output due to stress acting on moving boundaries is implied in the stream function when viscosity and density are given. In other words, *the real problem is to find the appropriate stream function; to extract the other pertinent information is mostly routine use of standard fluid dynamic relationships.*

We note that stream functions give the instantaneous velocities, the instantaneous strain rates, the instantaneous stress distribution etc. The evolution in finite

time of a model accordingly depends upon integration problems not related to the question of finding the stream function itself. However, even if integration over a finite time interval may pose formidable and perhaps even insoluble problems, quantitative knowledge of the instantaneous velocity, stress etc. is itself of great value for the understanding of the evolution of rock structures. See also p. 239.

For periodic structures such as, for example, buckle folds in layered rocks and periodic series of domes and diapirs, harmonic stream functions of type:

$$\psi = \exp(\pm \omega y) [A \cos(\omega x) \pm B \sin(\omega x)] \quad (23)$$

$$\psi = y \exp(\pm \omega y) [A \cos(\omega x) \pm B \sin(\omega x)] \quad (24)$$

( $\omega = 2\pi/\lambda$ ,  $\lambda$  is wavelength)

both being solutions of  $\nabla^4 \psi = 0$ —are applicable and yield useful results such as the dominant wavelength of folds, the spacing between diapirs, the rate of isostatic adjustment etc. as long as the amplitude is small compared with the wavelength. This is demonstrated and thoroughly discussed in some of the works cited above (e.g., Ramberg, 1968, 1981) and will not be repeated here. Instead we shall consider polynomial forms of stream functions, which are applicable to various non-periodic geologic structures.

#### A USEFUL DOUBLE-POLYNOMIAL STREAM FUNCTION

The application of a polynomial stream function to the slow “creeping” gravitational spreading of a viscous nappe was published in Ramberg (1981, pp. 267–226). (Unfortunately a numerical error affected the calculated strain energy of the model, but a correction has been published, see Ramberg, 1985.)

In the cited book (Ramberg, 1981) the stream function was applied to a simple nappe model with a rather special velocity field. The nappe was coherent to the rigid basement, and it was symmetric about a vertical plane through its center. This means that the velocity components  $u$  and  $v$  vanish at the base, that  $u$  vanishes also at the central cross section and that the stream function developed was not useable for nappes with more realistic boundary conditions.

In the present study we shall develop a polynomial stream function which is versatile enough to simulate a variety of non-periodic structures, including nappes with non-vanishing velocity at the base. Nappes described by stream functions of this nature are not only permitted to slide along the base while spreading gravitationally, but also allow a “push from behind”. Incidentally, it is interesting to note that the double-polynomial function to be developed (eqn. 31) is comprehensive enough to contain the periodic solutions (23) and (24). This can be demonstrated by appropriate adjustment of the arbitrary coefficients using Taylor-Maclaurin series for  $\sin(\omega x)$ ,  $\cos(\omega x)$ ,  $\exp(\omega y)$ .

To develop the general polynomial stream function it is convenient to start by considering the velocity component  $u$  and its variation with  $y$  at distance  $x$  from

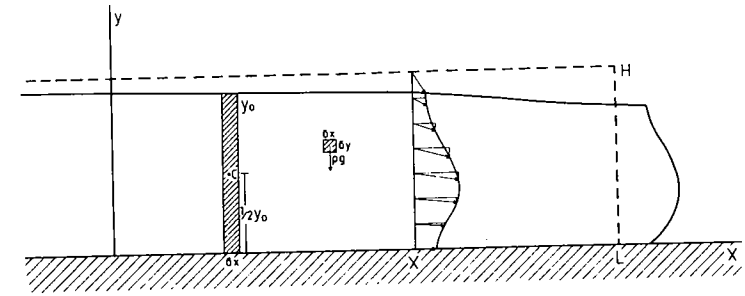


Fig. 1. Right-hand half of viscous body with initially rectangular cross section parallel with infinite length in  $z$ . Initial cross section dashed, profile after arbitrary time of deformation solid lines. Displacement of vertical straight marker at  $x$  indicated by velocity vector  $u$ .

the central plane (Fig. 1). As the material of the nappe is supposed to be homogeneous and Newtonian,  $u$  is evidently a continuous and smooth function at constant  $x$ . Hence  $u$  can be expressed as a polynomial in  $y$ :

$$u = -[a + 2by + 3cy^2 + 4dy^3 + \dots + nwy^{(n-1)}]$$

(cf. Weierstrass' theorem which states that any continuous function can be approximated by a polynomial—Courant, 1953, p. 423).

The reason for the negative sign and the factors 2, 3...  $n$  in the coefficients is to obtain a positive and simple form of the corresponding stream function—see below. In polynomial (25) the coefficients are unknown functions of  $x$ , and each of the coefficients may be expressed in polynomial form:

$$\begin{aligned} a &= a_1 + a_2x + a_3x^2 + \dots + a_mx^{(m-1)} \\ b &= b_1 + b_2x + b_3x^2 + \dots + b_mx^{(m-1)} \\ c &= c_1 + c_2x + c_3x^2 + \dots + c_mx^{(m-1)} \\ &\vdots \\ w &= w_1 + w_2x + w_3x^2 + \dots + w_mx^{(m-1)} \end{aligned}$$

Using the definition  $u = -\partial\psi/\partial y$  we form a function  $\psi$  by integrating  $u$  with respect to  $y$ :

$$\psi = ay + by^2 + cy^3 + dy^4 + \dots + wy^n + f(x)$$

Here  $f(x)$  is a function of  $x$  alone. From the definition  $v = \partial\psi/\partial x$  it follows that  $f(x)$  determines the velocity component  $v$  at a constant  $y$ . It is reasonable to express  $f(x)$  as a polynomial in  $x$ :

$$f(x) = \alpha_1 + \alpha_2x + \alpha_3x^2 + \dots + \alpha_mx^{(m-1)}$$

(Clearly, eqn. (27) as it stands is not a stream function unless it is correlated in accordance with the constraint  $\nabla^4\psi = 0$ . The result is shown below, p. 214–215).

model accordingly depends upon integration problems not related to the finding the stream function itself. However, even if integration over a interval may pose formidable and perhaps even insoluble problems, knowledge of the instantaneous velocity, stress etc. is itself of great understanding of the evolution of rock structures. See also p. 239.

periodic structures such as, for example, buckle folds in layered rocks and profiles of domes and diapirs, harmonic stream functions of type:

$$v(y) [A \cos(\omega x) \pm B \sin(\omega x)] \quad (23)$$

$$w(y) [A \cos(\omega x) \pm B \sin(\omega x)] \quad (24)$$

$\lambda$  is wavelength)

Solutions of  $\nabla^4 \psi = 0$ —are applicable and yield useful results such as the wavelength of folds, the spacing between diapirs, the rate of isostatic etc. as long as the amplitude is small compared with the wavelength. Constrated and thoroughly discussed in some of the works cited above (e.g., 1968, 1981) and will not be repeated here. Instead we shall consider forms of stream functions, which are applicable to various non-periodic structures.

#### DOUBLE-POLYNOMIAL STREAM FUNCTION

Application of a polynomial stream function to the slow “creeping” gravitational flow of a viscous nappe was published in Ramberg (1981, pp. 267–226). Slightly a numerical error affected the calculated strain energy of the model, correction has been published, see Ramberg, 1985.)

In the book (Ramberg, 1981) the stream function was applied to a simple model with a rather special velocity field. The nappe was coherent to the rigid substrate and it was symmetric about a vertical plane through its center. This model assumed the velocity components  $u$  and  $v$  vanish at the base, that  $u$  vanishes also at the free surface cross section and that the stream function developed was not useable with more realistic boundary conditions.

In the present study we shall develop a polynomial stream function which is sufficient enough to simulate a variety of non-periodic structures, including nappes with vanishing velocity at the base. Nappes described by stream functions of this type are not only permitted to slide along the base while spreading gravitationally but also allow a “push from behind”. Incidentally, it is interesting to note that the double-polynomial function to be developed (eqn. 31) is comprehensive enough to contain the periodic solutions (23) and (24). This can be demonstrated by adjustment of the arbitrary coefficients using Taylor-Maclaurin series  $\cos(\omega x)$ ,  $\exp(\omega y)$ .

From the general polynomial stream function it is convenient to start by describing the velocity component  $u$  and its variation with  $y$  at distance  $x$  from

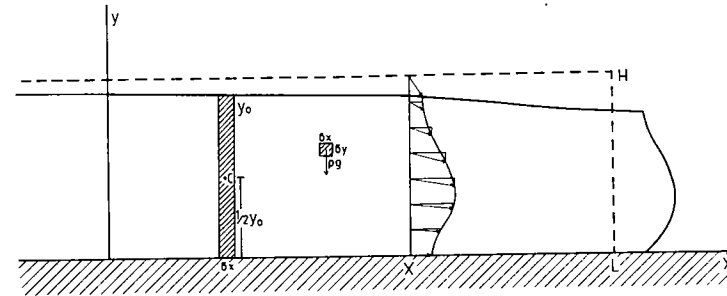


Fig. 1. Right-hand half of viscous body with initially rectangular cross section parallel to plane  $xy$  and with infinite length in  $z$ . Initial cross section dashed, profile after arbitrary time of deformation shown in solid lines. Displacement of vertical straight marker at  $x$  indicated by velocity vectors.

the central plane (Fig. 1). As the material of the nappe is supposed to be homogeneous and Newtonian,  $u$  is evidently a continuous and smooth function of  $y$  at constant  $x$ . Hence  $u$  can be expressed as a polynomial in  $y$ :

$$u = -[a + 2by + 3cy^2 + 4dy^3 + \dots + nwy^{(n-1)}] \quad (25)$$

(cf. Weierstrass' theorem which states that any continuous function can be approximated by a polynomial—Courant, 1953, p. 423).

The reason for the negative sign and the factors 2, 3... $n$  in front of the coefficients is to obtain a positive and simple form of the corresponding stream function—see below. In polynomial (25) the coefficients are unknown functions of  $x$ , and each of the coefficients may be expressed in polynomial form:

$$\begin{aligned} a &= a_1 + a_2x + a_3x^2 + \dots + a_mx^{(m-1)} \\ b &= b_1 + b_2x + b_3x^2 + \dots + b_mx^{(m-1)} \\ c &= c_1 + c_2x + c_3x^2 + \dots + c_mx^{(m-1)} \\ &\vdots \\ w &= w_1 + w_2x + w_3x^2 + \dots + w_mx^{(m-1)} \end{aligned} \quad (26)$$

Using the definition  $u = -\partial\psi/\partial y$  we form a function  $\psi$  by integration:

$$\psi = ay + by^2 + cy^3 + dy^4 + \dots + wy^n + f(x) \quad (27)$$

Here  $f(x)$  is a function of  $x$  alone. From the definition  $v = \partial\psi/\partial x$  and the above form of  $\psi$  follow that  $f(x)$  determines the velocity component  $v$  at  $y=0$ , and it is reasonable to express  $f(x)$  as a polynomial in  $x$ :

$$f(x) = \alpha_1 + \alpha_2x + \alpha_3x^2 + \dots + \alpha_mx^{(m-1)} \quad (28)$$

(Clearly, eqn. (27) as it stands is not a stream function unless the coefficients are correlated in accordance with the constraint  $\nabla^4\psi = 0$ . The result of this correlation is shown below, p. 214–215).

EQUATION 29

	1	$y$	$y^2$	$y^3$	$y^4$	$y^5$	...	$y^{(n-1)}$
1	$a_1$	$a_1$	$b_1$	$c_1$	$d_1$	$e_1$	...	$w_1$
$x$	$a_2$	$a_2$	$b_2$	$c_2$	$d_2$	$e_2$	...	$w_2$
$x^2$	$a_3$	$a_3$	$b_3$	$c_3$	$d_3$	$e_3$	...	$w_3$
$x^3$	$a_4$	$a_4$	$b_4$	$c_4$	$d_4$	$e_4$	...	$w_4$
$x^4$	$a_5$	$a_5$	$b_5$	$c_5$	$d_5$	$e_5$	...	$w_5$
$x^5$	$a_6$	$a_6$	$b_6$	$c_6$	$d_6$	$e_6$	...	$w_6$
$\vdots$	$\vdots$	$\vdots$	$\vdots$	$\vdots$	$\vdots$	$\vdots$		$\vdots$
$x^{(m-1)}$	$a_m$	$a_m$	$b_m$	$c_m$	$d_m$	$e_m$	...	$w_m$

The function  $\psi$  is conveniently presented in the form of a two-dimensional array, eqn. (29).

This arrangement means that each element in the array is the coefficient for the product  $x^p y^q$  in which  $x^p$  is the multiplier for the row, and  $y^q$  the multiplier for the column, in which the element occurs.  $d_4$ , for example, is the coefficient for  $x^3 y^4$ ,  $c_6$  the coefficient for  $x^5 y^3$ ,  $b_5$  for  $x^4 y^2$  etc., thus  $d_4 x^3 y^4$ ,  $c_6 x^5 y^3$  and  $b_5 x^4 y^2$  are examples of terms in the polynomial.

When the coefficients of the double polynomial are presented in array form it is desirable to use the more self-explanatory double-index notation expressed in eqn. (30).

In the double polynomial (30) the number of unknown coefficients is  $m \cdot n$  when the degree of the polynomial is  $(m-1)$  with respect to  $x$  and  $(n-1)$  with respect to  $y$ . We see that the number of unknown coefficients is considerably reduced by the constraint  $\nabla^4 \psi = 0$ . After some cumbersome algebraic and arithmetic operations the correlations recorded in eqn. (31) based on degree 14 in both  $x$  and  $y$ , are determined.

(To determine the coefficient correlation we derive  $\partial^4 \psi / \partial x^4$ ,  $\partial^4 \psi / \partial y^4$  and  $\partial^4 \psi / \partial x^2 \partial y^2$  from polynomial (30), collect terms with same power of  $x$  and same

EQUATION 30

	1	$y$	$y^2$	$y^3$	$y^4$	$y^5$	...	$y^{(n-1)}$
1	$a_{11}$	$a_{12}$	$a_{13}$	$a_{14}$	$a_{15}$	$a_{16}$	...	$a_{1n}$
$x$	$a_{21}$	$a_{22}$	$a_{23}$	$a_{24}$	$a_{25}$	$a_{26}$	...	$a_{2n}$
$x^2$	$a_{31}$	$a_{32}$	$a_{33}$	$a_{34}$	$a_{35}$	$a_{36}$	...	$a_{3n}$
$x^3$	$a_{41}$	$a_{42}$	$a_{43}$	$a_{44}$	$a_{45}$	$a_{46}$	...	$a_{4n}$
$x^4$	$a_{51}$	$a_{52}$	$a_{53}$	$a_{54}$	$a_{55}$	$a_{56}$	...	$a_{5n}$
$x^5$	$a_{61}$	$a_{62}$	$a_{63}$	$a_{64}$	$a_{65}$	$a_{66}$	...	$a_{6n}$
$\vdots$	$\vdots$	$\vdots$	$\vdots$	$\vdots$	$\vdots$	$\vdots$		$\vdots$
$x^{(m-1)}$	$a_{m1}$	$a_{m2}$	$a_{m3}$	$a_{m4}$	$a_{m5}$	$a_{m6}$	...	$a_{mn}$

power of  $y$ , put each collection of equal-power terms in the form:  $2\partial^4 \psi / \partial x^2 \partial y^2 + \partial^4 \psi / \partial y^4$  and equate to zero. From the set of eqs. obtained the coefficient correlation follows.)

We find that the coefficients in the two first columns and in the two rows are arbitrary while the remaining coefficients either vanish or are the coefficients in rows 1 and 2, and in columns 1 and 2.

Row 1 constitutes a polynomial in  $y$ , and row 2 a polynomial in  $y$  multiplied by  $x$  in the first power. Column 1 constitutes a polynomial in  $x$ , and column 2 a polynomial in  $x$  multiplied by  $y$  in the first power. These four polynomials incidentally have the coefficients  $a_{11}$ ,  $a_{12}$ ,  $a_{21}$ ,  $a_{22}$  in common—are polynomials whose coefficients are not constrained by the condition  $\nabla^4 \psi = 0$  are instead free to assume any values determined by the conditions in the special model studied.

One notes that the four arbitrary polynomials in the double-power series of the partial differential equation  $\nabla^4 \psi = 0$  play the same role as constants in series solution of ordinary differential equations (see, e.g., Tranter, 1961, p. 111 ff.).

In the following we distinguish between the arbitrary coefficient-dependent coefficients, the latter being functions of the former.

It is interesting to note that the high-degree cross terms,  $a_{ij} x^{(i-1)} y^{(j-1)}$  when  $i+j > p+2$  where  $p$  is the degree of the arbitrary polynomial:  $p=14$  and we see that all coefficients whose index sum  $i+j > 16$ , are zero. It is worth noting that the degree of the arbitrary polynomials in  $y$  is the same as the degree of the arbitrary polynomials in  $x$ , i.e.  $m=n$ . This is a consequence of  $\nabla^4 \psi = 0$ .

It is rarely necessary to use the comprehensive polynomial (31) of degree 14. Truncated versions will usually do to analyse physical models. The correlations are therefore perhaps needed concerning the procedure of truncating the polynomial in such a manner that the altered version remains a solution of  $\nabla^4 \psi = 0$ , and hence a valid stream function.

If we look carefully, we note that only coefficients with equal index sum  $p=i+j$ , are correlated. This means that correlation involves only coefficients on the same diagonal running from upper right to lower left. It is also interesting to note that only coefficients in alternating sites are correlated. For example,  $a_{3,13}$ ,  $a_{5,11}$ ,  $a_{7,9}$ ,  $a_{9,7}$ ,  $a_{11,5}$  and  $a_{13,3}$  are interrelated because they are all functions of the two arbitrary coefficients  $a_{1,15}$  and  $a_{15,1}$ . Similarly  $a_{10,6}$  and  $a_{12,4}$  are interrelated because all are functions of the two arbitrary coefficients  $a_{2,14}$  and  $a_{14,2}$ .

It follows from the first relationship that the polynomial can be truncated without violating the constraint  $\nabla^4 \psi = 0$ , by cutting out diagonal coefficients with a successively smaller index sum,  $p=i+j$ .

Another way of altering the comprehensive polynomial without



$y$	$y^2$	$y^3$	$y^4$	$y^5$	...	$y^{(n-1)}$
$a_1$	$b_1$	$c_1$	$d_1$	$e_1$	...	$w_1$
$a_2$	$b_2$	$c_2$	$d_2$	$e_2$	...	$w_2$
$a_3$	$b_3$	$c_3$	$d_3$	$e_3$	...	$w_3$
$a_4$	$b_4$	$c_4$	$d_4$	$e_4$	...	$w_4$
$a_5$	$b_5$	$c_5$	$d_5$	$e_5$	...	$w_5$
$a_6$	$b_6$	$c_6$	$d_6$	$e_6$	...	$w_6$
$\vdots$	$\vdots$	$\vdots$	$\vdots$	$\vdots$		$\vdots$
$a_m$	$b_m$	$c_m$	$d_m$	$e_m$	...	$w_m$

tion  $\psi$  is conveniently presented in the form of a two-dimensional array,

ngement means that each element in the array is the coefficient for the  $y^q$  in which  $x^p$  is the multiplier for the row, and  $y^q$  the multiplier for in which the element occurs.  $d_4$ , for example, is the coefficient for  $x^3y^4$ ,  $c_6$  for  $x^5y^3$ ,  $b_5$  for  $x^4y^2$  etc., thus  $d_4x^3y^4$ ,  $c_6x^5y^3$  and  $b_5x^4y^2$  are terms in the polynomial.

coefficients of the double polynomial are presented in array form it is use the more self-explanatory double-index notation expressed in eqn.

ble polynomial (30) the number of unknown coefficients is  $m \cdot n$  when the polynomial is  $(m - 1)$  with respect to  $x$  and  $(n - 1)$  with respect to  $y$ . After some cumbersome algebraic and arithmetic operations the number of unknown coefficients is considerably reduced by the condition  $\nabla^4\psi = 0$ . After some cumbersome algebraic and arithmetic operations the result is recorded in eqn. (31) based on degree 14 in both  $x$  and  $y$ , are

nine the coefficient correlation we derive  $\partial^4\psi/\partial x^4$ ,  $\partial^4\psi/\partial y^4$  and from polynomial (30), collect terms with same power of  $x$  and same

	$y^2$	$y^3$	$y^4$	$y^5$	...	$y^{(n-1)}$
12	$a_{13}$	$a_{14}$	$a_{15}$	$a_{16}$	...	$a_{1n}$
22	$a_{23}$	$a_{24}$	$a_{25}$	$a_{26}$	...	$a_{2n}$
32	$a_{33}$	$a_{34}$	$a_{35}$	$a_{36}$	...	$a_{3n}$
42	$a_{43}$	$a_{44}$	$a_{45}$	$a_{46}$	...	$a_{4n}$
52	$a_{53}$	$a_{54}$	$a_{55}$	$a_{56}$	...	$a_{5n}$
62	$a_{63}$	$a_{64}$	$a_{65}$	$a_{66}$	...	$a_{6n}$
$\vdots$	$\vdots$	$\vdots$	$\vdots$	$\vdots$		$\vdots$
$m2$	$a_{m3}$	$a_{m4}$	$a_{m5}$	$a_{m6}$	...	$a_{mn}$

power of  $y$ , put each collection of equal-power terms in the form:  $\partial^4\psi/\partial x^4 + 2\partial^4\psi/\partial x^2\partial y^2 + \partial^4\psi/\partial y^4$  and equate to zero. From the set of equations thus obtained the coefficient correlation follows.)

We find that the coefficients in the two first columns and in the two uppermost rows are arbitrary while the remaining coefficients either vanish or are functions of the coefficients in rows 1 and 2, and in columns 1 and 2.

Row 1 constitutes a polynomial in  $y$ , and row 2 a polynomial in  $y$  multiplied by  $x$  in the first power. Column 1 constitutes a polynomial in  $x$ , and column 2 a polynomial in  $x$  multiplied by  $y$  in the first power. These four polynomials—which incidentally have the coefficients  $a_{11}$ ,  $a_{12}$ ,  $a_{21}$ ,  $a_{22}$  in common—are the arbitrary polynomials whose coefficients are not constrained by the condition  $\nabla^4\psi = 0$ , but are instead free to assume any values determined by the conditions imposed by the special model studied.

One notes that the four arbitrary polynomials in the double-power series solution of the partial differential equation  $\nabla^4\psi = 0$  play the same role as the arbitrary constants in series solution of ordinary differential equations (see, e.g., Lamb and Tranter, 1961, p. 111 ff.).

In the following we distinguish between the arbitrary coefficients and the dependent coefficients, the latter being functions of the former.

It is interesting to note that the high-degree cross terms,  $a_{ij}x^{(i-1)}y^{(j-1)}$ , vanish when  $i + j > p + 2$  where  $p$  is the degree of the arbitrary polynomials. In eqn. (31)  $p = 14$  and we see that all coefficients whose index sum  $i + j > 16$ , are zero. It is also worth noting that the degree of the arbitrary polynomials in  $y$  is the same as the degree of the arbitrary polynomials in  $x$ , i.e.  $m = n$ . This is a consequence of  $\nabla^4\psi = 0$ .

It is rarely necessary to use the comprehensive polynomial (31) of as high degree as 14. Truncated versions will usually do to analyse physical models. A few remarks are therefore perhaps needed concerning the procedure of truncating and otherwise altering the polynomial in such a manner that the altered version remains a solution of  $\nabla^4\psi = 0$ , and hence a valid stream function.

If we look carefully, we note that only coefficients with equal index sum,  $p = i + j$ , are correlated. This means that correlation involves only coefficients in the same diagonal running from upper right to lower left. It is also interesting that in one and the same diagonal only coefficients in alternating sites are related. For example,  $a_{3,13}$ ,  $a_{5,11}$ ,  $a_{7,9}$ ,  $a_{9,7}$ ,  $a_{11,5}$  and  $a_{13,3}$  are interrelated because they are all functions of the two arbitrary coefficients  $a_{1,15}$  and  $a_{15,1}$ . Similarly  $a_{4,12}$ ,  $a_{6,10}$ ,  $a_{8,8}$ ,  $a_{10,6}$  and  $a_{12,4}$  are interrelated because all are functions of the two arbitrary coefficients  $a_{2,14}$  and  $a_{14,2}$ .

It follows from the first relationship that the polynomial can be shortened without violating the constraint  $\nabla^4\psi = 0$ , by cutting out diagonal after diagonal of coefficients with a successively smaller index sum,  $p = i + j$ .

Another way of altering the comprehensive polynomial without nullifying the

EQUATION 31

	1	$y$	$y^2$	$y^3$	$y^4$	$y^5$	$y^6$	$y^7$	$y^8$	$y^9$	$y^{10}$	$y^{11}$	$y^{12}$	$y^{13}$
1	$a_{11}$	$a_{12}$	$a_{13}$	$a_{14}$	$a_{15}$	$a_{16}$	$a_{17}$	$a_{18}$	$a_{19}$	$a_{1,10}$	$a_{1,11}$	$a_{1,12}$	$a_{1,13}$	$a_{1,14}$
$x$	$a_{21}$	$a_{22}$	$a_{23}$	$a_{24}$	$a_{25}$	$a_{26}$	$a_{27}$	$a_{28}$	$a_{29}$	$a_{2,10}$	$a_{2,11}$	$a_{2,12}$	$a_{2,13}$	$a_{2,14}$
$x^2$	$a_{31}$	$a_{32}$	$a_{33} =$ $-3(a_{15}$ $+ a_{51})$	$a_{34} =$ $-5a_{16}$ $- a_{52}$	$a_{35} =$ $-10a_{17}$ $+ 5a_{71}$	$a_{36} =$ $-14a_{18}$ $+ a_{72}$	$a_{37} =$ $-21a_{19}$ $- 7a_{91}$	$a_{38} =$ $-27a_{1,10}$ $- a_{92}$	$a_{39} =$ $-36a_{1,11}$ $+ 9a_{11,1}$	$a_{3,10} =$ $-44a_{1,12}$ $+ a_{11,2}$	$a_{3,11} =$ $-55a_{1,13}$ $- 11a_{13,1}$	$a_{3,12} =$ $-(65a_{1,14}$ $+ a_{13,2})$	$a_{3,13} =$ $13(-6a_{1,15}$ $+ a_{15,1})$	
$x^3$	$a_{41}$	$a_{42}$	$a_{43} =$ $-a_{25}$ $-5a_{61}$	$a_{44} =$ $-\frac{5}{3}(a_{26}$ $+ a_{62})$	$a_{45} =$ $-\frac{10}{3}a_{27}$ $+ \frac{35}{3}a_{81}$	$a_{46} =$ $-\frac{14}{3}a_{28}$ $+ \frac{7}{3}a_{82}$	$a_{47} =$ $-7(a_{29}$ $+ 3a_{10,1})$	$a_{48} =$ $-3(3a_{2,10}$ $+ a_{10,2})$	$a_{49} =$ $-12a_{2,11}$ $+ 33a_{12,1}$	$a_{4,10} =$ $\frac{11}{3}(-4a_{2,12}$ $+ a_{12,2})$	$a_{4,11} =$ $-\frac{55}{3}(a_{2,13}$ $+ 2.6a_{14,1})$	$a_{4,12} =$ $-\frac{13}{3}(5a_{2,14}$ $+ 10a_{14,2})$		
$x^4$	$a_{51}$	$a_{52}$	$a_{53} =$ $5a_{17}$ $-10a_{71}$	$a_{54} =$ $\frac{35}{3}a_{18}$ $-\frac{10}{3}a_{72}$	$a_{55} =$ $35(a_{19}$ $+ a_{91})$	$a_{56} =$ $63a_{1,10}$ $+ 7a_{92}$	$a_{57} =$ $126a_{1,11}$ $- 84a_{11,1}$	$a_{58} =$ $198a_{1,12}$ $- 12a_{11,2}$	$a_{59} =$ $165(2a_{1,13}$ $+ a_{13,1})$	$a_{5,10} =$ $\frac{55}{3}(26a_{1,14}$ $+ a_{13,2})$	$a_{5,11} =$ $286(2.5a_{1,15}$ $- a_{15,1})$			
$x^5$	$a_{61}$	$a_{62}$	$a_{63} =$ $a_{27}$ $-14a_{81}$	$a_{64} =$ $\frac{7}{3}a_{28}$ $-\frac{14}{3}a_{82}$	$a_{65} =$ $7a_{29}$ $+ 63a_{10,1}$	$a_{66} =$ $\frac{63}{5}(a_{2,10}$ $+ a_{10,2})$	$a_{67} =$ $\frac{126}{5}a_{2,11}$ $-\frac{924}{5}a_{12,1}$	$a_{68} =$ $\frac{198}{5}a_{2,12}$ $-\frac{132}{5}a_{12,2}$	$a_{69} =$ $66(a_{2,13} +$ $6.5a_{14,1})$	$a_{6,10} =$ $\frac{143}{3}(2a_{2,14} +$ $+ a_{14,2})$				
$x^6$	$a_{71}$	$a_{72}$	$a_{73} =$ $-7(a_{19}$ $+ 3a_{9,1})$	$a_{74} =$ $-7(3a_{1,10}$ $+ a_{9,2})$	$a_{75} =$ $-84a_{1,11}$ $+ 126a_{11,1}$	$a_{76} =$ $-\frac{924}{5}a_{1,12}$ $+ \frac{126}{5}a_{11,2}$	$a_{77} =$ $-462(a_{1,13}$ $+ a_{13,1})$	$a_{78} =$ $-66(13a_{1,14}$ $+ a_{13,2})$	$a_{79} =$ $-1716a_{1,15}$ $+ 1287a_{15,1}$					
$x^7$	$a_{81}$	$a_{82}$	$a_{83} =$ $-a_{29}$ $-27a_{10,1}$	$a_{84} =$ $-3(a_{2,10} +$ $+ 3a_{10,2})$	$a_{85} =$ $-12a_{2,11} +$ $+ 198a_{12,1}$	$a_{86} =$ $-\frac{132}{5}a_{2,12}$ $+ \frac{198}{5}a_{12,2}$	$a_{87} =$ $-66(a_{2,13} +$ $+ 13a_{14,1})$	$a_{88} =$ $-858/7$ $(a_{2,14} + a_{14,2})$						
$x^8$	$a_{91}$	$a_{92}$	$a_{93} =$ $9a_{1,11}$ $-36a_{11,1}$	$a_{94} =$ $33a_{1,12}$ $-12a_{11,2}$	$a_{95} =$ $165(a_{1,13}$ $+ 2a_{13,1})$	$a_{96} =$ $66(6.5a_{1,14}$ $+ a_{13,2})$	$a_{97} =$ $1287a_{1,15}$ $- 1716a_{15,1}$							
$x^9$	$a_{10,1}$	$a_{10,2}$	$a_{10,3} =$ $a_{2,11}$ $-44a_{12,1}$	$a_{10,4} =$ $\frac{11}{3}(a_{2,12}$ $- 4a_{12,2})$	$a_{10,5} =$ $\frac{55}{3}(a_{2,13}$ $+ 2.6a_{14,1})$	$a_{10,6} =$ $\frac{143}{3}(a_{2,14}$ $+ 2a_{14,2})$								
$x^{10}$	$a_{11,1}$	$a_{11,2}$	$a_{11,3} =$ $-11(a_{1,13}$ $+ 5a_{13,1})$	$a_{11,4} =$ $-\frac{55}{3}(2.6a_{1,14}$ $+ a_{13,2})$	$a_{11,5} =$ $286(-a_{1,15}$ $+ 2.5a_{15,1})$									
$x^{11}$	$a_{12,1}$	$a_{12,2}$	$a_{12,3} =$ $-(a_{2,13}$ $+ 6.5a_{14,1})$	$a_{12,4} =$ $-\frac{13}{3}(a_{2,14}$ $+ 5a_{14,2})$										
$x^{12}$	$a_{13,1}$	$a_{13,2}$	$a_{13,3} =$ $13(a_{1,15}$ $- 6a_{15,1})$											
$x^{13}$	$a_{14,1}$	$a_{14,2}$												
$x^{14}$	$a_{15,1}$													

biharmonic constraint is to cancel rows or columns. To find out how to note that all rows with dependent coefficients whose  $i$ -index is even are arbitrary coefficients whose  $i$ -index is also even, and all rows with coefficients having odd  $i$ -index contain only arbitrary coefficients whose  $i$ -index is also odd. Hence one can either cancel *all* rows with even index  $i$ , or *all* rows with odd index  $i$ , yet the condition  $\nabla^4\psi = 0$  remains satisfied resulting altered polynomial. If the rows with odd  $i$ -index are cancelled obtain the polynomial valid for the symmetrical model without motion. If in the same polynomial all arbitrary coefficients with  $j$  index = 1 are cancelled we obtain a polynomial which yields  $v = u = 0$  at  $y = 0$ ; that function valid for a symmetrical model welded to the base has been obtained.

Returning now to the columns, a parallel situation is noted. Coefficients with dependent coefficients have an even  $j$ -index contain only arbitrary coefficients whose  $j$ -index is also even; and columns with dependent coefficients whose  $j$ -index contain only arbitrary coefficients with an odd  $j$ -index. Thus none of the coefficients in columns with an odd  $j$ -index are related to coefficients in columns with an even index  $j$ , while at least some coefficients in a column with, say an even index  $j$  are related to some coefficients in a column with an even  $j$ -index, and the same interrelation holds for columns

	$y$	$y^2$	$y^3$	$y^4$	$y^5$	$y^6$	$y^7$
11	$a_{12}$	$a_{13}$	$a_{14}$	$a_{15}$	$a_{16}$	$a_{17}$	$a_{18}$
21	$a_{22}$	$a_{23}$	$a_{24}$	$a_{25}$	$a_{26}$	$a_{27}$	$a_{28}$
31	$a_{32}$	$a_{33} =$ $-3(a_{15}$ $+ a_{51})$	$a_{34} =$ $-5a_{16}$ $- a_{52}$	$a_{35} =$ $-10a_{17}$ $+ 5a_{71}$	$a_{36} =$ $-14a_{18}$ $+ a_{72}$	$a_{37} =$ $-21a_{19}$ $- 7a_{91}$	$a_{38} =$ $-27a_{1,10}$ $- a_{92}$
41	$a_{42}$	$a_{43} =$ $- a_{25}$ $- 5a_{61}$	$a_{44} =$ $-\frac{5}{3}(a_{26}$ $+ a_{62})$	$a_{45} =$ $-\frac{10}{3}a_{27}$ $+ \frac{35}{3}a_{81}$	$a_{46} =$ $-\frac{14}{3}a_{28}$ $+ \frac{7}{3}a_{82}$	$a_{47} =$ $-7(a_{29}$ $+ 3a_{10,1})$	$a_{48} =$ $-3(3a_{2,10}$ $+ a_{10,2})$
51	$a_{52}$	$a_{53} =$ $5a_{17}$ $- 10a_{71}$	$a_{54} =$ $\frac{35}{3}a_{18}$ $- \frac{10}{3}a_{72}$	$a_{55} =$ $35(a_{19}$ $+ a_{91})$	$a_{56} =$ $63a_{1,10}$ $+ 7a_{92}$	$a_{57} =$ $126a_{1,11}$ $- 84a_{11,1}$	$a_{58} =$ $198a_{1,12}$ $- 12a_{11,2}$
61	$a_{62}$	$a_{63} =$ $a_{27}$ $- 14a_{81}$	$a_{64} =$ $\frac{7}{3}a_{28}$ $- \frac{14}{3}a_{82}$	$a_{65} =$ $7a_{29}$ $+ 63a_{10,1}$	$a_{66} =$ $\frac{63}{5}(a_{2,10}$ $+ a_{10,2})$	$a_{67} =$ $\frac{126}{5}a_{2,11}$ $+ \frac{924}{5}a_{12,1}$	$a_{68} =$ $\frac{198}{5}a_{2,12}$ $- \frac{132}{5}a_{12,2}$
71	$a_{72}$	$a_{73} =$ $-7(a_{19}$ $+ 3a_{9,1})$	$a_{74} =$ $-7(3a_{1,10}$ $+ a_{9,2})$	$a_{75} =$ $-84a_{1,11}$ $+ 126a_{11,1}$	$a_{76} =$ $-\frac{924}{5}a_{1,12}$ $+ \frac{126}{5}a_{11,2}$	$a_{77} =$ $-462(a_{1,13}$ $+ a_{13,1})$	$a_{78} =$ $-66(13a_{1,14}$ $+ a_{13,2})$
81	$a_{82}$	$a_{83} =$ $- a_{29}$ $- 27a_{10,1}$	$a_{84} =$ $-3(a_{2,10}$ $+ 3a_{10,2})$	$a_{85} =$ $-12a_{2,11}$ $+ 198a_{12,1}$	$a_{86} =$ $-\frac{132}{5}a_{2,12}$ $+ \frac{198}{5}a_{12,2}$	$a_{87} =$ $-66(a_{2,13}$ $+ 13a_{14,1})$	$a_{88} =$ $-858/7$ $(a_{2,14} + a_{14,2})$
91	$a_{92}$	$a_{93} =$ $9a_{1,11}$ $- 36a_{11,1}$	$a_{94} =$ $33a_{1,12}$ $- 12a_{11,2}$	$a_{95} =$ $165(a_{1,13}$ $+ 2a_{13,1})$	$a_{96} =$ $66(6.5a_{1,14}$ $+ a_{13,2})$	$a_{97} =$ $1287a_{1,15}$ $- 1716a_{15,1}$	
101	$a_{10,2}$	$a_{10,3} =$ $a_{2,11}$ $- 44a_{12,1}$	$a_{10,4} =$ $\frac{11}{3}(a_{2,12}$ $- 4a_{12,2})$	$a_{10,5} =$ $\frac{55}{3}(a_{2,13}$ $+ 26a_{14,1})$	$a_{10,6} =$ $\frac{143}{3}(a_{2,14}$ $+ 2a_{14,2})$		
111	$a_{11,2}$	$a_{11,3} =$ $-11(a_{1,13}$ $+ 5a_{13,1})$	$a_{11,4} =$ $-\frac{55}{3}(2.6a_{1,14}$ $+ a_{13,2})$	$a_{11,5} =$ $286(-a_{1,15}$ $+ 2.5a_{15,1})$			
121	$a_{12,2}$	$a_{12,3} =$ $-(a_{2,13}$ $+ 65a_{14,1})$	$a_{12,4} =$ $-\frac{13}{3}(a_{2,14}$ $+ 5a_{14,2})$				
131	$a_{13,2}$	$a_{13,3} =$ $13(a_{1,15}$ $- 6a_{15,1})$					
141	$a_{14,2}$						

$y^8$	$y^9$	$y^{10}$	$y^{11}$	$y^{12}$	$y^{13}$	$y^{14}$
$a_{19}$	$a_{1,10}$	$a_{1,11}$	$a_{1,12}$	$a_{1,13}$	$a_{1,14}$	$a_{1,15}$
$a_{29}$	$a_{2,10}$	$a_{2,11}$	$a_{2,12}$	$a_{2,13}$	$a_{2,14}$	
$a_{39} =$ $-36a_{1,11}$ $+ 9a_{11,1}$	$a_{3,10} =$ $-44a_{1,12}$ $+ a_{11,2}$	$a_{3,11} =$ $-55a_{1,13}$ $- 11a_{13,1}$	$a_{3,12} =$ $-(65a_{1,14}$ $+ a_{13,2})$	$a_{3,13} =$ $13(-6a_{1,15}$ $+ a_{15,1})$		
$a_{49} =$ $-12a_{2,11}$ $+ 33a_{12,1}$	$a_{4,10} =$ $\frac{11}{3}(-4a_{2,12}$ $+ a_{12,2})$	$a_{4,11} =$ $-\frac{55}{3}(a_{2,13}$ $+ 2.6a_{14,1})$	$a_{4,12} =$ $-\frac{13}{3}(5a_{2,14}$ $+ 10a_{14,2})$			
$a_{59} =$ $165(2a_{1,13}$ $+ a_{13,1})$	$a_{5,10} =$ $\frac{55}{3}(26a_{1,14}$ $+ a_{13,2})$	$a_{5,11} =$ $286(2.5a_{1,15}$ $- a_{15,1})$				
$a_{69} =$ $66(a_{2,13}$ $+ 6.5a_{14,1})$	$a_{6,10} =$ $\frac{143}{3}(2a_{2,14}$ $+ a_{14,2})$					
$a_{79} =$ $-1716a_{1,15}$ $+ 1287a_{15,1}$						

biharmonic constraint is to cancel rows or columns. To find out how to do this we note that all rows with dependent coefficients whose  $i$ -index is even contain only arbitrary coefficients whose  $i$ -index is also even, and all rows with dependent coefficients having odd  $i$ -index contain only arbitrary coefficients whose  $i$ -index is also odd. Hence one can either cancel *all* rows with even index  $i$ , or one can cancel *all* rows with odd index  $i$ , yet the condition  $\nabla^4\psi = 0$  remains satisfied for the resulting altered polynomial. If the rows with odd  $i$ -index are cancelled, we in fact obtain the polynomial valid for the symmetrical model without motion at the base. If in the same polynomial all arbitrary coefficients with  $j$  index = 1 and 2 are also cancelled we obtain a polynomial which yields  $v = u = 0$  at  $y = 0$ ; that is the stream function valid for a symmetrical model welded to the base has been obtained.

Returning now to the columns, a parallel situation is noted. Columns whose dependent coefficients have an even  $j$ -index contain only arbitrary coefficients whose  $j$ -index is also even; and columns with dependent coefficients with an odd  $j$ -index contain only arbitrary coefficients with an odd  $j$ -index. This means that none of the coefficients in columns with an odd  $j$ -index are related to any of the coefficients in columns with an even index  $j$ , while at least some coefficients in a column with, say an even index  $j$  are related to some coefficients in all columns with an even  $j$ -index, and the same interrelation holds for columns with an odd

index  $j$ . It follows from these relationships that the comprehensive polynomial may be altered, and still remain a solution of  $\nabla^4\psi = 0$ , if either *all* columns with coefficients with an even  $j$ -index are cancelled, or *all* columns with coefficients with an odd  $j$ -index are cancelled.

Before applying stream function (31) to physical models, it is desirable to comment on certain problems related to stream-function simulation.

#### THE PROBLEM OF SATISFYING BOUNDARY STRESSES AND STRAINS

It is important to be aware of the difficulty in polynomial stream functions of satisfying completely the surface strains and stresses existing in physical models. In the model described by Ramberg (1981, pp. 207 ff.), for example, it was not possible to satisfy the condition of vanishing shear at the free vertical front face of the collapsing nappe. The shear at the front face could only be made to vanish if all coefficients in the stream function were reduced to zero, obviously a meaningless situation.

Because the polynomial used in Ramberg (1981) was of rather low degree—degree 5 in  $y$  and 3 in  $x$ —it seems not an unreasonable assumption that the larger number of arbitrary coefficients in a higher degree polynomial would permit the shear at the front face to vanish without reducing all coefficients to zero. This is unfortunately not so, a fact which can be demonstrated by applying the expression:

$$\dot{\gamma}_{xy} = \partial u / \partial y + \partial v / \partial x = -\partial^2 \psi / \partial y^2 + \partial^2 \psi / \partial x^2 = 0 \quad (32)$$

at  $x = \pm L$ ,  $0 \leq y \leq H$  on stream functions of high degree.

In addition to the problem of simulating a stress free front face when using polynomial stream functions, there are limitations when it comes to exact simulation of a stress free top surface of models. It poses no difficulty to *either* apply a condition of vanishing shear stress at the top face, *or* a condition of vanishing normal stress but it seems not always possible to apply both conditions simultaneously in a polynomial stream function, at least not if the degree is low or moderate.

#### COEFFICIENT DETERMINATION BY THE METHOD OF EXTREMIZING THE RATE OF ENERGY CHANGE

One drawback due to the above noted discrepancy between physical models and their mathematical stream-function images is that the true physical boundary conditions  $\dot{\gamma}_{xy} = 0$  and  $\sigma_x = 0$  at the front face or the condition of simultaneous vanishing of  $\dot{\gamma}_{xy}$  and  $\sigma_y$  at the top surface cannot be used to determine coefficients, and one may wonder how then the coefficients can be determined? Earlier the author applied the principle of extremum rate of dissipation of energy—or the equivalent extremum rate of decline of potential energy—as a means of determining

coefficients (Ramberg, 1981, p. 211). Depending upon whether the for velocities are considered constant during the procedure of determining extremum, the latter is either a maximum (at constant forces) or a minimum (at constant velocities).

In the model of a gravitationally spreading nappe not horizontally spreading driving force is fixed, viz. the body force of gravity, and the potential gradient is the sole supply of energy which keeps the system moving and spreading. Therefore gravitational spreading will take the path characterized by maximum rate of decline of potential energy, coupled with the side condition that the rate of potential energy change balances the rate of dissipation due to viscous stresses. The maximum rate of dissipation if one prefers—controls the values of the coefficients in the stream function in such a manner that the corresponding velocity field assumes a geometry, which—under the prevailing constraints—gives minimum resistance and accordingly maximum rate of collapse and maximum rate of spreading of the body. (Cf. Gauss' "Principle of Least Constraint": "The minimum influence takes place so that the constraints on the system are the least." Van Nostrand's Scientific Encyclopedia, 1959, p. 731.)

With the theory of non-equilibrium thermodynamics in mind, e.g. Prigogine (1970), interesting to consider the change of entropy associated with spreading changes. In Newtonian viscous flow of incompressible fluids, the structure of the fluid before and after flowage is the same, and the entropy of the material remains unchanged during flow at constant temperature. The change of entropy which takes place is therefore due to the heat produced by viscous dissipation divided by the instantaneous temperature. Maximum rate of dissipation is accordingly equivalent to maximum rate of production of entropy.

The energy-extremizing method generates enough relationships to determine all coefficients in the polynomial. Examples of this kind of calculation are found below.

It admittedly gives grounds for worry that the lack of stress at the front face in the physical model cannot be expressed by derivation from a polynomial stream function, and one wonders how significant this lack of exact correspondence between physical- and mathematical model may be.

A crucial aspect of this problem is the condition that energy is not conserved when derived from a stream function as pointed out on p. 2.

For the model considered the principle of conservation of energy is expressed by eqn. (33):

$$\Delta \dot{E}_{pot} + \Delta \dot{E}_{\epsilon_y} - \Delta \dot{E}_{\sigma_r} = 0$$

Here the change of potential energy is reckoned positive when increasing and negative when decreasing; the strain energy is always positive and the

j. It follows from these relationships that the comprehensive polynomial may be truncated, and still remain a solution of  $\nabla^4\psi = 0$ , if either all columns with coefficients with an even j-index are cancelled, or all columns with coefficients with an odd j-index are cancelled.

Before applying stream function (31) to physical models, it is desirable to be aware of certain problems related to stream-function simulation.

PROBLEM OF SATISFYING BOUNDARY STRESSES AND STRAINS

It is important to be aware of the difficulty in polynomial stream functions of satisfying completely the surface strains and stresses existing in physical models. In the model described by Ramberg (1981, pp. 207 ff.), for example, it was not possible to satisfy the condition of vanishing shear at the free vertical front face of the spreading nappe. The shear at the front face could only be made to vanish if all coefficients in the stream function were reduced to zero, obviously a meaningless solution.

Because the polynomial used in Ramberg (1981) was of rather low degree—degree 2 in y and 3 in x—it seems not an unreasonable assumption that the larger number of arbitrary coefficients in a higher degree polynomial would permit the shear at the front face to vanish without reducing all coefficients to zero. This is generally not so, a fact which can be demonstrated by applying the expression:

$$v/\partial y + \partial v/\partial x = -\partial^2\psi/\partial y^2 + \partial^2\psi/\partial x^2 = 0 \tag{32}$$

on stream functions of high degree. In addition to the problem of simulating a stress free front face when using polynomial stream functions, there are limitations when it comes to exact simulation of a stress free top surface of models. It poses no difficulty to either apply a condition of vanishing shear stress at the top face, or a condition of vanishing normal stress but it seems not always possible to apply both conditions simultaneously in a polynomial stream function, at least not if the degree is low or moderate.

PROBLEM OF COEFFICIENT DETERMINATION BY THE METHOD OF EXTREMIZING THE RATE OF CHANGE

A drawback due to the above noted discrepancy between physical models and mathematical stream-function images is that the true physical boundary conditions  $\dot{\gamma}_{xy} = 0$  and  $\sigma_x = 0$  at the front face or the condition of simultaneous satisfaction of  $\dot{\gamma}_{xy}$  and  $\sigma_y$  at the top surface cannot be used to determine coefficients, one may wonder how then the coefficients can be determined? Earlier the principle of extremum rate of dissipation of energy—or the principle of extremum rate of decline of potential energy—as a means of determining

coefficients (Ramberg, 1981, p. 211). Depending upon whether the forces or the velocities are considered constant during the procedure of determining the energy extremum, the latter is either a maximum (at constant forces) or a minimum (at constant velocities).

In the model of a gravitationally spreading nappe not horizontally pushed, the driving force is fixed, viz. the body force of gravity, and the potential gravity energy is the sole supply of energy which keeps the system moving and deforming. Therefore gravitational spreading will take the path characterized by maximum rate of decline of potential energy, coupled with the side condition that the rate of potential energy change balances the rate of dissipation due to viscous strain. What happens is that the principle of maximum rate of decline of potential energy—or maximum rate of dissipation if one prefers—controls the values of the coefficients in the stream function in such a manner that the corresponding velocity field assumes a geometry, which—under the prevailing constraints—gives minimum resistance and accordingly maximum rate of collapse and maximum rate of spreading of the body. (Cf. Gauss' "Principle of Least Constraint": "The motion of a system of interconnected points, interconnected in any way and submitted to any influence takes place so that the constraints on the system are the least possible". Van Nostrand's Scientific Encyclopedia, 1959, p. 731.)

With the theory of non-equilibrium thermodynamics in mind, e.g., Gyarmati (1970), interesting to consider the change of entropy associated with the energy changes. In Newtonian viscous flow of incompressible fluids, the microscopic structure of the fluid before and after flowage is the same, and the entropy of the material remains unchanged during flow at constant temperature. The only entropy change which takes place is therefore due to the heat produced by viscous strain, divided by the instantaneous temperature. Maximum rate of dissipation of energy is accordingly equivalent to maximum rate of production of entropy.

The energy-extremizing method generates enough relationships to allow us to determine all coefficients in the polynomial. Examples of this kind of calculation are found below.

It admittedly gives grounds for worry that the lack of stress at the free front face in the physical model cannot be expressed by derivation from a polynomial stream function, and one wonders how significant this lack of exact correspondence between physical- and mathematical model may be.

A crucial aspect of this problem is the condition that energy is automatically conserved when derived from a stream function as pointed out on p. 208.

For the model considered the principle of conservation of energy is expressed in eqn. (33):

$$\Delta \dot{E}_{pot} + \Delta \dot{E}_{\epsilon\gamma} - \Delta \dot{E}_{\sigma\tau} = 0 \tag{33}$$

Here the change of potential energy is reckoned positive when increasing and negative when decreasing; the strain energy is always positive and the energy change

due to stress acting on moving parts of the boundary is positive if energy is introduced into the body and negative if the body imparts energy to the surroundings.

In the procedure for determining the coefficients by maximizing the rate of energy change, the rate of decline of potential energy was equated with the rate of dissipation due to viscous strain, i.e.,  $\dot{E}_{\text{pot}} + \dot{E}_{\text{cy}}$  was put equal to zero, in agreement with the fact that potential energy was the only driving power in the system. From eqn. (33) we see that a consequence of this is that  $\dot{E}_{\text{str}} = 0$ . In other words, the energy change due to the discrepant boundary stresses—i.e., the stresses which cannot be made to vanish when derived from the stream function even though they are zero in the corresponding physical model—vanishes when integrated over the entire boundary. Or expressed differently: the average energy change due to the discrepant boundary stresses is zero. From this crucial information we conclude that the lack of exact correspondence as regards boundary stresses between a physical model and its polynomial stream-function image may only be of marginal consequence for the dynamic behaviour of the mathematical model. Thus the velocity field calculated from a polynomial stream function should approximate quite well the physical model as long as correct input values for viscosity, density and geometric shapes and dimensions are used.

In view of the above comments it is reassuring to find that the validity of the method of maximizing the rate of dissipation—or rate of declining potential energy—during gravitational viscous collapse has been demonstrated experimentally, (Mulugeta and Ramberg, in prep.).

#### SIMULATION OF A SPREADING COMPOSITE NAPPE

##### *The use of continuity of velocity and stresses at layer interface*

Complete coherence at the base and free slip along the base discussed in Ramberg (1981) represents two extreme situations not likely to be found in the real world. In many nappes and thrust sheets motion occurs along the basal plane in contrast to the coherent model, but the motion is clearly not frictionless as it would be in a free slip model. To incorporate restricted basal motion in the model one could apply a reasonable coefficient of friction assuming slide along a rigid surface, but one could also consider motion in the form of concentrated viscous shear in a relatively thin basal layer. We shall treat the latter possibility and in so doing assign a relatively low Newtonian viscosity to the basal layer whose contact to the overlaying complex is coherent and mobile while exhibiting immobile contact to the rigid basement.

The model to consider is indicated in Fig. 2. It is a double-layer complex riding on a rigid horizontal basement. Both layers are homogeneous with respect to density, viscosity and thickness:  $\rho_1$ ,  $\eta_1$ , and  $H_1$  are valid for the bottom layer, and

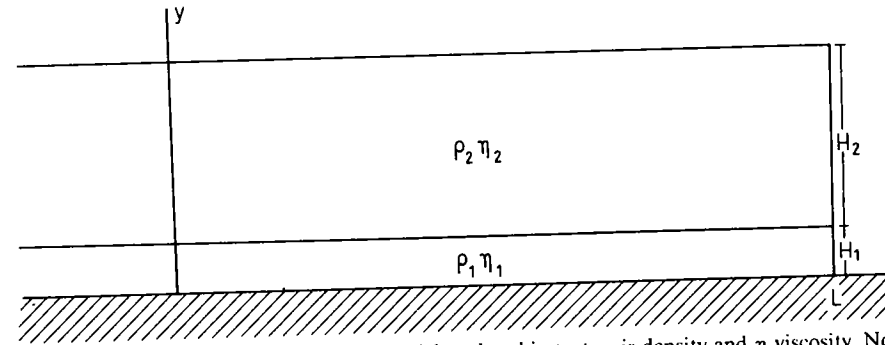


Fig. 2. Right-hand half of double-layer model analysed in text.  $\rho$  is density and  $\eta$  viscosity. No symbol  $\rho$  is replaced by  $R_0$  and  $\eta$  by  $Mu$  in the computer-plotted drawings later in this paper.

$\rho_2$ ,  $\eta_2$  and  $H_2$  for the top layer. By making  $H_1$  much less than  $H_2$  and  $\eta_1$  than  $\eta_2$  the conditions noted above are simulated. However, the theory follows applies to a variety of values of  $\rho$ ,  $\eta$ , and  $H$ .  $L$  is the half-length symmetric body whose semi-aspect ratios are  $R_1 = L/H_1$  and  $R_2 = L/H_2$  to two layers.

To simulate the model, stream functions of moderately high degree are used. Stream function (34), valid for vanishing velocity at the base, is used for the bottom layer, and stream function (35) which permits motion both at the upper and lower boundaries, is applied to the top layer. Both functions are truncated versions of a comprehensive  $\psi$ -function (31). In both functions the rows of terms with odd  $i$ -index (and even power of  $x$ ) are excluded, meaning that symmetry exists in the vertical plane normal to  $x$  at  $x = 0$  and that the velocity component  $u$  in both layers is zero here.

$$\begin{aligned} \psi_1 = & (a'_{23}y_1^2 + a'_{24}y_1^3 + a'_{25}y_1^4 + a'_{26}y_1^5 + a'_{27}y_1^6 + a'_{28}y_1^7)x_1 \\ & - (a'_{25}y_1^2 + \frac{5}{3}a'_{26}y_1^3 + \frac{10}{3}a'_{27}y_1^4 + \frac{14}{3}a'_{28}y_1^5)x_1^3 \\ & + (a'_{27}y_1^2 + \frac{7}{3}a'_{28}y_1^3)x_1^5 \\ = & - (ay_1^2 + by_1^3 + cy_1^4 + dy_1^5 + ey_1^6 + fy_1^7)x \\ & + (cy_1^2 + \frac{5}{3}dy_1^3 + \frac{10}{3}ey_1^4 + \frac{14}{3}fy_1^5)x^3 \\ & - (ey_1^2 + \frac{7}{3}fy_1^3)x^5 \\ \psi_2 = & (a_{21} + a_{22}y_2 + a_{23}y_2^2 + a_{24}y_2^3 + a_{25}y_2^4 + a_{26}y_2^5)x \\ & + [a_{41} + a_{42}y_2 - (a_{25} + 5a_{61})y_2^2 - \frac{5}{3}(a_{26} + a_{62})y_2^3]x^3 \\ & + (a_{61} + a_{62}y_2)x^5 \end{aligned}$$

stress acting on moving parts of the boundary is positive if energy is ced into the body and negative if the body imparts energy to the surround-

the procedure for determining the coefficients by maximizing the rate of change, the rate of decline of potential energy was equated with the rate of ion due to viscous strain, i.e.,  $\dot{E}_{pot} + \dot{E}_{\epsilon\gamma}$  was put equal to zero, in agreement fact that potential energy was the only driving power in the system. From ) we see that a consequence of this is that  $\dot{E}_{\sigma\tau} = 0$ . In other words, the change due to the discrepant boundary stresses—i.e., the stresses which be made to vanish when derived from the stream function even though they in the corresponding physical model—vanishes when integrated over the boundary. Or expressed differently: the average energy change due to the nt boundary stresses is zero. From this crucial information we conclude that of exact correspondence as regards boundary stresses between a physical and its polynomial stream-function image may only be of marginal conse- for the dynamic behaviour of the mathematical model. Thus the velocity ulated from a polynomial stream function should approximate quite well sical model as long as correct input values for viscosity, density and c shapes and dimensions are used.

ow of the above comments it is reassuring to find that the validity of the f maximizing the rate of dissipation—or rate of declining potential energy gravitational viscous collapse has been demonstrated experimentally, a and Ramberg, in prep.).

ION OF A SPREADING COMPOSITE NAPPE

*f continuity of velocity and stresses at layer interface*

ete coherence at the base and free slip along the base discussed in (1981) represents two extreme situations not likely to be found in the real many nappes and thrust sheets motion occurs along the basal plane in o the coherent model, but the motion is clearly not frictionless as it would ee slip model. To incorporate restricted basal motion in the model one y a reasonable coefficient of friction assuming slide along a rigid surface, ould also consider motion in the form of concentrated viscous shear in a thin basal layer. We shall treat the latter possibility and in so doing assign y low Newtonian viscosity to the basal layer whose contact to the complex is coherent and mobile while exhibiting immobile contact to the nent.

del to consider is indicated in Fig. 2. It is a double-layer complex riding l horizontal basement. Both layers are homogeneous with respect to oscosity and thickness:  $\rho_1, \eta_1$ , and  $H_1$  are valid for the bottom layer, and

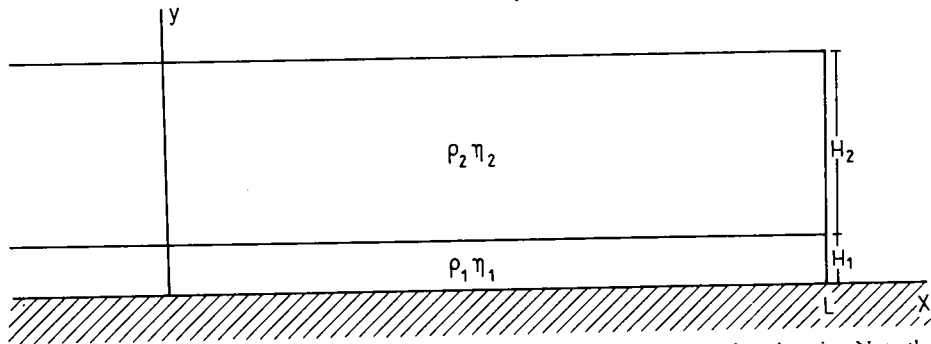


Fig. 2. Right-hand half of double-layer model analysed in text.  $\rho$  is density and  $\eta$  viscosity. Note that the symbol  $\rho$  is replaced by  $R_0$  and  $\eta$  by  $Mu$  in the computer-plotted drawings later in this paper.

$\rho_2, \eta_2$  and  $H_2$  for the top layer. By making  $H_1$  much less than  $H_2$  and  $\eta_1$  smaller than  $\eta_2$  the conditions noted above are simulated. However, the theory which follows applies to a variety of values of  $\rho, \eta$ , and  $H$ .  $L$  is the half-length of the symmetric body whose semi-aspect ratios are  $R_1 = L/H_1$  and  $R_2 = L/H_2$  for the two layers.

To simulate the model, stream functions of moderately high degree are chosen. Stream function (34), valid for vanishing velocity at the base, is used for the basal layer, and stream function (35) which permits motion both at the upper and lower boundaries, is applied to the top layer. Both functions are truncated versions of the comprehensive  $\psi$ -function (31). In both functions the rows of terms with an odd  $i$ -index (and even power of  $x$ ) are excluded, meaning that symmetry exists about a vertical plane normal to  $x$  at  $x = 0$  and that the velocity component  $u$  in both layers is zero here.

$$\begin{aligned} \psi_1 = & (a'_{23}y_1^2 + a'_{24}y_1^3 + a'_{25}y_1^4 + a'_{26}y_1^5 + a'_{27}y_1^6 + a'_{28}y_1^7)x_1 \\ & - (a'_{25}y_1^2 + \frac{5}{3}a'_{26}y_1^3 + \frac{10}{3}a'_{27}y_1^4 + \frac{14}{3}a'_{28}y_1^5)x_1^3 \\ & + (a'_{27}y_1^2 + \frac{7}{3}a'_{28}y_1^3)x_1^5 \\ = & -(ay_1^2 + by_1^3 + cy_1^4 + dy_1^5 + ey_1^6 + fy_1^7)x \\ & + (cy_1^2 + \frac{5}{3}dy_1^3 + \frac{10}{3}ey_1^4 + \frac{14}{3}fy_1^5)x^3 \\ & - (ey_1^2 + \frac{7}{3}fy_1^3)x^5 \end{aligned} \tag{34}$$

$$\begin{aligned} \psi_2 = & (a_{21} + a_{22}y_2 + a_{23}y_2^2 + a_{24}y_2^3 + a_{25}y_2^4 + a_{26}y_2^5)x \\ & + [a_{41} + a_{42}y_2 - (a_{25} + 5a_{61})y_2^2 - \frac{5}{3}(a_{26} + a_{62})y_2^3]x^3 \\ & + (a_{61} + a_{62}y_2)x^5 \end{aligned} \tag{35}$$

In  $\psi_2$  and in the first version of  $\psi_1$  the coefficients are indexed exactly as in the comprehensive eqn. (31) in order to show clearly how the truncation and modification of the comprehensive polynomial are performed. We shall keep the original subscripts of the coefficients in  $\psi_2$  but it is practical for the operation that follows that the coefficient notation in  $\psi_1$  is changed as shown in its second version. In  $\psi_1$  the condition  $u_1 = v_1 = 0$  at  $y = 0$  is accounted for by letting coefficients  $a_{i1}$  and  $a_{i2}$  vanish,  $i = 2, 4$  and  $6$ .

A condition for dynamic equilibrium is that the velocity be continuous across the contact (i.e.,  $u_1 = u_2$ ;  $v_1 = v_2$  at the contact). A further condition is that the tangential shear stress and the normal stress are continuous at the contact. Together with extremizing the rate of energy dissipation—or rate of potential energy decline—these conditions will be used to determine coefficients.

Equation (34) is valid for  $0 \leq y_1 \leq H_1$ , and eqn. (35) for  $0 \leq y_2 \leq H_2$ . Both equations are valid for  $-L \leq x \leq +L$ .

The following velocities are derived from the stream functions;

$$u_1 = -\frac{\partial \psi_1}{\partial y} = (2ay_1 + 3by_1^2 + 4cy_1^3 + 5dy_1^4 + 6ey_1^5 + 7fy_1^6)x - (2cy_1 + 5dy_1^2 + \frac{40}{3}ey_1^3 + \frac{70}{3}fy_1^4)x^3 + (2ey_1 + 7fy_1^2)x^5 \quad (36)$$

$$v_1 = \frac{\partial \psi_1}{\partial x} = -(ay_1^2 + by_1^3 + cy_1^4 + dy_1^5 + ey_1^6 + fy_1^7) + (3cy_1^2 + 5dy_1^3 + 10ey_1^4 + 14fy_1^5)x^2 - (5ey_1^2 + \frac{35}{3}fy_1^3)x^4 \quad (37)$$

$$u_2 = -\frac{\partial \psi_2}{\partial y} = -(a_{22} + 2a_{23}y_2 + 3a_{24}y_2^2 + 4a_{25}y_2^3 + 5a_{26}y_2^4)x + [-a_{42} + (2a_{25} + 10a_{61})y_2 + (5a_{26} + 5a_{62})y_2^2]x^3 - a_{62}x^5 \quad (38)$$

$$v_2 = \frac{\partial \psi_2}{\partial x} = a_{21} + a_{22}y_2 + a_{23}y_2^2 + a_{24}y_2^3 + a_{25}y_2^4 + a_{26}y_2^5 + [3a_{41} + 3a_{42}y_2 - (3a_{25} + 15a_{61})y_2^2 - (5a_{26} + 5a_{62})y_2^3]x^2 + 5(a_{61} + a_{62}y_2)x^4 \quad (39)$$

At the contact between the two layers  $y_1 = H_1$  and  $y_2 = 0$ . Introduced in eqns. (36) and (38) this leads to:

$$u_1 = (2aH_1 + 3bH_1^2 + 4cH_1^3 + 5dH_1^4 + 6eH_1^5 + 7fH_1^6)x - (2cH_1 + 5dH_1^2 + \frac{40}{3}eH_1^3 + \frac{70}{3}fH_1^4)x^3 + (2eH_1 + 7fH_1^2)x^5 \quad (40)$$

$$u_2 = -(a_{22}x + a_{42}x^3 + a_{62}x^5) \quad (41)$$

for the horizontal velocity component. Because  $u$  is continuous at the contact for all

values of  $x$  between  $-L$  and  $+L$  the sum of terms with the same power of  $x$  be equal in the two equations, and we find:

$$a_{62} = -2eH_1 - 7fH_1^2$$

$$a_{42} = 2cH_1 + 5dH_1^2 + \frac{40}{3}eH_1^3 + \frac{70}{3}fH_1^4$$

$$a_{22} = -2aH_1 - 3bH_1^2 - 4cH_1^3 - 5dH_1^4 - 6eH_1^5 - 7fH_1^6$$

Similarly the condition  $v_1 = v_2$  at  $y_1 = H_1$  and  $y_2 = 0$  yields:

$$a_{61} = -eH_1^2 - \frac{7}{3}fH_1^3$$

$$a_{41} = cH_1^2 + \frac{5}{3}dH_1^3 + \frac{10}{3}eH_1^4 + \frac{14}{3}fH_1^5$$

$$a_{21} = -aH_1^2 - bH_1^3 - cH_1^4 - dH_1^5 - eH_1^6 - fH_1^7$$

To apply the condition  $\tau_{x,y_1} = \tau_{x,y_2}$  at the contact we derive the expression  $\tau_{x,y} = \eta(\partial u/\partial y + \partial v/\partial x) = \eta(\partial^2 \psi/\partial x^2 - \partial^2 \psi/\partial y^2)$  for the two layers:

$$\begin{aligned} \tau_{x,y_1} &= \eta_1 \dot{\gamma}_{x,y_1} = \eta_1 \left[ (2a + 6by_1 + 18cy_1^2 + 30dy_1^3 + 50ey_1^4 + 70fy_1^5)x \right. \\ &\quad \left. - (2c + 10dy_1 + 60ey_1^2 + 140fy_1^3)x^3 + (2e + 14fy_1)x^5 \right] \\ \tau_{x,y_2} &= \eta_2 \dot{\gamma}_{x,y_2} = \eta_2 \left\{ [-2a_{23} + 6a_{41} - (6a_{24} - 6a_{42})y_2 - (18a_{25} + 30a_{61})y_2^2 \right. \\ &\quad \left. - (30a_{26} + 10a_{62})y_2^3 \right\} x + \{ 2a_{25} + 30a_{61} + (10a_{26} + 30a_{62})y_2 \} x^3 \end{aligned}$$

As continuous shear stress is required at all points—at all  $x$ —on the contact after equating  $\tau_{x,y_1}$  at  $y_1 = H_1$  with  $\tau_{x,y_2}$  at  $y_2 = 0$ :

$$f = -\frac{1}{7}H_1^{-1}e$$

$$\eta_2(2a_{25} + 30a_{61}) = -\eta_1(2c + 10dH_1 + 40eH_1^2)$$

and:

$$\eta_2(-2a_{23} + 6a_{41}) = \eta_1(2a + 6bH_1 + 18cH_1^2 + 30dH_1^3 + 40eH_1^4)$$

To make use of the condition  $\sigma_{y_1} = \sigma_{y_2}$  at the contact we start with the form

$$\sigma_y = 2\eta \dot{\epsilon}_y - P$$

and:

$$dP = \frac{\partial P}{\partial x} dx + \frac{\partial P}{\partial y} dy$$

in which  $\dot{\epsilon}_y$  and the partial derivatives are derived from the two stream functions using relations  $\dot{\epsilon}_y = \partial v/\partial y = \partial^2 \psi/\partial x \partial y$ ;

$$\partial P/\partial x = \eta \left( \frac{\partial^2 u}{\partial x^2} + \frac{\partial^2 v}{\partial y^2} \right) = -\eta \left( \frac{\partial^3 \psi}{\partial x \partial y^2} + \frac{\partial^3 \psi}{\partial y^3} \right)$$

and:

$$\partial P/\partial y = \eta \left( \frac{\partial^2 v}{\partial x^2} + \frac{\partial^2 v}{\partial y^2} \right) - \rho g = \eta \left( \frac{\partial^3 \psi}{\partial x^3} + \frac{\partial^3 \psi}{\partial x \partial y^2} \right) - \rho g$$



$\psi_2$  and in the first version of  $\psi_1$  the coefficients are indexed exactly as in the comprehensive eqn. (31) in order to show clearly how the truncation and modification of the comprehensive polynomial are performed. We shall keep the original subscripts of the coefficients in  $\psi_2$  but it is practical for the operation that follows to change the coefficient notation in  $\psi_1$  as shown in its second version. In  $\psi_1$  the condition  $u_1 = v_1 = 0$  at  $y = 0$  is accounted for by letting coefficients  $a_{i1}$  and  $a_{i2}$  be zero,  $i = 2, 4$  and  $6$ .

The condition for dynamic equilibrium is that the velocity be continuous across the contact (i.e.,  $u_1 = u_2$ ;  $v_1 = v_2$  at the contact). A further condition is that the tangential shear stress and the normal stress are continuous at the contact. Together with extremizing the rate of energy dissipation—or rate of potential energy decline—these conditions will be used to determine coefficients.

Equation (34) is valid for  $0 \leq y_1 \leq H_1$ , and eqn. (35) for  $0 \leq y_2 \leq H_2$ . Both equations are valid for  $-L \leq x \leq +L$ .

The following velocities are derived from the stream functions;

$$\frac{\partial \psi_1}{\partial y} = (2ay_1 + 3by_1^2 + 4cy_1^3 + 5dy_1^4 + 6ey_1^5 + 7fy_1^6)x - (2cy_1 + 5dy_1^2 + \frac{40}{3}ey_1^3 + \frac{70}{3}fy_1^4)x^3 + (2ey_1 + 7fy_1^2)x^5 \quad (36)$$

$$\frac{v_1}{x} = -(ay_1^2 + by_1^3 + cy_1^4 + dy_1^5 + ey_1^6 + fy_1^7) + (3cy_1^2 + 5dy_1^3 + 10ey_1^4 + 14fy_1^5)x^2 - (5ey_1^2 + \frac{35}{3}fy_1^3)x^4 \quad (37)$$

$$\frac{\partial \psi_2}{\partial y} = -(a_{22} + 2a_{23}y_2 + 3a_{24}y_2^2 + 4a_{25}y_2^3 + 5a_{26}y_2^4)x + [-a_{42} + (2a_{25} + 10a_{61})y_2 + (5a_{26} + 5a_{62})y_2^2]x^3 - a_{62}x^5 \quad (38)$$

$$\frac{v_2}{x} = a_{21} + a_{22}y_2 + a_{23}y_2^2 + a_{24}y_2^3 + a_{25}y_2^4 + a_{26}y_2^5 + [3a_{41} + 3a_{42}y_2 - (3a_{25} + 15a_{61})y_2^2 - (5a_{26} + 5a_{62})y_2^3]x^2 + 5(a_{61} + a_{62}y_2)x^4 \quad (39)$$

At the contact between the two layers  $y_1 = H_1$  and  $y_2 = 0$ . Introduced in eqns. (36) and (37) this leads to:

$$H_1 + 3bH_1^2 + 4cH_1^3 + 5dH_1^4 + 6eH_1^5 + 7fH_1^6)x - (2cH_1 + 5dH_1^2 + \frac{40}{3}eH_1^3 + \frac{70}{3}fH_1^4)x^3 + (2eH_1 + 7fH_1^2)x^5 \quad (40)$$

$$a_{22}x + a_{42}x^3 + a_{62}x^5 \quad (41)$$

The horizontal velocity component. Because  $u$  is continuous at the contact for all

values of  $x$  between  $-L$  and  $+L$  the sum of terms with the same power of  $x$  must be equal in the two equations, and we find:

$$a_{62} = -2eH_1 - 7fH_1^2 \quad (42)$$

$$a_{42} = 2cH_1 + 5dH_1^2 + \frac{40}{3}eH_1^3 + \frac{70}{3}fH_1^4 \quad (43)$$

$$a_{22} = -2aH_1 - 3bH_1^2 - 4cH_1^3 - 5dH_1^4 - 6eH_1^5 - 7fH_1^6 \quad (44)$$

Similarly the condition  $v_1 = v_2$  at  $y_1 = H_1$  and  $y_2 = 0$  yields:

$$a_{61} = -eH_1^2 - \frac{7}{3}fH_1^3 \quad (45)$$

$$a_{41} = cH_1^2 + \frac{5}{3}dH_1^3 + \frac{10}{3}eH_1^4 + \frac{14}{3}fH_1^5 \quad (46)$$

$$a_{21} = -aH_1^2 - bH_1^3 - cH_1^4 - dH_1^5 - eH_1^6 - fH_1^7 \quad (47)$$

To apply the condition  $\tau_{xy_1} = \tau_{xy_2}$  at the contact we derive the expression  $\tau_{xy} = \eta \dot{\gamma}_{xy} = \eta(\partial u / \partial y + \partial v / \partial x) = \eta(\partial^2 \psi / \partial x^2 - \partial^2 \psi / \partial y^2)$  for the two layers:

$$\tau_{xy_1} = \eta_1 \dot{\gamma}_{xy_1} = \eta_1 [(2a + 6by_1 + 18cy_1^2 + 30dy_1^3 + 50ey_1^4 + 70fy_1^5)x - (2c + 10dy_1 + 60ey_1^2 + 140fy_1^3)x^3 + (2e + 14fy_1)x^5] \quad (48)$$

$$\tau_{xy_2} = \eta_2 \dot{\gamma}_{xy_2} = \eta_2 \{ [-2a_{23} + 6a_{41} - (6a_{24} - 6a_{42})y_2 - (18a_{25} + 30a_{61})y_2^2 - (30a_{26} + 10a_{62})y_2^3]x + \{2a_{25} + 30a_{61} + (10a_{26} + 30a_{62})y_2\}x^3 \} \quad (49)$$

As continuous shear stress is required at all points—at all  $x$ —on the contact we find after equating  $\tau_{xy_1}$  at  $y_1 = H_1$  with  $\tau_{xy_2}$  at  $y_2 = 0$ :

$$f = -\frac{1}{7}H_1^{-1}e \quad (50)$$

$$\eta_2(2a_{25} + 30a_{61}) = -\eta_1(2c + 10dH_1 + 40eH_1^2) \quad (51)$$

and:

$$\eta_2(-2a_{23} + 6a_{41}) = \eta_1(2a + 6bH_1 + 18cH_1^2 + 30dH_1^3 + 40eH_1^4) \quad (52)$$

To make use of the condition  $\sigma_{y_1} = \sigma_{y_2}$  at the contact we start with the formulas:

$$\sigma_y = 2\eta \dot{\epsilon}_y - P \quad (53)$$

and:

$$dP = \frac{\partial P}{\partial x} dx + \frac{\partial P}{\partial y} dy \quad (54)$$

in which  $\dot{\epsilon}_y$  and the partial derivatives are derived from the two stream functions using relations  $\dot{\epsilon}_y = \partial v / \partial y = \partial^2 \psi / \partial x \partial y$ ;

$$\partial P / \partial x = \eta \left( \frac{\partial^2 u}{\partial x^2} + \frac{\partial^2 u}{\partial y^2} \right) = -\eta \left( \frac{\partial^3 \psi}{\partial x \partial y^2} + \frac{\partial^3 \psi}{\partial y^3} \right) \quad (55)$$

and:

$$\partial P / \partial y = \eta \left( \frac{\partial^2 v}{\partial x^2} + \frac{\partial^2 v}{\partial y^2} \right) - \rho g = \eta \left( \frac{\partial^3 \psi}{\partial x^3} + \frac{\partial^3 \psi}{\partial x \partial y^2} \right) - \rho g \quad (56)$$

When applied to stream function  $\psi_1$  this procedure leads to:

$$dP = \eta_1 \left[ (6b + 12cy_1 + 30dy_1^2 + 40ey_1^3 + 70fy_1^4)x - (10d + 40ey_1 + 140fy_1^2)x^3 + 14fx^5 \right] dx + \left[ \eta_1 \left\{ -2a - 6by_1 - 6cy_1^2 - 10dy_1^3 - 10ey_1^4 - 14fy_1^5 + (6c + 30dy_1 + 60ey_1^2 + 140fy_1^3)x^2 - (10e + 70fy_1)x^4 \right\} - \rho_1 g \right] dy \quad (57)$$

It can be demonstrated that  $dP$  in this equation is an exact differential, and integration can be performed accordingly:

$$P = \eta_1 \left[ (3b + 6cy_1 + 15dy_1^2 + 20ey_1^3 + 35fy_1^4)x^2 - \left( \frac{10}{4}d + 10ey_1 + 35fy_1^2 \right)x^4 + \frac{14}{6}fx^6 \right] + f(y) \quad (58)$$

Here  $f(y)$  is an unknown function which may be found when eqn. (58) is differentiated with respect to  $y$  and the resulting derivative is equated with the partial derivative  $\partial P/\partial y$  in eqn. (57). Thus:

$$\partial P/\partial y = \eta_1 (6c + 30dy_1 + 60ey_1^2 + 140fy_1^3)x^2 - (10e + 70fy_1)x^4 + \partial f(y)/\partial y \quad (59)$$

must equate with the term  $\partial P/\partial y$  in eqn. (57), i.e., the quantity in the parenthesis in front of  $dy$ . An expression for  $\partial f(y)/\partial y$  is accordingly obtained:

$$\partial f(y)/\partial y = \eta_1 (-2a - 6by_1 - 6cy_1^2 - 10dy_1^3 - 10ey_1^4 - 14fy_1^5) - \rho_1 g \quad (60)$$

which upon integration yields:

$$f(y) = \eta_1 (-2ay_1 - 3by_1^2 - 2cy_1^3 - \frac{5}{2}dy_1^4 - 2ey_1^5 - \frac{7}{3}fy_1^6) - \rho_1 gy_1 + c_1 \quad (61)$$

Here  $c_1$  is a constant of integration.

$f(y)$  can be introduced in eqn. (58) which in its turn goes into eqn. (53), and the normal stress parallel to  $y$  in layer 1 follows when:

$$\epsilon_y = \frac{\partial v}{\partial y} = \frac{\partial^2 \psi}{\partial x \partial y}$$

is also inserted as derived from stream function  $\psi_1$ .

$$\sigma_{y_1} = 2\eta_1 \epsilon_{y_1} - P_1 = \eta_1 \left( -2ay - 3by_1^2 - 6cy_1^3 - \frac{15}{2}dy_1^4 - 10ey_1^5 - \frac{35}{3}fy_1^6 + (-3b + 6cy_1 + 15dy_1^2 + 60ey_1^3 + 105fy_1^4)x^2 + \left( \frac{5}{2}d - 10ey_1 - 35fy_1^2 \right)x^4 - \frac{7}{3}fx^6 \right) + \rho_1 gy_1 - c_1 \quad (62)$$

A corresponding procedure performed using stream function  $\psi_2$  produces an expression for the normal stress  $\sigma_2$  in the top layer:

$$\sigma_{y_2} = 2\eta_2 \epsilon_{y_2} - P_1 = \eta_2 \left[ 2a_{22} + 2a_{23}y_2 - 6a_{41}y_2 + (3a_{24} - 3a_{42})y_2^2 + (6a_{25} + 10a_{62})y_2^3 + \left( \frac{15}{2}a_{26} + \frac{5}{3}a_{62} \right)y_2^4 + \left\{ 3a_{24} + 9a_{42} - (6a_{25} + 90a_{61})y_2 - (15a_{26} + 45a_{62})y_2^2 \right\} x^2 - \left( \frac{5}{2}a_{26} - \frac{35}{3}a_{62} \right)x^4 \right] + \rho g y_2 - c_2 \quad (63)$$

Here again  $c_2$  is a constant of integration. Incidentally, neither  $c_1$  nor  $c_2$  are necessary for the determination of coefficients in the stream functions, but the values of  $a$  and  $c_2$  are necessary if we wish to know the magnitude of the normal stress in two layers.

$\sigma_{y_1}$  must equate with  $\sigma_{y_2}$  at all  $x$  between  $-L$  and  $+L$  when  $y_1$  is put equal to  $H_1$  and  $y_2 = 0$  in eqns. (62) and (63). Performing this operation we immediately obtain that:

$$f = 0$$

(because  $\frac{7}{3}fx^6$  is the only term containing  $f$ ). A consequence of this is:

$$e = a_{62} = a_{61} = 0 \quad (\text{see eqns. (50), (42) and (45)})$$

Application of these results on the terms multiplied by  $x^4$  in eqns. (62) and (63) leads to:

$$a_{26} = -\eta_1/\eta_2 d \equiv -md \quad (\text{here } m \equiv \eta_1/\eta_2)$$

Equating the collection of terms multiplied by  $x^2$  in the two equations one obtains:

$$\eta_2 (3a_{24} + 9a_{42}) = \eta_1 (-3b + 6cH_1 + 15dH_1^2),$$

and the relation:

$$2\eta_2 a_{22} - c_2 = -\eta_1 (2aH_1 + 3bH_1^2 + 6cH_1^3 + \frac{15}{2}dH_1^4) - c_1 + \rho_1 g H_1$$

follows when the constant terms are collected and equated

Equation (67) with the expression for  $a_{42}$  introduced (eqn. 43) gives:

$$a_{24} = -mb + (2m - 6)cH_1 + (5m - 15)dH_1^2$$

From eqns. (52), (45) and (65) follows:

$$a_{23} = -m \left[ a + 3bH_1 + (9 - 3m^{-1})cH_1^2 + (15 - 5m^{-1})dH_1^3 \right]$$

and from eqns. (51) and (65):

$$a_{25} = -m(c + 5dH_1)$$

Now all coefficients in stream function  $\psi_2$  are expressed as functions of  $a$  to  $d$  in stream function  $\psi_1$ . The said relationships are:

$$a_{21} = -aH_1^2 - bH_1^3 - cH_1^4 - dH_1^5$$

$$a_{22} = -2aH_1 - 3bH_1^2 - 4cH_1^3 - 5dH_1^4$$

$$a_{23} = -m \left[ a + 3bH_1 + (9 - 3/m)cH_1^2 + (15 - 5/m)dH_1^3 \right]$$

$$a_{24} = -mb + (2m - 6)cH_1 + (5m - 15)dH_1^2$$

$$a_{25} = -m(c + 5dH_1)$$

$$a_{26} = -md$$

$$a_{41} = cH_1^2 + \frac{5}{3}dH_1^3$$

$$a_{42} = 2cH_1 + 5dH_1^2$$

All other coefficients are zero.

an applied to stream function  $\psi_1$  this procedure leads to:

$$= \eta_1 \left[ (6b + 12cy_1 + 30dy_1^2 + 40ey_1^3 + 70fy_1^4)x - (10d + 40ey_1 + 140fy_1^2)x^3 + 14fx^5 \right] dx + \left[ \eta_1 \left\{ -2a - 6by_1 - 6cy_1^2 - 10dy_1^3 - 10ey_1^4 - 14fy_1^5 + (6c + 30dy_1 + 60ey_1^2 + 140fy_1^3)x^2 - (10e + 70fy_1)x^4 \right\} - \rho_1 g \right] dy \quad (57)$$

It can be demonstrated that  $dP$  in this equation is an exact differential, and integration can be performed accordingly:

$$P_1 \left[ (3b + 6cy_1 + 15dy_1^2 + 20ey_1^3 + 35fy_1^4)x^2 - \left( \frac{10}{4}d + 10ey_1 + 35fy_1^2 \right)x^4 + \frac{14}{6}fx^6 \right] + f(y) \quad (58)$$

$f(y)$  is an unknown function which may be found when eqn. (58) is differentiated with respect to  $y$  and the resulting derivative is equated with the partial derivative  $\partial P / \partial y$  in eqn. (57). Thus:

$$= \eta_1 (6c + 30dy_1 + 60ey_1^2 + 140fy_1^3)x^2 - (10e + 70fy_1)x^4 + \partial f(y) / \partial y \quad (59)$$

Equating with the term  $\partial P / \partial y$  in eqn. (57), i.e., the quantity in the parenthesis in eqn. (57), an expression for  $\partial f(y) / \partial y$  is accordingly obtained:

$$\partial f(y) / \partial y = \eta_1 (-2a - 6by_1 - 6cy_1^2 - 10dy_1^3 - 10ey_1^4 - 14fy_1^5) - \rho_1 g \quad (60)$$

Upon integration yields:

$$\eta_1 \left( -2ay_1 - 3by_1^2 - 2cy_1^3 - \frac{5}{2}dy_1^4 - 2ey_1^5 - \frac{7}{3}fy_1^6 \right) - \rho_1 gy_1 + c_1 \quad (61)$$

where  $c_1$  is a constant of integration.

Equation (61) can be introduced in eqn. (58) which in its turn goes into eqn. (53), and the normal stress parallel to  $y$  in layer 1 follows when:

$$= \frac{\partial^2 \psi}{\partial x \partial y}$$

and is inserted as derived from stream function  $\psi_1$ .

$$\sigma_{y1} - P_1 = \eta_1 \left( -2ay_1 - 3by_1^2 - 6cy_1^3 - \frac{15}{2}dy_1^4 - 10ey_1^5 - \frac{35}{3}fy_1^6 + (-3b + 6cy_1 + 15dy_1^2 + 60ey_1^3 + 105fy_1^4)x^2 + \left( \frac{5}{2}d - 10ey_1 - 35fy_1^2 \right)x^4 - \frac{7}{3}fx^6 \right) + \rho_1 gy_1 - c_1 \quad (62)$$

The corresponding procedure performed using stream function  $\psi_2$  produces an expression for the normal stress  $\sigma_2$  in the top layer:

$$\sigma_{y2} - P_1 = \eta_2 \left[ 2a_{22} + 2a_{23}y_2 - 6a_{41}y_2 + (3a_{24} - 3a_{42})y_2^2 + (6a_{25} + 10a_{62})y_2^3 + \left( \frac{15}{2}a_{26} + \frac{5}{2}a_{62} \right)y_2^4 + \left\{ 3a_{24} + 9a_{42} - (6a_{25} + 90a_{61})y_2 - (15a_{26} + 45a_{62})y_2^2 \right\} x^2 - \left( \frac{5}{2}a_{26} - \frac{25}{2}a_{62} \right)x^4 \right] + \rho g y_2 - c_2 \quad (63)$$

Here again  $c_2$  is a constant of integration. Incidentally, neither  $c_1$  nor  $c_2$  are needed for the determination of coefficients in the stream functions, but the values of  $c_1$  and  $c_2$  are necessary if we wish to know the magnitude of the normal stress in the two layers.

$\sigma_{y1}$  must equate with  $\sigma_{y2}$  at all  $x$  between  $-L$  and  $+L$  when  $y_1$  is put equal to  $H_1$  and  $y_2 = 0$  in eqns. (62) and (63). Performing this operation we immediately see that:

$$f = 0 \quad (64)$$

(because  $\frac{7}{3}fx^6$  is the only term containing  $f$ ). A consequence of this is:

$$e = a_{62} = a_{61} = 0 \quad (\text{see eqns. (50), (42) and (45)}) \quad (65)$$

Application of these results on the terms multiplied by  $x^4$  in eqns. (62) and (63) leads to:

$$a_{26} = -\eta_1 / \eta_2 d \equiv -md \quad (\text{here } m \equiv \eta_1 / \eta_2) \quad (66)$$

Equating the collection of terms multiplied by  $x^2$  in the two equations one obtains:

$$\eta_2 (3a_{24} + 9a_{42}) = \eta_1 (-3b + 6cH_1 + 15dH_1^2), \quad (67)$$

and the relation:

$$2\eta_2 a_{22} - c_2 = -\eta_1 (2aH_1 + 3bH_1^2 + 6cH_1^3 + \frac{15}{2}dH_1^4) - c_1 + \rho_1 g H_1 \quad (68)$$

which follows when the constant terms are collected and equated

Equation (67) with the expression for  $a_{42}$  introduced (eqn. 43) gives:

$$a_{24} = -mb + (2m - 6)cH_1 + (5m - 15)dH_1^2 \quad (69)$$

From eqns. (52), (45) and (65) follows:

$$a_{23} = -m \left[ a + 3bH_1 + (9 - 3m^{-1})cH_1^2 + (15 - 5m^{-1})dH_1^3 \right] \quad (70)$$

and from eqns. (51) and (65):

$$a_{25} = -m(c + 5dH_1) \quad (71)$$

Now all coefficients in stream function  $\psi_2$  are expressed as functions of the coefficients  $a$  to  $d$  in stream function  $\psi_1$ . The said relationships are:

$$a_{21} = -aH_1^2 - bH_1^3 - cH_1^4 - dH_1^5 \quad (72)$$

$$a_{22} = -2aH_1 - 3bH_1^2 - 4cH_1^3 - 5dH_1^4 \quad (73)$$

$$a_{23} = -m \left[ a + 3bH_1 + (9 - 3/m)cH_1^2 + (15 - 5/m)dH_1^3 \right] \quad (74)$$

$$a_{24} = -mb + (2m - 6)cH_1 + (5m - 15)dH_1^2 \quad (75)$$

$$a_{25} = -m(c + 5dH_1) \quad (76)$$

$$a_{26} = -md \quad (77)$$

$$a_{41} = cH_1^2 + \frac{5}{3}dH_1^3 \quad (78)$$

$$a_{42} = 2cH_1 + 5dH_1^2 \quad (79)$$

All other coefficients are zero.

In order to reduce the number of unknown coefficients further, we use the condition of vanishing shear stress parallel to the surface at  $y_2 = H_2$ . Equation (49) with  $f = e = a_{62} = a_{61} = 0$  and  $y_2 = H_2$  introduced takes the form:

$$\tau_{xy_2} = \eta_2 \left[ (-2a_{23} + 6a_{41} - 6(a_{24} - a_{42})H_2 - 18a_{25}H^2 - 30a_{26}H_2^3)x + (2a_{25} + 10a_{26}H_2)x^3 \right] = 0 \quad (80)$$

When in this equation  $a_{23}$ ,  $a_{24}$  etc. are transformed to  $a$ ,  $b$ ,  $c$ , and  $d$  by means of the formulas on p. 223, and the terms in the two parentheses in front of  $x^3$  and  $x$  are separately equated to zero,  $c$  and  $d$  follow as functions of  $a$  and  $b$ :

$$c = [a + (3 + 3/h)H_1b] / DH_1^2 = \frac{\alpha_1}{H_1^2}a + \frac{\beta_1}{H_1}b \quad (81)$$

and:

$$d = -[a + (3 + 3/h)H_1b] / [D(5 + 5/h)H_1^3] = \frac{\alpha_2}{H_1^3}a + \frac{\beta_2}{H_1^2}b \quad (82)$$

Here:

$$D = 6/h - 9 - 9/h^2 - 24/hm + (3 + 3/h^3 - 3/h + 9/h^2 + 12/hm)/(1 + 1/h),$$

$$h = H_1/H_2, \quad m = \eta_1/\eta_2; \quad \alpha_1 = 1/D; \quad \beta_1 = (3 + 3/h)/D;$$

$$\alpha_2 = -1/D(5 + 5/h); \quad \beta_2 = -(3 + 3/h)/D(5 + 5/h)$$

These formulas, combined with the expressions for  $a_{ij}$  as functions of  $a$ ,  $b$ ,  $c$ , and  $d$ , transform all coefficients in the stream functions and their derivatives to  $a$  and  $b$ . Hence we end up with only two unknown coefficients,  $a$  and  $b$ , and these will be determined by the method of energy extremization. To use this method, expressions for the strain-energy rate as well as the rate of change of potential energy are needed. Unfortunately the energies require quite lengthy expressions and these are given in full in Appendix A. Here only a brief summary of the procedure for determining the energies will be given.

The instantaneous rate of change of strain energy is obtained by integrating the "specific" strain energy rate (i.e., the energy rate per unit volume),

$$4\eta_i \dot{\epsilon}_x^2 = 4\eta_i \left( -\frac{\partial^2 \psi}{\partial y \partial x} \right)^2 \quad \text{and} \quad \eta_i \dot{\gamma}_{xy}^2 = \eta_i \left( \frac{\partial^2 \psi}{\partial x^2} - \frac{\partial^2 \psi}{\partial y^2} \right)^2$$

over a vertical slice of unit thickness parallel to the  $xy$  plane across the model, using  $\eta_1$  and  $\psi_1$  for the part of the slice which cuts layer 1 and  $\eta_2$  and  $\psi_2$  for the part which cuts layer 2. This leads to equations (A1) to (A4) in Appendix A. When in

these equations the coefficients,  $c$ ,  $d$ ,  $A_{22}$ ,  $A_{23}$  etc are transformed to  $a$  and the equations on p. 223, we find:

$$\dot{E}_{\epsilon\gamma_1} = \eta_1 (A_{\epsilon\gamma_1} H_2^4 a^2 + B_{\epsilon\gamma_1} H_2^6 b^2 + C_{\epsilon\gamma_1} H_2^5 ab)$$

and:

$$\dot{E}_{\epsilon\gamma_2} = \eta_2 (A_{\epsilon\gamma_2} H_2^4 a^2 + B_{\epsilon\gamma_2} H_2^6 b^2 + C_{\epsilon\gamma_2} H_2^5 ab)$$

for the instantaneous strain-energy rates referring to the portions of the slice through layer 1 and layer 2, respectively. Here the coefficients  $A_{\epsilon\gamma_i}$ ,  $C_{\epsilon\gamma_i}$ ,  $i = 1, 2$ , are quite involved functions of material and geometric properties of the two layers, much too lengthy to present in full here. The interested reader is referred to the computer program, Appendix B, in which the symbols correspond to  $A_{\epsilon\gamma_1}$ ,  $Estrb1$  to  $B_{\epsilon\gamma_1}$ ,  $Estrab1$  to  $C_{\epsilon\gamma_1}$ ,  $Estra2$  to  $A_{\epsilon\gamma_2}$ ,  $Estrl$  and finally  $Estrab2$  corresponds to  $C_{\epsilon\gamma_2}$ . Note that  $H_2$  is also used in the equations for layer 1; here the transformation  $H_1 \rightarrow H_2$  is "hidden" in the coefficients  $B_{\epsilon\gamma_1}$  and  $C_{\epsilon\gamma_1}$ .

The rate of change of potential energy for the slice across the model is obtained by integrating the "specific" potential energy rate,  $\rho_i g v_i$  over the cross-cut using  $\rho_1$  and  $v_1$  for the part which cuts layer 1 and  $\rho_2$  and  $v_2$  for the part through layer 2; see eqns. (A5) and (A6) in Appendix A and see also p. 223. Transforming  $c$ ,  $d$ ,  $a_{22}$ ,  $a_{23}$  etc to  $a$  and  $b$  by use of the equations on p. 223, the instantaneous potential energy rate is expressed as follows:

$$\dot{E}_{pot_1} = \rho_1 g (A_{p_1} H_2^4 a + B_{p_1} H_2^5 b)$$

$$\dot{E}_{pot_2} = \rho_2 g (A_{p_2} H_2^4 a + B_{p_2} H_2^5 b)$$

Here the transformation  $H_1 \rightarrow H_2$  in eqn. (85) is concealed in the coefficients  $A_{p_i}$  and  $B_{p_i}$ ,  $i = 1, 2$ . The somewhat involved terms of the coefficients  $A_{p_i}$  and  $B_{p_i}$ ,  $i = 1, 2$  found in the computer program, Appendix B, where  $Epotal$ ,  $Epotbl$ ,  $Epot2a$ ,  $Epot2b$  correspond to  $A_{p_1}$ ,  $B_{p_1}$ ,  $A_{p_2}$  and  $B_{p_2}$ , respectively.

A condition to consider when using the rate of energy change for determining the coefficients is that the only energy available for deforming and moving the model is gravitational energy. Hence the theorem of conservation of energy requires that the rate of decline of potential energy equals the rate of dissipation of energy by viscous resistance, and the Gaussian principle of least constraint requires that the rate of decline of potential energy shall assume maximal value under the boundary conditions. Since potential energy change equals energy dissipation by viscous strain we may also say that the rate of dissipation of energy by viscous resistance shall assume maximal value.

The problem is accordingly to maximize the potential energy rate as a function of the unknown coefficients  $a$  and  $b$ , and/or to maximize the strain energy rate as a function of  $a$  and  $b$ .

use of vanishing shear strain at top face and energy extremization

order to reduce the number of unknown coefficients further, we use the condition of vanishing shear stress parallel to the surface at  $y_2 = H_2$ . Equation (49)  $f = e = a_{62} = a_{61} = 0$  and  $y_2 = H_2$  introduced takes the form:

$$= \eta_2 \left[ (-2a_{23} + 6a_{41} - 6(a_{24} - a_{42})H_2 - 18a_{25}H^2 - 30a_{26}H_2^3)x + (2a_{25} + 10a_{26}H_2)x^3 \right] = 0 \quad (80)$$

in this equation  $a_{23}$ ,  $a_{24}$  etc. are transformed to  $a$ ,  $b$ ,  $c$ , and  $d$  by means of formulas on p. 223, and the terms in the two parentheses in front of  $x^3$  and  $x$  separately equated to zero,  $c$  and  $d$  follow as functions of  $a$  and  $b$ :

$$+ (3 + 3/h)H_1b] / DH_1^2 = \frac{\alpha_1}{H_1^2}a + \frac{\beta_1}{H_1}b \quad (81)$$

$$[a + (3 + 3/h)H_1b] / [D(5 + 5/h)H_1^3] = \frac{\alpha_2}{H_1^3}a + \frac{\beta_2}{H_1^2}b \quad (82)$$

$$h - 9 - 9/h^2 - 24/hm + (3 + 3/h^3 - 3/h + 9/h^2 + 12/hm)/(1 + 1/h),$$

$$/H_2, \quad m = \eta_1/\eta_2; \quad \alpha_1 = 1/D; \quad \beta_1 = (3 + 3/h)/D;$$

$$1/D(5 + 5/h); \quad \beta_2 = -(3 + 3/h)/D(5 + 5/h)$$

formulas, combined with the expressions for  $a_{ij}$  as functions of  $a$ ,  $b$ ,  $c$ , and  $d$ , form all coefficients in the stream functions and their derivatives to  $a$  and  $b$ . We end up with only two unknown coefficients,  $a$  and  $b$ , and these will be determined by the method of energy extremization. To use this method, expressions for the strain-energy rate as well as the rate of change of potential energy are required. Unfortunately the expressions require quite lengthy expressions and these are given in full in Appendix A. Here only a brief summary of the procedure for determining the energies will be given.

The instantaneous rate of change of strain energy is obtained by integrating the "strain energy rate (i.e., the energy rate per unit volume),

$$\eta_i \left( -\frac{\partial^2 \psi}{\partial y \partial x} \right)^2 \quad \text{and} \quad \eta_i \dot{\gamma}_{x,y}^2 = \eta_i \left( \frac{\partial^2 \psi}{\partial x^2} - \frac{\partial^2 \psi}{\partial y^2} \right)^2$$

for a vertical slice of unit thickness parallel to the  $xy$  plane across the model, using  $\eta_1$  and  $\psi_1$  for the part of the slice which cuts layer 1 and  $\eta_2$  and  $\psi_2$  for the part which cuts layer 2. This leads to equations (A1) to (A4) in Appendix A. When in

these equations the coefficients,  $c$ ,  $d$ ,  $A_{22}$ ,  $A_{23}$  etc are transformed to  $a$  and  $b$ , using the equations on p. 223, we find:

$$\dot{E}_{\epsilon\gamma 1} = \eta_1 (A_{\epsilon\gamma 1} H_2^4 a^2 + B_{\epsilon\gamma 1} H_2^6 b^2 + C_{\epsilon\gamma 1} H_2^5 ab) \quad (83)$$

and:

$$\dot{E}_{\epsilon\gamma 2} = \eta_2 (A_{\epsilon\gamma 2} H_2^4 a^2 + B_{\epsilon\gamma 2} H_2^6 b^2 + C_{\epsilon\gamma 2} H_2^5 ab) \quad (84)$$

for the instantaneous strain-energy rates referring to the portions of the slice which cut through layer 1 and layer 2, respectively. Here the coefficients  $A_{\epsilon\gamma}$ ,  $B_{\epsilon\gamma}$  and  $C_{\epsilon\gamma}$ ,  $i = 1, 2$ , are quite involved functions of material and geometric properties of the two layers, much too lengthy to present in full here. The interested reader is referred to the computer program, Appendix B, in which the symbol *Estral* corresponds to  $A_{\epsilon\gamma 1}$ , *Estrbl* to  $B_{\epsilon\gamma 1}$ , *Estrabl* to  $C_{\epsilon\gamma 1}$ , *Estra2* to  $A_{\epsilon\gamma 2}$ , *Estrb2* to  $B_{\epsilon\gamma 2}$  and finally *Estrab2* corresponds to  $C_{\epsilon\gamma 2}$ . Note that  $H_2$  is also used in the equation for layer 1; here the transformation  $H_1 \rightarrow H_2$  is "hidden" in the coefficients  $A_{\epsilon\gamma 1}$ ,  $B_{\epsilon\gamma 1}$  and  $C_{\epsilon\gamma 1}$ .

The rate of change of potential energy for the slice across the model is found by integrating the "specific" potential energy rate,  $\rho_i g v_i$  over the cross-cutting slice, using  $\rho_1$  and  $v_1$  for the part which cuts layer 1 and  $\rho_2$  and  $v_2$  for the part cutting through layer 2; see eqns. (A5) and (A6) in Appendix A and see also p. 239. After transforming  $c$ ,  $d$ ,  $a_{22}$ ,  $a_{23}$  etc to  $a$  and  $b$  by use of the equations on p. 223, the instantaneous potential energy rate is expressed as follows:

$$\dot{E}_{\text{pot} 1} = \rho_1 g (A_{p_1} H_2^4 a + B_{p_1} H_2^5 b) \quad (85)$$

$$\dot{E}_{\text{pot} 2} = \rho_2 g (A_{p_2} H_2^4 a + B_{p_2} H_2^5 b) \quad (86)$$

Here the transformation  $H_1 \rightarrow H_2$  in eqn. (85) is concealed in the coefficients  $A_{p_1}$  and  $B_{p_1}$ . The somewhat involved terms of the coefficients  $A_{p_i}$  and  $B_{p_i}$ ,  $i = 1, 2$ , are found in the computer program, Appendix B, where *Epotal*, *Epotbl*, *Epota2* and *Epotb2* correspond to  $A_{p_1}$ ,  $B_{p_1}$ ,  $A_{p_2}$  and  $B_{p_2}$ , respectively.

A condition to consider when using the rate of energy change for determining coefficients is that the only energy available for deforming and moving the present model is gravitational energy. Hence the theorem of conservation of energy requires that the rate of decline of potential energy equals the rate of dissipation due to viscous resistance, and the Gaussian principle of least constraint requires that the rate of decline of potential energy shall assume maximal value under the prevailing boundary conditions. Since potential energy change equals energy dissipation due to strain we may also say that the rate of dissipation of energy by viscous strain will assume maximal value.

The problem is accordingly to maximize the potential energy rate treated as a function of the unknown coefficients  $a$  and  $b$ , and/or to maximize the strain energy

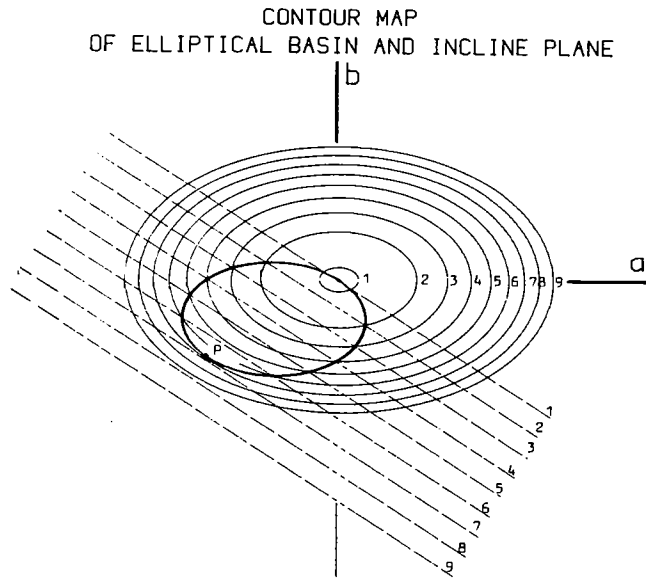


Fig. 3. Contours representing energy increasing from arbitrary values 1 to 9. Solid closed curve passing through origin and the point  $P$  marks the intersection between the basin and the plane,  $P$  coinciding with maximum energy on the intersection curve. The coordinates for the point  $P$  are the sought values for the coefficients  $a$  and  $b$ . Example showing general principle.

rate also treated as a function of  $a$  and  $b$  subject to the side-condition that  $\dot{E}_{\text{pot}} = \dot{E}_{\epsilon\gamma}$ . The situation may be visualized (Fig. 3) when one realizes that  $\dot{E}_{\epsilon\gamma} = \dot{E}_{\epsilon\gamma_1} + \dot{E}_{\epsilon\gamma_2}$  describes a quadric surface in the space defined by the axes  $\dot{E}_{\epsilon\gamma}$ ,  $a$  and  $b$ ; and  $\dot{E}_{\text{pot}} = \dot{E}_{\text{pot}_1} + \dot{E}_{\text{pot}_2}$  describes a plane in the same space, the axes for  $\dot{E}_{\epsilon\gamma}$  and  $\dot{E}_{\text{pot}}$  coinciding. Assuming that the  $\dot{E}_{\epsilon\gamma}$ - or  $\dot{E}_{\text{pot}}$  axis is vertical and the  $a$ - and  $b$  axes are horizontal one finds that  $\dot{E}_{\epsilon\gamma} = f_{\epsilon\gamma}(a, b)$  defines a basin whose lowest point coincides with the origin of the coordinate system, and whose elliptical horizontal cross-section area increases with height on the  $\dot{E}$ -axis. The plane  $\dot{E}_{\text{pot}} = f_{\text{pot}}(a, b)$  is generally inclined to the axes and contains the origin. The side condition  $\dot{E}_{\epsilon\gamma} + \dot{E}_{\text{pot}} = 0$  defines the intersection curve between the two surfaces. It is the maximal  $\dot{E}$ -value on this intersection we seek, and especially the  $a$ - and  $b$  values which correspond to maximum energy rate. As demonstrated in Fig. 3 the extreme values coincide with the condition  $(\partial a / \partial b)_{\epsilon\gamma} = (\partial a / \partial b)_{\text{pot}}$ . Here subscripts  $\epsilon\gamma$  and  $\text{pot}$  refer to the partial derivative  $\partial a / \partial b$  of the strain energy function and of the potential energy function, respectively.

It is easy to see that one extremum—the minimum—coincides with  $\dot{E} = 0$ ,  $a = b = 0$ , but the maximum depends upon the inclination of the plane  $\dot{E}_{\text{pot}} = f_{\text{pot}}(a, b)$  with respect to the  $\dot{E}$ -axis, and upon the exact shape of the surface  $\dot{E}_{\epsilon\gamma} = f_{\epsilon\gamma}(a, b)$ .

It is convenient to put the energy equations:

$$\dot{E}_{\epsilon\gamma} = \dot{E}_{\epsilon\gamma_1} + \dot{E}_{\epsilon\gamma_2} = \eta_2 \left[ (\eta_{1:2} A_{\epsilon\gamma_1} + A_{\epsilon\gamma_2}) a^2 H_2^4 + (\eta_{1:2} B_{\epsilon\gamma_1} + B_{\epsilon\gamma_2}) b^2 H_2^6 + (\eta_{1:2} C_{\epsilon\gamma_1} + C_{\epsilon\gamma_2}) ab H_2^5 \right]$$

and:

$$\dot{E}_{\text{pot}} = \dot{E}_{\text{pot}_1} + \dot{E}_{\text{pot}_2} = \rho_2 g \left[ (\rho_{1:2} A_{\text{pot}_1} + A_{\text{pot}_2}) a H_2^4 + (\rho_{1:2} B_{\text{pot}_1} + B_{\text{pot}_2}) b H_2^5 \right]$$

in the simpler identical forms below:

$$\dot{E}_{\epsilon\gamma} = \eta_2 (A_{\epsilon\gamma} a^2 H_2^4 + B_{\epsilon\gamma} b^2 H_2^6 + C_{\epsilon\gamma} ab H_2^5)$$

and:

$$\dot{E}_{\text{pot}} = \rho_2 g (A_{\text{pot}a} H_2^4 + B_{\text{pot}b} H_2^5)$$

Here the new coefficients  $A_{\epsilon\gamma}$ ,  $B_{\epsilon\gamma}$ ,  $C_{\epsilon\gamma}$ ,  $A_{\text{pot}}$  and  $B_{\text{pot}}$  follow from the id eqns. (87) and (89) and of eqns. (88) and (90), respectively.

By implicit differentiation we find:

$$\left. \frac{\partial a}{\partial b} \right]_{\epsilon\gamma} = - \frac{2B_{\epsilon\gamma} b H_2^2 + C_{\epsilon\gamma} a H_2}{2A_{\epsilon\gamma} a + C_{\epsilon\gamma} b H_2}$$

$$\left. \frac{\partial a}{\partial b} \right]_{\text{pot}} = - \frac{B_{\text{pot}} H_2}{A_{\text{pot}}}$$

When  $\left. \frac{\partial a}{\partial b} \right]_{\epsilon\gamma}$  is put equal to  $\left. \frac{\partial a}{\partial b} \right]_{\text{pot}}$ ,  $a$  and  $b$  become related:

$$b = \frac{2A_{\epsilon\gamma} \frac{B_{\text{pot}}}{A_{\text{pot}}} - C_{\epsilon\gamma}}{2B_{\epsilon\gamma} H_2 - \frac{B_{\text{pot}}}{A_{\text{pot}}} C_{\epsilon\gamma} H_2} a \equiv \pi a$$

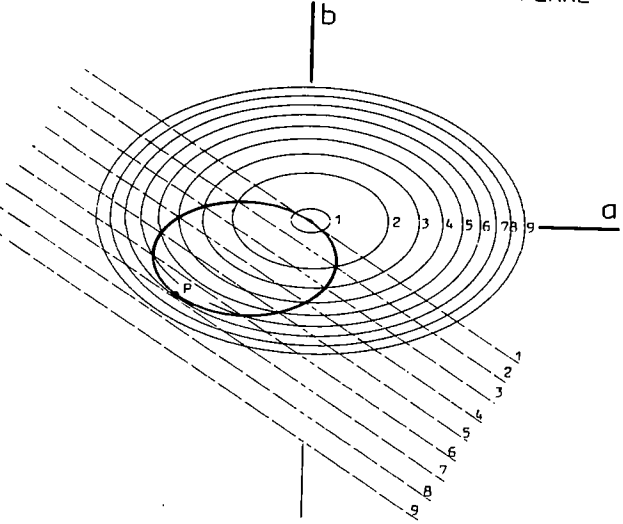
The use of this relationship in connection with the condition  $\dot{E}_{\epsilon\gamma} + \dot{E}_{\text{pot}} = 0$  two values of  $a$ , namely  $a = 0$  and:

$$a = - \frac{\rho_2 g (A_{\text{pot}} + B_{\text{pot}} \pi H_2)}{\eta_2 (A_{\epsilon\gamma} + B_{\epsilon\gamma} \pi^2 H_2^2 + C_{\epsilon\gamma} \pi H_2)}$$

The corresponding values of  $b$  follow when  $a$  is introduced in eqn. (93) used as a symbol for the fraction in front of  $a$ , not as a symbol for 3.14

Now all coefficients in the two stream functions (34) and (35) for the known functions of material and geometric parameters of the two la model. The pertinent material parameters are viscosities and density relevant geometric parameters are thicknesses and aspect ratios. This me

CONTOUR MAP  
OF ELLIPTICAL BASIN AND INCLINE PLANE



3. Contours representing energy increasing from arbitrary values 1 to 9. Solid closed curve passing through origin and the point P marks the intersection between the basin and the plane. P coinciding with maximum energy on the intersection curve. The coordinates for the point P are the sought values in coefficients a and b. Example showing general principle.

also treated as a function of a and b subject to the side-condition that  $\dot{E}_{\epsilon\gamma} = \dot{E}_{\epsilon\gamma_1}$ . The situation may be visualized (Fig. 3) when one realizes that  $\dot{E}_{\epsilon\gamma_1}$  describes a quadric surface in the space defined by the axes  $\dot{E}_{\epsilon\gamma}$ , a and b;  $\dot{E}_{\text{pot}} = \dot{E}_{\text{pot}_1} + \dot{E}_{\text{pot}_2}$  describes a plane in the same space, the axes for  $\dot{E}_{\epsilon\gamma}$  and  $\dot{E}_{\text{pot}}$  coinciding. Assuming that the  $\dot{E}_{\epsilon\gamma}$ - or  $\dot{E}_{\text{pot}}$  axis is vertical and the a- and b axes horizontal one finds that  $\dot{E}_{\epsilon\gamma} = f_{\epsilon\gamma}(a, b)$  defines a basin whose lowest point coincides with the origin of the coordinate system, and whose elliptical horizontal cross-section area increases with height on the  $\dot{E}$ -axis. The plane  $\dot{E}_{\text{pot}} = f_{\text{pot}}(a, b)$  is equally inclined to the axes and contains the origin. The side condition  $\dot{E}_{\epsilon\gamma} + \dot{E}_{\text{pot}}$  defines the intersection curve between the two surfaces. It is the maximal energy rate on this intersection we seek, and especially the a- and b values which correspond to maximum energy rate. As demonstrated in Fig. 3 the extreme values of a and b depend with the condition  $(\partial a / \partial b)_{\epsilon\gamma} = (\partial a / \partial b)_{\text{pot}}$ . Here subscripts  $\epsilon\gamma$  and pot refer to the partial derivative  $\partial a / \partial b$  of the strain energy function and of the potential energy function, respectively. It is easy to see that one extremum—the minimum—coincides with  $\dot{E} = 0$ , but the maximum depends upon the inclination of the plane  $\dot{E}_{\text{pot}} = f_{\text{pot}}(a, b)$  with respect to the  $\dot{E}$ -axis, and upon the exact shape of the surface  $\dot{E}_{\epsilon\gamma}(a, b)$ .

It is convenient to put the energy equations:

$$\dot{E}_{\epsilon\gamma} = \dot{E}_{\epsilon\gamma_1} + \dot{E}_{\epsilon\gamma_2} = \eta_2 \left[ (\eta_{1:2} A_{\epsilon\gamma_1} + A_{\epsilon\gamma_2}) a^2 H_2^4 + (\eta_{1:2} B_{\epsilon\gamma_1} + B_{\epsilon\gamma_2}) b^2 H_2^6 + (\eta_{1:2} C_{\epsilon\gamma_1} + C_{\epsilon\gamma_2}) ab H_2^5 \right] \quad (87)$$

and:

$$\dot{E}_{\text{pot}} = \dot{E}_{\text{pot}_1} + \dot{E}_{\text{pot}_2} = \rho_2 g \left[ (\rho_{1:2} A_{\text{pot}_1} + A_{\text{pot}_2}) a H_2^4 + (\rho_{1:2} B_{\text{pot}_1} + B_{\text{pot}_2}) b H_2^5 \right] \quad (88)$$

in the simpler identical forms below:

$$\dot{E}_{\epsilon\gamma} = \eta_2 (A_{\epsilon\gamma} a^2 H_2^4 + B_{\epsilon\gamma} b^2 H_2^6 + C_{\epsilon\gamma} ab H_2^5) \quad (89)$$

and:

$$\dot{E}_{\text{pot}} = \rho_2 g (A_{\text{pot}} a H_2^4 + B_{\text{pot}} b H_2^5) \quad (90)$$

Here the new coefficients  $A_{\epsilon\gamma}$ ,  $B_{\epsilon\gamma}$ ,  $C_{\epsilon\gamma}$ ,  $A_{\text{pot}}$  and  $B_{\text{pot}}$  follow from the identity of eqns. (87) and (89) and of eqns. (88) and (90), respectively.

By implicit differentiation we find:

$$\left. \frac{\partial a}{\partial b} \right]_{\epsilon\gamma} = - \frac{2 B_{\epsilon\gamma} b H_2^2 + C_{\epsilon\gamma} a H_2}{2 A_{\epsilon\gamma} a + C_{\epsilon\gamma} b H_2} \quad (91)$$

$$\left. \frac{\partial a}{\partial b} \right]_{\text{pot}} = - \frac{B_{\text{pot}} H_2}{A_{\text{pot}}} \quad (92)$$

When  $\left. \frac{\partial a}{\partial b} \right]_{\epsilon\gamma}$  is put equal to  $\left. \frac{\partial a}{\partial b} \right]_{\text{pot}}$ , a and b become related:

$$b = \frac{2 A_{\epsilon\gamma} \frac{B_{\text{pot}}}{A_{\text{pot}}} - C_{\epsilon\gamma}}{2 B_{\epsilon\gamma} H_2 - \frac{B_{\text{pot}}}{A_{\text{pot}}} C_{\epsilon\gamma} H_2} a \equiv \pi a \quad (93)$$

The use of this relationship in connection with the condition  $\dot{E}_{\epsilon\gamma} + \dot{E}_{\text{pot}} = 0$  leads to two values of a, namely  $a = 0$  and:

$$a = - \frac{\rho_2 g (A_{\text{pot}} + B_{\text{pot}} \pi H_2)}{\eta_2 (A_{\epsilon\gamma} + B_{\epsilon\gamma} \pi^2 H_2^2 + C_{\epsilon\gamma} \pi H_2)} \quad (94)$$

The corresponding values of b follow when a is introduced in eqn. (93). ( $\pi$  is here used as a symbol for the fraction in front of a, not as a symbol for 3.14.)

Now all coefficients in the two stream functions (34) and (35) for the model are known functions of material and geometric parameters of the two layers in the model. The pertinent material parameters are viscosities and densities and the relevant geometric parameters are thicknesses and aspect ratios. This means that the

TABLE 1

Velocity  $u$  in cm/year at different levels at the right hand vertical boundary of model.  $R = 0.5$ ,  $\eta_2 = \eta_1 = 10^{22}$  P,  $\rho = 2.8$  g/cm<sup>3</sup>,  $H = 5000$  m,  $N$  is height in parts of  $H$  (see Figs. 4B, 5 and 6A)

$u_2$	$N$	$u_2$	$N$
-0.0353177800	1	0.1516899015	0.4
0.0186560141	0.9	0.1426623379	0.3
0.0645197947	0.8	0.1174261573	0.2
0.1017673992	0.7	0.0734505460	0.1
0.1295552230	0.6	0.0078672487	0
0.1467022198	0.5		

instantaneous velocity field and stress field of the model are known through eqns. (36) to (39) and eqns. (48), (49), (62) and (63) when the relevant viscosities, densities, thicknesses and aspect ratios are put in the coefficients. The instantaneous rate of decline of potential energy as well as the rate of dissipation also follow automatically via eqns. (A2) to (A6), Appendix A.

$H_2=5000M, H_1=50M, R_2=0.5, Mu=10^{22}, Ro_1=Ro_2=2.8$

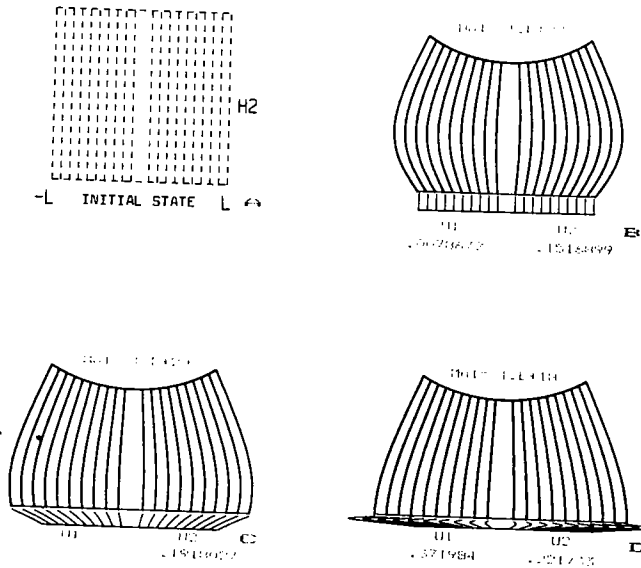


Fig. 4. Deformation of double-layer model with aspect ratio  $R_2 = 0.5$  for layer 2. In B, C and D height of layer 1 is exaggerated 10-fold to show the deformation of initially straight vertical markers. As the computer does not print Greek symbols the viscosity has been given the symbol  $Mu$  and density  $Ro$ , viscosity has been given in poises (P) and density in g/cm<sup>3</sup>. Velocities in cm/yr refer to maximal values at the right-hand initially vertical face. See also Table 1.

$H=5000M, R=0.5, Mu=10^{22}, Ro_1=2.8$

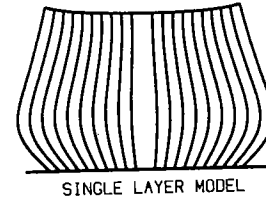
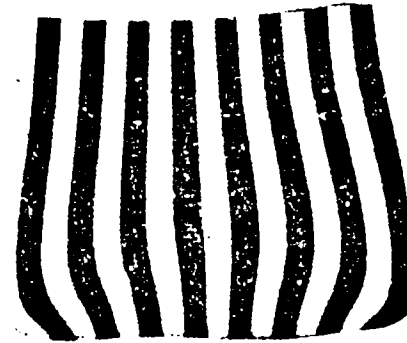


Fig. 5. Deformation of single-layer model after creep with unchanged initial velocity during 5·10<sup>10</sup> years. Compare experiment, Fig. 6A. Based on stream function (34) but with 2 orders higher degree.

(A)



(B)

(a)



Fig. 6. A. Spreading under own weight of rectangular parallelepiped of viscous silicone putty. Coherence at base. Early stage of deformation shown. Note similarity between early stage stream-function simulation, Fig. 5. B. Spreading under own weight of rectangular parallelepiped silicone putty.  $R = 0.5$ . Free slip at base (silicone body floating on mercury). Note similarity with Fig. 5.



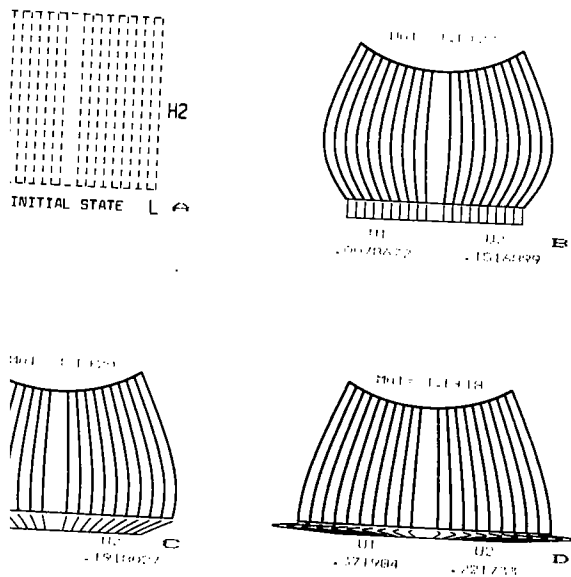
TABLE 1

velocity  $u$  in cm/year at different levels at the right hand vertical boundary of model.  $R = 0.5$ ,  $\eta_1 = 10^{22}$  P,  $\rho = 2.8$  g/cm<sup>3</sup>,  $H = 5000$  m,  $N$  is height in parts of  $H$  (see Figs. 4B, 5 and 6A)

	$N$	$u_2$	$N$
0353177800	1	0.1516899015	0.4
86560141	0.9	0.1426623379	0.3
45197947	0.8	0.1174261573	0.2
17673992	0.7	0.0734505460	0.1
95552230	0.6	0.0078672487	0
67022198	0.5		

Instantaneous velocity field and stress field of the model are known through eqns. (39) and eqns. (48), (49), (62) and (63) when the relevant viscosities, densities, thicknesses and aspect ratios are put in the coefficients. The instantaneous rate of change of potential energy as well as the rate of dissipation also follow automatically via eqns. (A2) to (A6), Appendix A.

$H_2=5000M, H_1=50M, R_2=0.5, \mu_1=10^{22}, \rho_1=\rho_2=2.8$



Deformation of double-layer model with aspect ratio  $R_2 = 0.5$  for layer 2. In B, C and D height of  $H_2$  is exaggerated 10-fold to show the deformation of initially straight vertical faces. As the velocity does not print Greek symbols the viscosity has been given the symbol  $\mu$  and density  $\rho$ , has been given in poises (P) and density in g/cm<sup>3</sup>. Velocities in cm/yr refer to maximal values at right-hand initially vertical face. See also Table 1.

$H=5000M, R=0.5, \mu_1=10^{22}, \rho_1=2.8$

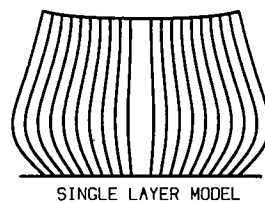


Fig. 5. Deformation of single-layer model after creep with unchanged initial velocity during  $5 \cdot 10^5$  years. Compare experiment, Fig. 6A. Based on stream function (34) but with 2 orders higher degree,  $x^7, y^9$ .

(A)



(B)

(a)

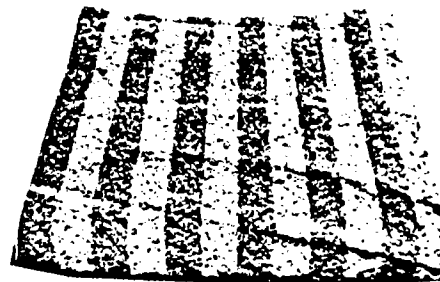


Fig. 6. A. Spreading under own weight of rectangular parallelepiped of viscous silicone putty  $R = 0.5$ . Coherence at base. Early stage of deformation shown. Note similarity between early stage (A) and stream-function simulation, Fig. 5. B. Spreading under own weight of rectangular parallelepiped of viscous silicone putty.  $R = 0.5$ . Free slip at base (silicone body floating on mercury). Note similarity with Fig. 4D.

## Numerical results of the simulation

As numerical examples of the simulation of spreading double layer nappes the following series of models, consisting of a 50 m thick basal sheet (layer 1) overlain by a 5000 m thick layer 2 are treated. The density of both layers is kept at  $2.8 \text{ g/cm}^3$  and the viscosity of layer 2 is kept at  $10^{22}$  poise ( $10^{21}$  Pa s), while the viscosity of layer 1 varies from model to model. The instantaneous velocity field of models with

$H_2=5000\text{M}, H_1=50\text{M}, R_2=2, \mu_2=10^{22}, \rho_1=\rho_2=2.8,$   
 $U_{\text{free}}=.5322, V_{\text{free}}=-.2661$

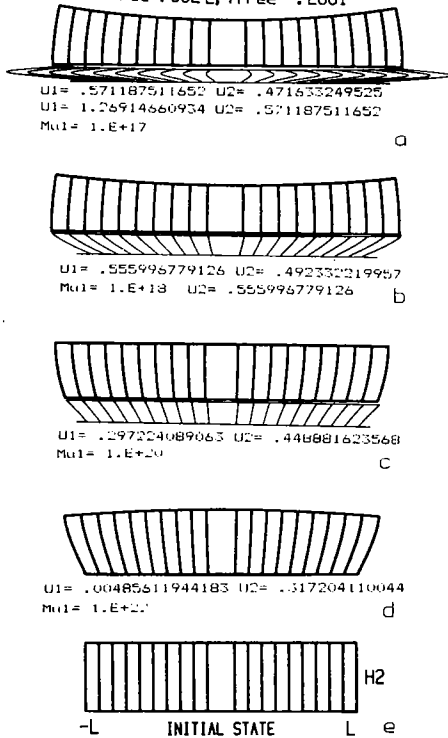


Fig. 7. Deformation after  $5 \cdot 10^5$  years of creep of double-layer model with  $R_2 = 2$  assuming constant initial velocity. Height of layer 1 in *a*, *b* and *c* is 50-fold exaggerated to show deformation of initially straight vertical markers. For explanation of symbols see Figs. 4 and 5; in addition:  $10^{22} \equiv 10^{22}$ ,  $U_{\text{free}}$  and  $V_{\text{free}}$  are velocity components at the corners  $y = H_2$ ,  $x = \pm L$  if there was free slip at the base. When two values for  $u_1$  and/or  $u_2$  are given, one refers to the velocity at the layer contact at the front face, the other  $u_2$  refers to the edge at  $X = L$ ,  $Y = H_2$ , while the other  $u_1$  refers to the middle level of layer 1. Note the change of deformed shape as a function of the viscosity of layer 1. With high viscosity of the basal layer  $u_2$  has maximum value at the top of layer 2, and  $v_2$  varies so as to generate a convex top boundary. Low  $\mu_{u1}$  gives maximal  $u_2$  at the base of layer 2 and maximal  $u_1$  in the middle of layer 1. Because of horizontal tensile strain in layer 2 the top surface assumes a concave shape. For discussion of these effects of an especially mobile basal layer see text pp. 38, 39. All velocities in cm/yr.

$H_2=5000\text{M}, H_1=50\text{M}, R_2=10, \mu_2=10^{22}, \rho_1=\rho_2=2.8, U_{\text{free}}=2.661, V_{\text{free}}=-.2661$

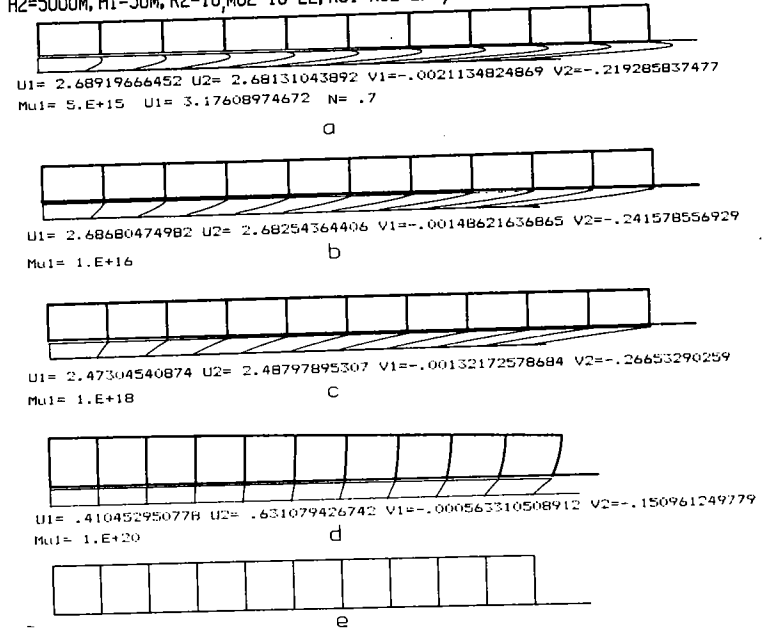


Fig. 8. Deformation after  $5 \cdot 10^5$  years of creep assuming unchanged initial velocity of double layer aspect ratio  $R_2 = 10$ . Only right-hand half of model shown. Height of layer 1 exaggerated ten fold. *b*, *c* and *d*. *e* is initial state. For explanation of symbols and definition of units, see Figs. 4 and 5; that the strained profiles of the model show similarities but also significant differences when compared with the shorter double layer in Fig. 7. The similarity is manifested by the increase of  $u_2$  with height at the front face (*d*), by the convex (though weak) top surface at low viscosity  $\mu_{u1}$  (*d*) and by excess of horizontal tensile strain in the back (middle) part of layer 2 (*a*). The difference is shown in the lack of variation of  $u_2$  with height at the front face of layer 2 when  $\mu_{u1}$  is small, and by the convex shape of the top surface in this model a lower viscosity  $\mu_{u1}$  is needed to produce "extrusion flow" in layer 1, i.e., the velocity here being maximum at intermediate levels.

selected aspect ratios ( $R_i = L/H_i$ ) and selected viscosity ratios ( $Rm = \eta_1/\eta_2$ ) computed. The deformed shape of the initially rectangular cross section of model shown, assuming that the initial instantaneous velocity was constant in the corner, over an initial period of 500,000 years.

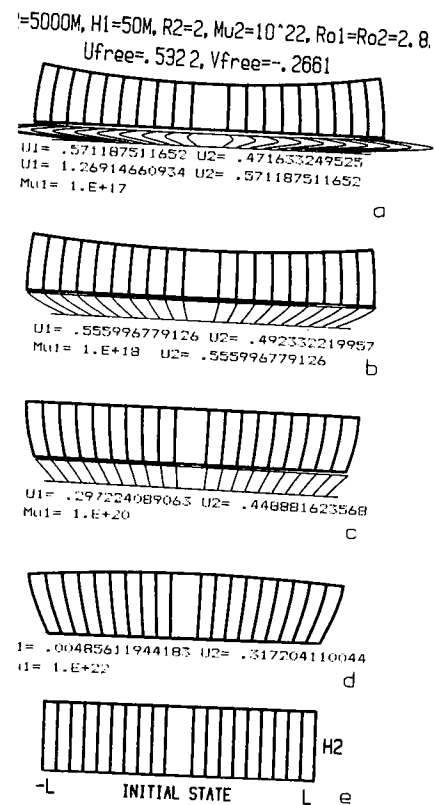
All pertinent results are shown in Figs. 4–15 and explained in the figure text. The instantaneous velocity at the front end of the models perhaps being the most interesting result.

### Extension of results by using simple scale-model rules

It is a consequence of scaling theory that the velocity field for models of different thicknesses, viscosities and densities different from those computed may be

## Numerical results of the simulation

As numerical examples of the simulation of spreading double layer nappes the following series of models, consisting of a 50 m thick basal sheet (layer 1) overlain by a 5000 m thick layer 2 are treated. The density of both layers is kept at  $2.8 \text{ g/cm}^3$  and the viscosity of layer 2 is kept at  $10^{22}$  poise ( $10^{21} \text{ Pa s}$ ), while the viscosity of layer 1 varies from model to model. The instantaneous velocity field of models with



Deformation after  $5 \cdot 10^5$  years of creep of double-layer model with  $R_2 = 2$  assuming constant velocity. Height of layer 1 in *a*, *b* and *c* is 50-fold exaggerated to show deformation of initially vertical markers. For explanation of symbols see Figs. 4 and 5; in addition:  $10^{22} \approx 10^{22}$ ,  $U_{\text{free}}$  are velocity components at the corners  $y = H_2$ ,  $x = \pm L$  if there was free slip at the base. No values for  $u_1$  and/or  $u_2$  are given, one refers so the velocity at the layer contact at the front; other  $u_2$  refers to the edge at  $X = L$ ,  $Y = H_2$ , while the other  $u_1$  refers to the middle level of layer 1. Note the change of deformed shape as a function of the viscosity of layer 1. With high viscosity basal layer  $u_2$  has maximum value at the top of layer 2, and  $v_2$  varies so as to generate a convex top surface. Low  $\mu_1$  gives maximal  $u_2$  at the base of layer 2 and maximal  $u_1$  in the middle of layer 2. Note the effects of horizontal tensile strain in layer 2 the top surface assumes a concave shape. For discussion of effects of an especially mobile basal layer see text pp. 38, 39. All velocities in cm/yr.

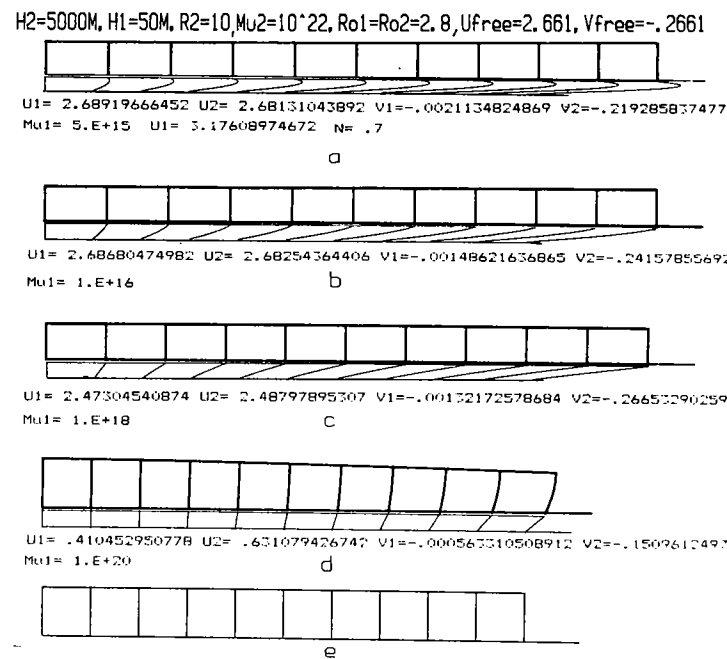


Fig. 8. Deformation after  $5 \cdot 10^5$  years of creep assuming unchanged initial velocity of double layer with aspect ratio  $R_2 = 10$ . Only right-hand half of model shown. Height of layer 1 exaggerated ten fold in *a*, *b*, *c* and *d*. *e* is initial state. For explanation of symbols and definition of units, see Figs. 4 and 7. Note that the strained profiles of the model show similarities but also significant differences when compared with the shorter double layer in Fig. 7. The similarity is manifested by the increase of  $u_2$  with height at the front face (*d*), by the convex (though weak) top surface at low viscosity  $\mu_1$  (*d*) and by a weak excess of horizontal tensile strain in the back (middle) part of layer 2 (*a*). The difference is shown by the lack of variation of  $u_2$  with height at the front face of layer 2 when  $\mu_1$  is small, and by the condition that in this model a lower viscosity  $\mu_1$  is needed to produce "extrusion flow" in layer 1, i.e., by the velocity here being maximum at intermediate levels.

selected aspect ratios ( $R_i = L/H_i$ ) and selected viscosity ratios ( $R_m = \eta_1/\eta_2$ ) are computed. The deformed shape of the initially rectangular cross section of models is shown, assuming that the initial instantaneous velocity was constant in the course of an initial period of 500,000 years.

All pertinent results are shown in Figs. 4–15 and explained in the figure texts, the instantaneous velocity at the front end of the models perhaps being the most interesting result.

### Extension of results by using simple scale-model rules

It is a consequence of scaling theory that the velocity field for models with thicknesses, viscosities and densities different from those computed may be esti-

R2=100, H2=5000M, H1=50M, Mu2=10<sup>22</sup>, Ro1=Ro2=2.8, Ufree=26.609625, Vfree=-.2660925

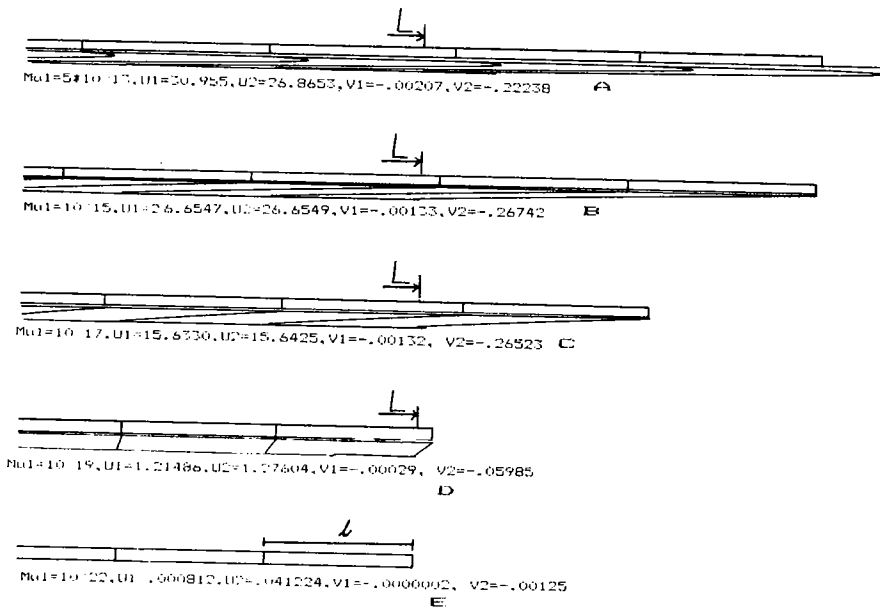


Fig. 9. Front part of spreading double-layer nappe with varying viscosity  $Mu1$ , showing initial velocity in cm/yr and displacement of front face after 500,000 yrs, assuming constant velocity. Thickness of layer 1 is 120 times exaggerated in order to show deformation of initially straight vertical markers.  $l = 50$  km.  $L$  marks the initial position of the front face at 500 km from centre of the symmetrical nappe; viscosities  $Mu1$  and  $Mu2$  in poises.

mated by simple proportionality factors provided that the ratios between significant parameters are the same as for the models computed.

Thus, for example, when in a series of models all parameters are fixed except the absolute viscosities while, however, the viscosity ratio,  $R_m$ , is the same, then the velocity at any corresponding point is inversely proportional to the absolute viscosities.

Similarly, if all parameters in the models—including the density ratio—are fixed except the absolute densities, then the velocity at any corresponding points is proportional to the absolute densities.

For variations in geometric dimension the rule of thumb is: if in a series of models all parameters including aspect ratios and the ratio between thicknesses, are fixed except the absolute thicknesses and lengths, then the velocity at corresponding points varies with the square of a defined linear dimension, e.g., the absolute thickness. In this case the strain rate at corresponding points varies linearly with the defined linear dimension (Table 2).

Using the above rules the information presented in Figs. 4–15 can be extended to

TABLE 2

Example demonstrating the second degree relation between geometric dimension and velocity. \*  $R_m = \rho_1 = \rho_2 = 2.8$  g/cm<sup>3</sup>,  $H_1/H_2 = 0.01$ ,  $\eta_1 = 10^{18}$  P  $\eta_2 = 10^{22}$  P

$H_2$ (m)	$u_2$ (cm/yr)
625	0.0864249627
1250	0.3456998510
2500	1.3827994038
5000	5.5311976153
10000	22.1247904614

\* As may be readily checked, with a pocket calculator for example, these values show that a doubling the linear dimension—in this case the height—corresponds to a four-fold increase of the velocity. The numerical relationship is very exact for the models under study.

any desired value of density, thickness and viscosity limited by the noted constraints as regards parameter ratios.

#### Strain in the basal layer

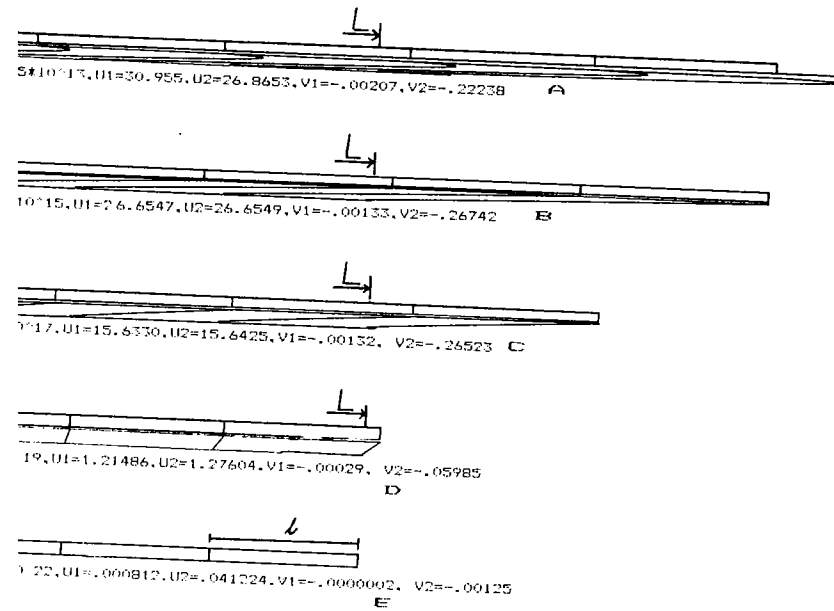
The rather complicated deformation of initially straight markers in layer 1 demonstrated in most models studied requires further comments. We may say that the strain in layer 1 is generated by the overlying layer since layer 1 is generally too thin to spread if not overlain by a heavy burden. The effect of layer 2 is twofold: (1) On account of its weight it squeezes the subjacent stratum and generates extrusion flow in the latter. This may be referred to as the “squeezing effect”; (2) on account of the gravitational spreading of layer 2, horizontal tensile strain is transmitted to the underlying layer 1 since the contact is welded (coherent) and may appropriately be termed the “transmitted tension effect.”

It is useful to be aware of these two distinct means by which layer 2 produces strain in layer 1. The two effects generally occur together, but that does not mean that they cannot be analysed separately. In fact, one of the effects may in practice occur without any noticeable contribution from the other. If the subjacent sheet is extremely viscous or rigid relative to the other it is unable to spread, but its weight will still squeeze layer 1 and generate extrusion there.

It is more difficult to “purify” the “transmitted tension effect” in the double-layer models here studied. The reason for this is that the relative viscosity required for gravitational spreading of layer 2 does of course not necessarily depend on its weight and its “squeezing effect”. However, by selecting the proper viscosity ratio between the two strata it is possible to construct numerical models in which the “transmitted tension” effect is the dominant one, see below.

In attempting to analyse the complex strain in layer 1 it helps to consider the aforementioned two effects separately. When studying the “transmitted tension

$R_2=100, H_2=5000\text{m}, H_1=50\text{m}, \mu_2=10^{22}, \rho_1=\rho_2=2.8, U_{\text{free}}=26.609625, V_{\text{free}}=-.2660925$



Front part of spreading double-layer nappe with varying viscosity  $\mu_1$ , showing initial velocity in and displacement of front face after 500,000 yrs, assuming constant velocity. Thickness of layer 1 is exaggerated in order to show deformation of initially straight vertical markers.  $l = 50$  km.  $L$  is the initial position of the front face at 500 km from centre of the symmetrical nappe; viscosities  $\mu_2$  in poises.

by simple proportionality factors provided that the ratios between significant parameters are the same as for the models computed.

For example, when in a series of models all parameters are fixed except the absolute viscosities while, however, the viscosity ratio,  $R_m$ , is the same, then the velocity at any corresponding point is inversely proportional to the absolute viscosities.

Similarly, if all parameters in the models—including the density ratio—are fixed except the absolute densities, then the velocity at any corresponding points is proportional to the absolute densities.

For variations in geometric dimension the rule of thumb is: if in a series of models all parameters including aspect ratios and the ratio between thicknesses, except the absolute thicknesses and lengths, then the velocity at corresponding points varies with the square of a defined linear dimension, e.g., the absolute thickness. In this case the strain rate at corresponding points varies linearly with the linear dimension (Table 2).

According to the above rules the information presented in Figs. 4-15 can be extended to

TABLE 2

Example demonstrating the second degree relation between geometric dimension and velocity. \*  $R_2 = 100$ ,  $\rho_1 = \rho_2 = 2.8 \text{ g/cm}^3$ ,  $H_1/H_2 = 0.01$ ,  $\eta_1 = 10^{18} \text{ P}$ ,  $\eta_2 = 10^{22} \text{ P}$

$H_2$ (m)	$u_2$ (cm/yr)
625	0.0864249627
1250	0.3456998510
2500	1.3827994038
5000	5.5311976153
10000	22.1247904614

\* As may be readily checked, with a pocket calculator for example, these values show that a doubling of the linear dimension—in this case the height—corresponds to a four-fold increase of the velocity. This numerical relationship is very exact for the models under study.

any desired value of density, thickness and viscosity limited by the noted constraints as regards parameter ratios.

#### Strain in the basal layer

The rather complicated deformation of initially straight markers in layer 1 as demonstrated in most models studied requires further comments. We may argue that the strain in layer 1 is generated by the overlying layer since layer 1 is generally too thin to spread if not overlain by a heavy burden. The effect of layer 2 is twofold: (1) On account of its weight it squeezes the subjacent stratum and generates extrusion flow in the latter. This may be referred to as the “squeezing effect”; (2) on account of the gravitational spreading of layer 2, horizontal tensile strain will be transmitted to the underlying layer 1 since the contact is welded (coherent). This may appropriately be termed the “transmitted tension effect.”

It is useful to be aware of these two distinct means by which layer 2 produces strain in layer 1. The two effects generally occur together, but that does not mean that they cannot be analysed separately. In fact, one of the effects may well in practice occur without any noticeable contribution from the other. If the superincumbent sheet is extremely viscous or rigid relative to the other it is unable to yield and spread, but its weight will still squeeze layer 1 and generate extrusion flow there.

It is more difficult to “purify” the “transmitted tension effect” in the type of double-layer models here studied. The reason for this is that the relatively low viscosity required for gravitational spreading of layer 2 does of course not nullify its weight and its “squeezing effect”. However, by selecting the proper viscosity ratio between the two strata it is possible to construct numerical models in which the “transmitted tension” effect is the dominant one, see below.

In attempting to analyse the complex strain in layer 1 it helps to consider the aforementioned two effects separately. When studying the “transmitted tension”

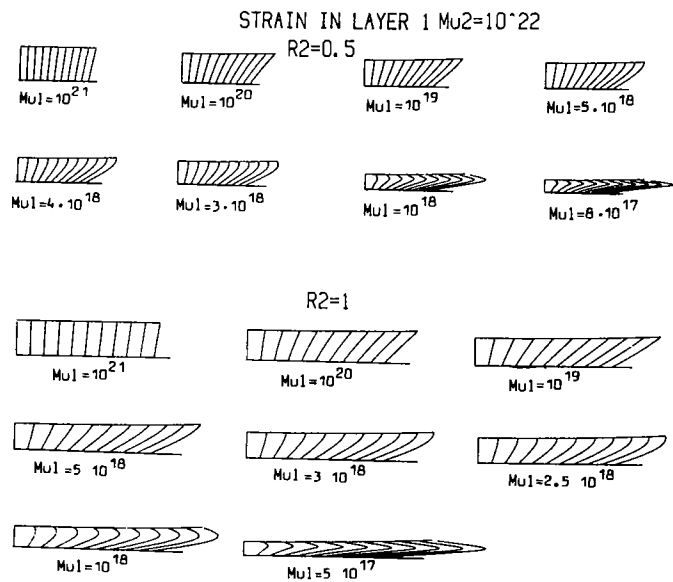
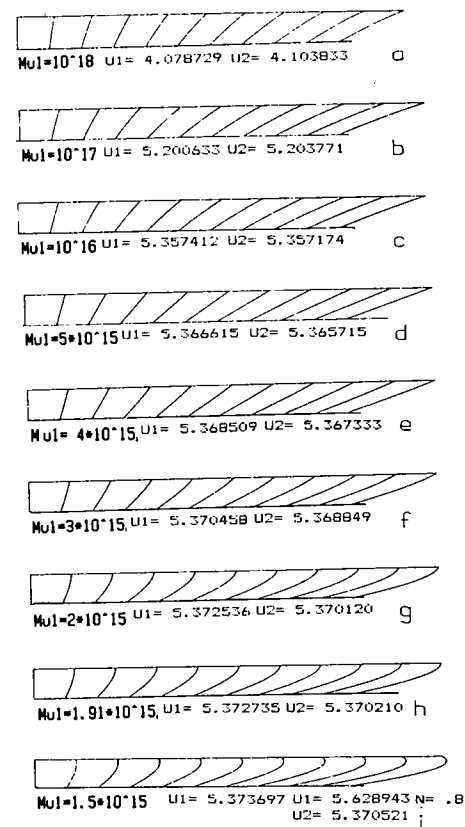


Fig. 10. Strain in layer 1 indicated by deformation of initially straight vertical markers shown at  $R_2 = 0.5$  and 1, and for selected viscosity values in poises (P) of layer 1 while  $Mu_2$  is fixed at  $10^{22}$  P. Note change of deformation with varying viscosity. When  $Mu_1$  is large the tilted markers are straight or show a gentle curvature, convex toward the (upper) left. With decreasing viscosity the curvature increases but now convex toward the (lower) right. As  $Mu_1$  decreases further the curvature sharpens and becomes pointed at the same time as the deformed markers below and above the sharp kinks bend gently in the opposite direction to the kinks. Note that the viscosity at the stage for "kinking" of the markers is less for aspect ratio  $R_2 = 1$  than for  $R_2 = 0.5$ . Compare also Figs. 11 and 12. See comment in text, p. 233 ff.

effect, we cancel out the squeezing effect by disregarding the weight of layer 2, but at the same time assuming a contact-parallel longitudinal strain identical to that which would have been produced by the gravitational spreading. Since the contact is coherent the longitudinal extension is the same on either side of the contact, and it follows that in layer 1 longitudinal layer-parallel stretch increases from zero at the

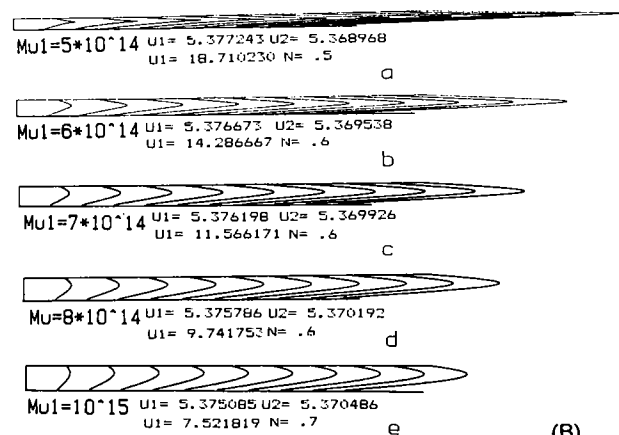
Fig. 11. A. Strain in layer 1 for selected viscosities at aspect ratio  $R_2 = 20$  which corresponds to  $R_1 = 2000$  since  $H_1 = H_2/100$  and the layers are equally long.  $Mu_2$  is constant  $= 10^{22}$  P. The switch of marker curvature (see Fig. 10) occurs at  $Mu_1 \approx 5 \cdot 10^5$  P compared with between  $10^{19}$  and  $10^{20}$  poise for  $R_2 = 0.5$  and about  $10^{19}$  for  $R_2 = 1$ . Velocities given in cm/yr at front end,  $u_2$  refers to upper right corner of layer 2 (not shown in figure), and  $u_1$  to the upper right corner of layer 1, i.e., to the contact between the layers, and for  $Mu_1 = 1.5 \cdot 10^5$  also at level  $N_1 = 0.8$  where  $u_1$  reaches maximal value. B. Same as 11A but the effect of additional viscosity values is demonstrated. Note especially the extremely sharp cusps in the deformed markers at  $Mu_1 = 5 \cdot 10^{14}$  P. It is also worth noting that the level  $N$  at which maximum  $u_1$  is reached moves close to the centre when viscosity decreases.  $N$  gives the level in tenths of  $H_1$ .

STRAIN IN LAYER 1,  $R_2=20, H_2=5000M, H_1=50M, Mu_2=10^{22}$



(A)

STRAIN IN LAYER 1:  $R_2=20, Mu_2=10^{22}$



(B)

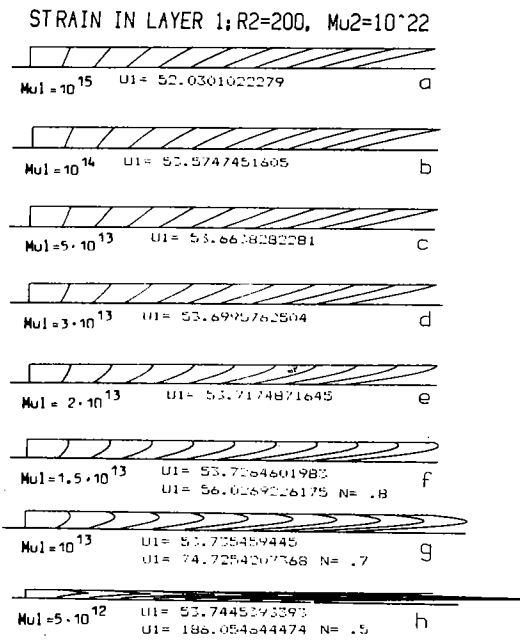


Fig. 12. With the extreme aspect of layer 1 in this example ( $R_1 = 20,000$ ) the switch of curvature in the deformed markers occurs at  $\mu_1$  between  $3 \cdot 10^{13}$  and  $5 \cdot 10^{13}$  P, and the sharp cusps develop at  $\mu_1 = 5 \cdot 10^{12}$  P; compare Figs. 9 and 10.  $u_1$  is given in cm/year at front face. For  $\mu_1 \leq 1.5 \cdot 10^{13}$  maximum  $u_1$  is also given, occurring at levels  $N = 0.8, 0.7$  and  $0.5$ , respectively. It is interesting that the computer-plotted figure indicates that shear at layer contact vanishes (the markers are normal to the top surface of layer 1) when  $\mu_1$  is between  $1.5 \cdot 10^{13}$  and  $2 \cdot 10^{13}$  P (see also Table 3).

contact with the rigid base to maximal value at the contact to the spreading layer 2. It can be demonstrated that a gradient across the layer of layer-parallel longitudinal strain causes initially straight passive markers not only to tilt but also to bend with the concave side of the curvature facing in the direction of motion, (see Fig. 13). This effect is detectable in some of the models computed in which the viscosity ratio happened to be sufficiently favourable for a certain dominance of "the transmitted tension" effect. This would mean relatively high viscosity of layer 1, thereby reducing the squeezing effect (see, e.g., Figs. 8, 10 and 11). However, the models studied were intended to illustrate the "lubrication" tendency of a relatively soft basal sheet in the problem of thrust motion. Hence all models computed so far have basal layers less viscous than the superincumbent layer. For illustration of the "transmitted tension" phenomenon it is desirable to select viscosities for the basal stratum which are higher than the viscosity of the layer above. An example of this is presented in Fig. 15. In this figure not only does the longitudinal strain increase across the stratum from base to top, but there is also a positive gradient of the longitudinal strain along the layer from back to front. This means that the gradient

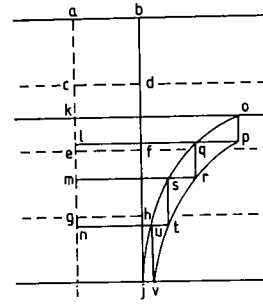


Fig. 13. Deformation of a straight marker ( $b$  to  $j$ ) caused by a gradient parallel to the marker longitudinal tensile strain normal to the marker. For demonstration the strain increases stepwise across the gradient, being small in the region  $ghij$ , larger in the region  $efgh$ , still larger in the region  $cdef$  assuming maximum value in the region  $abcd$ . The regions mentioned belong to zones extending normal to the marker, the strain within each zone being homogeneous and the thickness of the zones infinitesimal. The line  $a-i$  is in the centre of the strain so there is no motion across this line. In stepwise increasing strain the region  $ghij$  changes to  $nuiv$ , the region  $efgh$  to  $msnt$ , the region  $cdef$  to  $eqmr$ , and ultimately the region  $abcd$  goes to  $kolp$ . It is clear that if this operation was made in infinitesimal steps the marker  $bj$  will deform to a continuous smooth curve within the region bounded by  $prtv$  and  $qsuj$ .

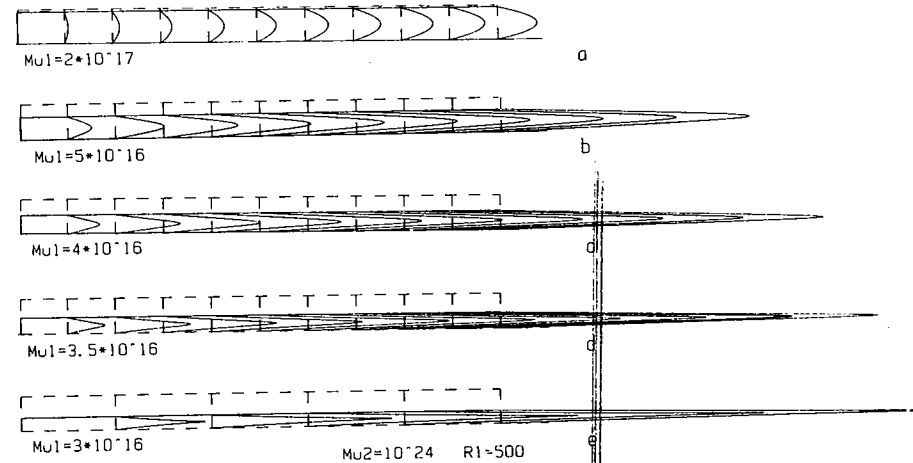
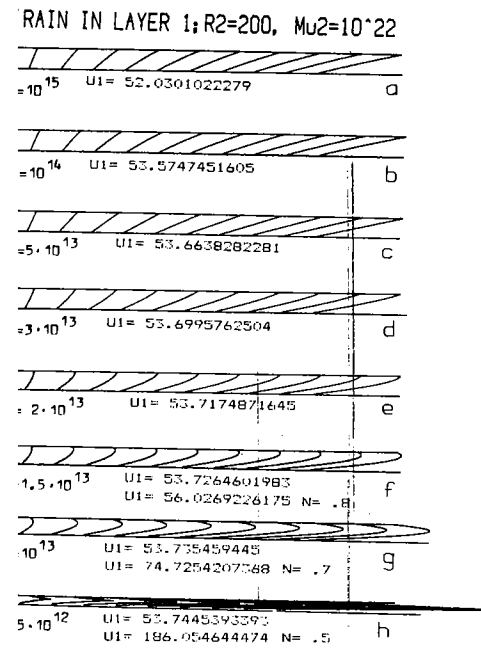


Fig. 14. Extrusion flow in layer 1 caused by the "squeezing effect" of layer 2 (not shown in the figure). Layer 2 is given the viscosity  $\eta_2 = 10^{24}$  P to make it practically immobile. Note the well developed symmetry of the flow in contrast to models where the "squeezing effect" is mixed with the "transmitted tension effect" (Figs. 10, 11 and 12). To show the well developed sharp cusps in the markers at the squeezing only every second marker is recorded. Dashed lines give initial outline of cross section. Deformed pattern based on initial velocity remaining unchanged for years.



2. With the extreme aspect of layer 1 in this example ( $R_1 = 20,000$ ) the switch of curvature in the markers occurs at  $Mu_1$  between  $3 \cdot 10^{13}$  and  $5 \cdot 10^{13}$  P, and the sharp cusps develop at  $5 \cdot 10^{12}$  P; compare Figs. 9 and 10.  $u_1$  is given in cm/year at front face. For  $Mu_1 \leq 1.5 \cdot 10^{13}$   $u_1$  is also given, occurring at levels  $N = 0.8, 0.7$  and  $0.5$ , respectively. It is interesting that the shear at layer contact vanishes (the markers are normal to the top of layer 1) when  $Mu_1$  is between  $1.5 \cdot 10^{13}$  and  $2 \cdot 10^{13}$  P (see also Table 3).

With the rigid base to maximal value at the contact to the spreading layer 2. It can be demonstrated that a gradient across the layer of layer-parallel longitudinal strain causes initially straight passive markers not only to tilt but also to bend with the concave side of the curvature facing in the direction of motion, (see Fig. 13). This effect is detectable in some of the models computed in which the viscosity ratio is sufficiently favourable for a certain dominance of "the transmitted tension" effect. This would mean relatively high viscosity of layer 1, thereby reducing the squeezing effect (see, e.g., Figs. 8, 10 and 11). However, the models were intended to illustrate the "lubrication" tendency of a relatively soft sheet in the problem of thrust motion. Hence all models computed so far have shown layers less viscous than the superincumbent layer. For illustration of the "transmitted tension" phenomenon it is desirable to select viscosities for the basal layer which are higher than the viscosity of the layer above. An example of this is given in Fig. 15. In this figure not only does the longitudinal strain increase from the stratum from base to top, but there is also a positive gradient of the longitudinal strain along the layer from back to front. This means that the gradient

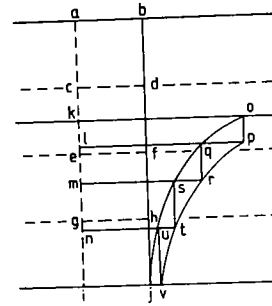


Fig. 13. Deformation of a straight marker ( $b$  to  $j$ ) caused by a gradient parallel to the marker of longitudinal tensile strain normal to the marker. For demonstration the strain increases stepwise along the gradient, being small in the region  $ghij$ , larger in the region  $efgh$ , still larger in the region  $cdef$  and assuming maximum value in the region  $abcd$ . The regions mentioned belong to zones extending normal to the marker, the strain within each zone being homogeneous and the thickness of the zones infinitesimal. The line  $a-i$  is in the centre of the strain so there is no motion across this line. In this stepwise increasing strain the region  $ghij$  changes to  $nuiv$ , the region  $efgh$  to  $msnt$ , the region  $cdef$  to  $eqmr$ , and ultimately the region  $abcd$  goes to  $kolp$ . It is clear that if this operation was made with infinitesimal steps the marker  $bj$  will deform to a continuous smooth curve within the region bounded by  $prtv$  and  $qsuj$ .

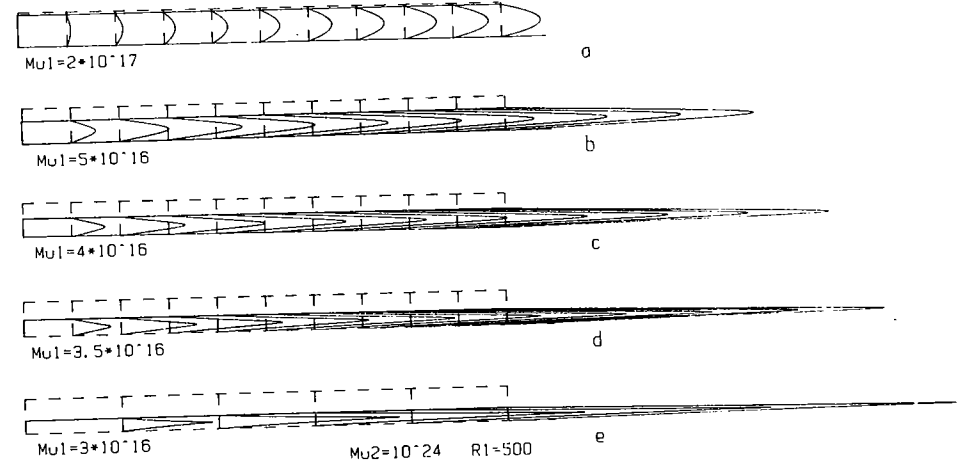


Fig. 14. Extrusion flow in layer 1 caused by the "squeezing effect" of layer 2 (not shown in the figure). Layer 2 is given the viscosity  $\eta_2 = 10^{24}$  P to make it practically immobile. Note the well developed symmetry of the flow in contrast to models where the "squeezing effect" is mixed with the "transmitted tension effect" (Figs. 10, 11 and 12). To show the well developed sharp cusps in the markers at strong squeezing only every second marker is recorded. Dashed lines give initial outline of cross section and indicate the initial markers. Deformed pattern based on initial velocity remaining unchanged for  $5 \cdot 10^5$  yrs.



MJ1=5·10<sup>-19</sup> MJ2=5·10<sup>-16</sup> R1=500

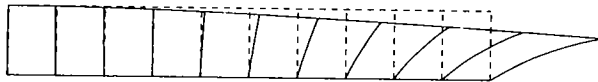


Fig. 15. The "transmitted tension effect" in layer 1 caused by horizontal spreading of layer 2 (not shown) and the transmission of longitudinal strain across the coherent boundary. Note the curvature in the deformed markers as caused by the strain increasing from bottom to top as well as from the back to the front. The vertical dimension is exaggerated by a factor of 90 in this figure. Compare with Fig. 13.

of the strain across the layer becomes steeper as the front is approached (since strain is zero at the base); a condition which explains why the curvature of the deformed markers is accentuated in the frontal region. (Incidentally, the increment of layer-parallel stretch in the frontal region in layer 1 is in good agreement with the strain in layer 2 in models with relatively competent basal layers, see, e.g., Figs. 11 and 12.) As pointed out above, the "squeezing effect" can be readily demonstrated in its "pure" state by selecting a rigid or highly viscous overburden. With vanishing spreading of the overburden layer-parallel stretch is zero both at the top and bottom of layer 1 and maximum tensile strain will be in the middle of the layer. This is well demonstrated in Fig. 14 in which the perfect symmetry of the "bulge" of deformed markers should be compared with the unsymmetric "bulge" in models allowing squeezing and tension transmission to occur with comparable intensity.

It is clear from the above discussion of the longitudinal strain gradient that the curvature and the extreme cusps on the markers in Fig. 14 and other examples arise from the gradients from both edges to the centre of layer parallel longitudinal strain.

At certain relations between the viscosity ratio and the aspect ratio of the model the shear strain vanishes at the boundary between the two layers; see Table 3. When this happens the second layer moves as if there was no friction at the base. If the

TABLE 3

Relation between aspect ratio  $R_2$  and viscosity ratio  $\eta_1/\eta_2$  at which the shear stress vanishes at layer 1/layer 2 contact

$R_2$	$\eta_1/\eta_2$	$\eta_1$	$\eta_2$
0.5	$4.0 \cdot 10^{-4}$	$4 \cdot 10^{18}$	$10^{22}$
1	$2.5 \cdot 10^{-4}$	$2.5 \cdot 10^{18}$	$10^{22}$
2	$4.3 \cdot 10^{-5}$	$4.3 \cdot 10^{17}$	$10^{22}$
5	$3.5 \cdot 10^{-6}$	$3.5 \cdot 10^{16}$	$10^{22}$
10	$7.6 \cdot 10^{-7}$	$7.6 \cdot 10^{15}$	$10^{22}$
20	$1.85 \cdot 10^{-7}$	$1.85 \cdot 10^{15}$	$10^{22}$
50	$2.9 \cdot 10^{-8}$	$2.9 \cdot 10^{14}$	$10^{22}$
100	$7.4 \cdot 10^{-9}$	$7.4 \cdot 10^{13}$	$10^{22}$
200	$1.9 \cdot 10^{-9}$	$1.9 \cdot 10^{13}$	$10^{22}$

viscosity of layer 1 is less than that given by this critical value, the flow in layer 2 generates a horizontal pull on layer 1, the pull being maximal in the centre of the nappe.

#### PROSPECTED DEVELOPMENT OF A STREAM FUNCTION-ENERGY EXTREMIZING METHOD

It is obviously a serious limitation of the combined "stream function-energy extremizing" method presented here that only the instantaneous velocity field is calculated. The goal for a user of the method must be to follow the complete evolution of the deforming process—in our case the complete history of spreading viscous "nappe". It is easy to see that this may be accomplished step-wise procedure, assuming that the velocity field is constant for a limited interval and then calculating a new velocity field based on the initially deformed model, the new velocity field giving rise to further deformation which in its turn produces an altered velocity field that is used to calculate the next step deformation, etc., etc. The new velocity field characterizing a deformed state of model is based on new values of the coefficients in the polynomial stream function. To obtain the new values of the coefficients strain- and potential energy must be calculated by integration over the deformed cross section of the model, using the formula for the "specific energy rate" as regards the strain energy, but calculated the potential energy change by a method different from the one used above for an infinitesimal instantaneous state. Now the potential energy must be calculated at the end of the first step, using the formula:

$$E_{pot1} = \rho g \int \int y \partial x \partial y$$

the boundary of the deformation profile being defined by the collection of position vectors  $y$  given by the formulas:

$$x = x_i + u \Delta t$$

and:

$$y = y_i + v \Delta t$$

Here  $x_i$  and  $y_i$  are position vectors for the initial profile boundary and the velocity components  $u$  and  $v$  are derived from the stream function whose coefficients have not yet been determined.  $\Delta t$  is an arbitrary short time interval.

The change of potential energy during the interval  $\Delta t$  is then:

$$\Delta E_{pot} = E_{pot1} - E_{pot0}$$

where:

$$E_{pot0} = \rho g \int \int y \partial x \partial y$$

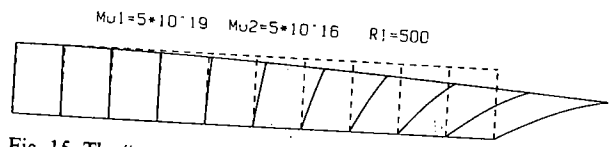


Fig. 15. The "transmitted tension effect" in layer 1 caused by horizontal spreading of layer 2 (not shown) and the transmission of longitudinal strain across the coherent boundary. Note the curvature in the deformed markers as caused by the strain increasing from bottom to top as well as from the back to the front. The vertical dimension is exaggerated by a factor of 90 in this figure. Compare with Fig. 13.

of the strain across the layer becomes steeper as the front is approached (since strain is zero at the base); a condition which explains why the curvature of the deformed markers is accentuated in the frontal region. (Incidentally, the increment of layer-parallel stretch in the frontal region in layer 1 is in good agreement with the strain in layer 2 in models with relatively competent basal layers, see, e.g., Figs. 11 and 12.) As pointed out above, the "squeezing effect" can be readily demonstrated in its "pure" state by selecting a rigid or highly viscous overburden. With vanishing spreading of the overburden layer-parallel stretch is zero both at the top and bottom of layer 1 and maximum tensile strain will be in the middle of the layer. This is well demonstrated in Fig. 14 in which the perfect symmetry of the "bulge" of deformed markers should be compared with the unsymmetric "bulge" in models allowing squeezing and tension transmission to occur with comparable intensity.

It is clear from the above discussion of the longitudinal strain gradient that the curvature and the extreme cusps on the markers in Fig. 14 and other examples arise from the gradients from both edges to the centre of layer parallel longitudinal strain.

At certain relations between the viscosity ratio and the aspect ratio of the model the shear strain vanishes at the boundary between the two layers; see Table 3. When this happens the second layer moves as if there was no friction at the base. If the

TABLE 3  
Relation between aspect ratio  $R_2$  and viscosity ratio  $\eta_1/\eta_2$  at which the shear stress vanishes at layer 2 contact

	$\eta_1/\eta_2$	$\eta_1$	$\eta_2$
5	$4.0 \cdot 10^{-4}$	$4 \cdot 10^{18}$	$10^{22}$
	$2.5 \cdot 10^{-4}$	$2.5 \cdot 10^{18}$	$10^{22}$
	$4.3 \cdot 10^{-5}$	$4.3 \cdot 10^{17}$	$10^{22}$
	$3.5 \cdot 10^{-6}$	$3.5 \cdot 10^{16}$	$10^{22}$
	$7.6 \cdot 10^{-7}$	$7.6 \cdot 10^{15}$	$10^{22}$
	$1.85 \cdot 10^{-7}$	$1.85 \cdot 10^{15}$	$10^{22}$
	$2.9 \cdot 10^{-8}$	$2.9 \cdot 10^{14}$	$10^{22}$
	$7.4 \cdot 10^{-9}$	$7.4 \cdot 10^{13}$	$10^{22}$
	$1.9 \cdot 10^{-9}$	$1.9 \cdot 10^{13}$	$10^{22}$

viscosity of layer 1 is less than that given by this critical value, the flow in layer 1 generates a horizontal pull on layer 2, the pull being maximal in the centre of the nappe.

PROSPECTED DEVELOPMENT OF A STREAM FUNCTION-ENERGY EXTREMIZING METHOD

It is obviously a serious limitation of the combined "stream function-energy-extremizing" method presented here that only the instantaneous velocity field is calculated. The goal for a user of the method must be to follow the complete evolution of the deforming process—in our case the complete history of the spreading viscous "nappe". It is easy to see that this may be accomplished by a step-wise procedure, assuming that the velocity field is constant for a limited time interval and then calculating a new velocity field based on the initially deformed model, the new velocity field giving rise to further deformation which in its turn produces an altered velocity field that is used to calculate the next step of deformation, etc., etc. The new velocity field characterizing a deformed state of the model is based on new values of the coefficients in the polynomial stream function. To obtain the new values of the coefficients strain- and potential energy must be calculated by integration over the deformed cross section of the model, using the formula for the "specific energy rate" as regards the strain energy, but calculating the potential energy change by a method different from the one used above for the infinitesimal instantaneous state. Now the potential energy must be calculated at the end of the first step, using the formula:

$$E_{pot1} = \rho g \int \int y \partial x \partial y \tag{95}$$

the boundary of the deformation profile being defined by the collection of points  $x, y$  given by the formulas:

$$x = x_i + u \Delta t \tag{96}$$

and:

$$y = y_i + v \Delta t \tag{97}$$

Here  $x_i$  and  $y_i$  are position vectors for the initial profile boundary and the velocity components  $u$  and  $v$  are derived from the stream function whose coefficients have not yet been determined.  $\Delta t$  is an arbitrary short time interval.

The change of potential energy during the interval  $\Delta t$  is then:

$$\Delta E_{pot} = E_{pot1} - E_{pot0} \tag{98}$$

where:

$$E_{pot0} = \rho g \int \int y \partial x \partial y \tag{99}$$

means integration over the initial profile.  $\Delta E_{\text{pot}}$  is to be equated with  $\dot{E}_{\text{strain}}\Delta t$ , and the optimizing method described above (keeping  $\Delta t$  constant) leads to determination of the coefficients in the stream function.

Tests have shown that this procedure leads to complications when it comes to optimizing the rate of energy change in attempts to determine the new coefficients in the stream function. Work is, however, in progress trying to solve this problem.

#### APPENDIX A

Applying the expressions:

$$\epsilon = \frac{\partial u}{\partial x} \quad \text{and} \quad \gamma = \left( \frac{\partial u}{\partial y} + \frac{\partial v}{\partial x} \right)$$

to eqn. (34) we obtain the strain energy rate per unit volume:

$$\dot{E}_{\epsilon\gamma_1} = \eta_1 (4\epsilon_x^2 + \gamma_{xy}^2) \quad (\text{A1})$$

which upon integration over the cross section  $0 \leq x \leq L$ ,  $0 \leq y \leq H_1$  gives the strain energy rate for that part of the cross section slice which cuts layer 1:

$$\begin{aligned} \dot{E}_{\epsilon\gamma_1} = \eta_1 \left[ \left( \frac{16}{3}R_1 + \frac{4}{3}R_1^3 \right) H_1^4 a^2 + \left( \frac{36}{5}R_1 + \frac{12}{3}R_1^3 \right) H_1^6 b^2 \right. \\ + \left( \frac{64}{7}R_1 + \frac{132}{15}R_1^3 + \frac{72}{15}R_1^5 + \frac{4}{7}R_1^7 \right) H^8 c^2 + \left( \frac{100}{9}R_1^3 + \frac{100}{9}R_1^5 + 12R_1^7 \right) \\ + \frac{100}{21}R_1^7 \left. \right] H^{10} d^2 + (12R_1 + 4R_1^3) H_1^5 ab + \left( \frac{64}{3}R_1 - \frac{24}{9}R_1^3 - \frac{8}{3}R_1^5 \right) H_1^6 ac \\ + \left( \frac{40}{3}R_1 - 10R_1^3 - 4R_1^5 \right) H_1^7 ad + (16R_1 + 6R_1^3 - \frac{24}{10}R_1^5) H_1^7 bc \\ + \left( \frac{120}{7}R_1 - 8R_1^5 \right) H_1^8 bd + (20R_1 + 20R_1^3 + 15R_1^5 + \frac{20}{7}R_1^7) H_1^9 cd \quad (\text{A2}) \end{aligned}$$

In the same way the energy of the part of the cross section slice which cuts through layer 2 is derived from stream function (35):

$$\begin{aligned} \dot{E}_{\epsilon\gamma_2} = \eta_2 \left[ 4a_{22}^2 H_2^2 R_2 + \left( \frac{16}{3}R_2 + \frac{4}{3}R_2^3 \right) a_{23}^2 H_2^4 + \left( \frac{36}{5}R_2 + 4R_2^3 \right) a_{24}^2 H_2^6 \right. \\ + \left( \frac{64}{7}R_2 + \frac{44}{5}R_2^3 + \frac{24}{5}R_2^5 + \frac{4}{7}R_2^7 \right) a_{25}^2 H_2^8 + \left( \frac{100}{9}R_2 + \frac{100}{7}R_2^3 \right) \\ + 12R_2^5 + \frac{100}{21}R_2^7 \left. \right] a_{26}^2 H_2^{10} + 12R_2^3 a_{24}^2 H_2^4 + (4R_2^3 + \frac{36}{5}R_2^5) a_{25}^2 H_2^6 \\ + a_{22} (8a_{23}R_2 H_2^3 + 8a_{24}R_2 H_2^4 + 8(R_2 - R_2^3) a_{25} H_2^5 + (8R_2 - \frac{40}{3}R_2^3) a_{26} H_2^6 \\ + 8R_2^3 a_{42} H_2^4) + a_{23} \left[ (12R_2 + 4R_2^3) a_{24} H_2^5 + \left( \frac{64}{5}R_2 - \frac{8}{3}R_2^3 - \frac{8}{3}R_2^5 \right) a_{25} H_2^6 \right. \\ + \left. \left( \frac{40}{3}R_2 - 10R_2^3 - 4R_2^5 \right) a_{26} H_2^7 - 8R_2^3 a_{41} H_2^4 + 4R_2^3 a_{42} H_2^5 \right] \\ + a_{24} \left\{ (16R_2 + 6R_2^3 - \frac{12}{5}R_2^5) a_{25} H_2^7 + \left( \frac{120}{7}R_2 - 8R_2^5 \right) a_{26} H_2^8 \right. \\ - 12R_2^3 a_{41} H_2^5 \left. \right\} + a_{25} \left\{ (20R_2 + 20R_2^3 + 12R_2^5 + \frac{20}{7}R_2^7) a_{26} H_2^9 \right. \\ - (10R_2^3 + 12R_2^5) a_{42} H_2^7 - (24R_2^3 - \frac{24}{5}R_2^5) a_{41} H_2^6 \left. \right\} \\ + a_{26} \left\{ -(16R_2^3 + 16R_2^5) a_{42} H_2^8 - (30R_2^3 - 12R_2^5) a_{41} H_2^7 \right\} \\ + 12R_2^3 a_{41} a_{42} H_2^5 \quad (\text{A3}) \end{aligned}$$

The strain energy rate for the total cross section slice of unit thickness through the model is then:

$$\dot{E}_{\epsilon\gamma} = \dot{E}_{\epsilon\gamma_1} + \dot{E}_{\epsilon\gamma_2}$$

The rate of change of potential energy for the unit slice follows upon integration of the expression:

$$\dot{E}_{\text{pot}} = \rho_i g v_i \partial x \partial y \quad (\text{see also p. 239}).$$

across layer 1 when  $i$  is 1 and layer 2 when  $i=2$ . Here the vertical velocity component is derived from the appropriate stream functions (34) or (35). This procedure leads to the potential energy rate for the whole unit section across model:

$$\begin{aligned} \dot{E}_{\text{pot}} = \dot{E}_{\text{pot}1} + \dot{E}_{\text{pot}2} = \rho_1 g \left[ - \left( \frac{1}{3}H_1^4 a + \frac{1}{4}H_1^5 b + \frac{1}{5}H_1^6 c + \frac{1}{6}H_1^7 d \right) R_1 \right. \\ + \left. \left( \frac{1}{3}H_1^6 c + \frac{5}{12}H_1^7 d \right) R_1^3 \right] + \rho_2 g \left[ \left( H_2^2 a_{21} + \frac{1}{2}H_2^3 a_{22} + \frac{1}{3}H_2^4 a_{23} \right. \right. \\ + \left. \frac{1}{4}H_2^5 a_{24} + \frac{1}{5}H_2^6 a_{25} + \frac{1}{6}H_2^7 a_{26} \right) R_2 + \left( H_2^4 a_{41} + \frac{1}{2}H_2^5 a_{42} \right. \\ \left. \left. - \frac{1}{3}H_2^6 a_{25} - \frac{5}{12}H_2^7 a_{26} \right) R_2^3 \right] \end{aligned}$$

$R_i$  ( $i=1$  to  $2$ ) is the aspect ratio,  $L/H_i$  of the layers.

#### APPENDIX B

```

10  !"COMBB6NAPW"
20  !A plotting,printing program for double-layer spreading nappe with vanishing
shear stress at top surface;valid for initial instantaneous velocities
30  !Theory and program (HPbasic,2,1;computer HP9816s) By Hans Ramberg,Uppsala
40  !Adjustment-if any-of viscosity,layer thickness,density (lines490,600) or p
velocity (line 230) must be done prior to pressing "RUN"
50  !Scale values (line 280) are generally input after start but may even be i
rted prior to start
60  !To start program put on the plotter and press "RUN"
70  !!
80  !The two polynomial STREAM FUNCTIONS are:
90  !Psi1=-(AY^2+BY^3+CY^4+DY^5+EY^6+FY^7)X+(Cy^2+5/3Dy^3+10/3Ey^4+14/3Fy^5)x^
Ey^2+7/3Fy^3)x^5
100 !Psi2=(A21+A22y+A23y^2+A24y^3+A25y^4+A26y^5)x+(A41+A42y-(A25+5*A61)y^2-5/
A26+A62)y^3)x^3+(A61+A62y)x^5
110 !!
120 !H1,H2 are thicknesses,Rh=H1/H2,L= length,R2(INPUT item!)=R=L/H2,R1=L/H1,
,Ro2 are densities,Rro=Ro1/Ro2,Mu1,Mu2 are viscosities,Rm(INPUT item!)=Mu1/Mu
130 !!
140 !Gr=acceleration of gravity, U1,V1,U2,V2 are horizontal (U) and vertical
velocity components in layer 1 and 2.
150 !!
160 !Ufree,Vfree are velocities at front face of free-slip model;X1,Y1;X2,Y2 a
position vectors in layer 1,resp.layer 2;Mi=X/L, Ni=Y/H in lines 1470,1490 ff.
170 ! are normalized position vectors
180 !!
190 ! If hight is in cm, density in g/cm^3, Gr in cm/s^2 and viscosity in po
then velocity is in cm/year;with hight in m, density in kg/m^3, viscosity in
200 !Pascal s and Gr in m/s^2 then velocity is in meter per year
210 !!
220 PRINTER IS 705 !(705 is really a plotter:HP7470A)
230 PRINT "IN;IF,VS2;";!This prepares for PLOTTING, and specifies PEN VELOCIT
240 TRACE PAUSE

```

means integration over the initial profile.  $\Delta E_{\text{pot}}$  is to be equated with  $\dot{E}_{\text{strain}} \Delta t$ , and the optimizing method described above (keeping  $\Delta t$  constant) leads to determination of the coefficients in the stream function.

Tests have shown that this procedure leads to complications when it comes to optimizing the rate of energy change in attempts to determine the new coefficients in the stream function. Work is, however, in progress trying to solve this problem.

#### PENDIX A

Applying the expressions:

$$\frac{\partial u}{\partial x} \quad \text{and} \quad \gamma = \left( \frac{\partial u}{\partial y} + \frac{\partial v}{\partial x} \right)$$

in eqn. (34) we obtain the strain energy rate per unit volume:

$$= \eta_1 (4\epsilon_x^2 + \gamma_{xy}^2) \quad (\text{A1})$$

which upon integration over the cross section  $0 \leq x \leq L$ ,  $0 \leq y \leq H_1$  gives the strain energy rate for that part of the cross section slice which cuts layer 1:

$$\begin{aligned} = \eta_1 & \left[ \left( \frac{16}{3} R_1 + \frac{4}{3} R_1^3 \right) H_1^4 a^2 + \left( \frac{36}{5} R_1 + \frac{12}{3} R_1^3 \right) H_1^6 b^2 \right. \\ & + \left( \frac{64}{7} R_1 + \frac{132}{15} R_1^3 + \frac{72}{15} R_1^5 + \frac{4}{7} R_1^7 \right) H^8 c^2 + \left( \frac{100}{9} R_1^3 + \frac{100}{7} R_1^5 + 12 R_1^7 \right) \\ & + \left. \frac{100}{21} R_1^7 \right) H^{10} d^2 + (12 R_1 + 4 R_1^3) H_1^5 ab + \left( \frac{64}{5} R_1 - \frac{24}{9} R_1^3 - \frac{8}{5} R_1^5 \right) H_1^6 ac \\ & + \left( \frac{40}{3} R_1 - 10 R_1^3 - 4 R_1^5 \right) H_1^7 ad + (16 R_1 + 6 R_1^3 - \frac{24}{10} R_1^5) H_1^7 bc \\ & + \left. \left( \frac{120}{7} R_1 - 8 R_1^5 \right) H_1^8 bd + (20 R_1 + 20 R_1^3 + 15 R_1^5 + \frac{20}{7} R_1^7) H_1^9 cd \right] \quad (\text{A2}) \end{aligned}$$

in the same way the energy of the part of the cross section slice which cuts through layer 2 is derived from stream function (35):

$$\begin{aligned} = \eta_2 & \left[ 4a_{22}^2 H_2^2 R_2 + \left( \frac{16}{3} R_2 + \frac{4}{3} R_2^3 \right) a_{23}^2 H_2^4 + \left( \frac{36}{5} R_2 + 4 R_2^3 \right) a_{24}^2 H_2^6 \right. \\ & + \left( \frac{64}{7} R_2 + \frac{44}{5} R_2^3 + \frac{24}{5} R_2^5 + \frac{4}{7} R_2^7 \right) a_{25}^2 H_2^8 + \left( \frac{100}{9} R_2 + \frac{100}{7} R_2^3 \right. \\ & + \left. 12 R_2^5 + \frac{100}{21} R_2^7 \right) a_{26}^2 H_2^{10} + 12 R_2^3 a_{41}^2 H_2^4 + \left( 4 R_2^3 + \frac{36}{5} R_2^5 \right) a_{42}^2 H_2^6 \\ & + a_{22} (8a_{23} R_2 H_2^3 + 8a_{24} R_2 H_2^4 + 8(R_2 - R_2^3) a_{25} H_2^5 + (8R_2 - \frac{40}{3} R_2^3) a_{26} H_2^6 \\ & + 8R_2^3 a_{42} H_2^4) + a_{23} \left[ (12 R_2 + 4 R_2^3) a_{24} H_2^5 + \left( \frac{64}{5} R_2 - \frac{8}{3} R_2^3 - \frac{8}{5} R_2^5 \right) a_{25} H_2^6 \right. \\ & + \left. \left( \frac{40}{3} R_2 - 10 R_2^3 - 4 R_2^5 \right) a_{26} H_2^7 - 8 R_2^3 a_{41} H_2^4 + 4 R_2^3 a_{42} H_2^5 \right] \\ & + a_{24} \left\{ (16 R_2 + 6 R_2^3 - \frac{12}{5} R_2^5) a_{25} H_2^7 + \left( \frac{120}{7} R_2 - 8 R_2^5 \right) a_{26} H_2^8 \right. \\ & - \left. 12 R_2^3 a_{41} H_2^5 \right\} + a_{25} \left\{ (20 R_2 + 20 R_2^3 + 12 R_2^5 + \frac{20}{7} R_2^7) a_{26} H_2^9 \right. \\ & - \left. (10 R_2^3 + 12 R_2^5) a_{42} H_2^7 - (24 R_2^3 - \frac{24}{5} R_2^5) a_{41} H_2^6 \right\} \\ & + a_{26} \left\{ - (16 R_2^3 + 16 R_2^5) a_{42} H_2^8 - (30 R_2^3 - 12 R_2^5) a_{41} H_2^7 \right\} \\ & + \left. 12 R_2^3 a_{41} a_{42} H_2^5 \right] \quad (\text{A3}) \end{aligned}$$

The strain energy rate for the total cross section slice of unit thickness through the model is then:

$$\dot{E}_{\epsilon\gamma} = \dot{E}_{\epsilon\gamma_1} + \dot{E}_{\epsilon\gamma_2} \quad (\text{A4})$$

The rate of change of potential energy for the unit slice follows upon integration of the expression:

$$\dot{e}_{\text{pot}} = \rho_i g v_i \partial x \partial y \quad (\text{see also p. 239}). \quad (\text{A5})$$

across layer 1 when  $i$  is 1 and layer 2 when  $i=2$ . Here the vertical velocity component is derived from the appropriate stream functions (34) or (35). This procedure leads to the potential energy rate for the whole unit section across the model:

$$\begin{aligned} \dot{E}_{\text{pot}} = \dot{E}_{\text{pot1}} + \dot{E}_{\text{pot2}} = \rho_1 g & \left[ - \left( \frac{1}{3} H_1^4 a + \frac{1}{4} H_1^5 b + \frac{1}{5} H_1^6 c + \frac{1}{6} H_1^7 d \right) R_1 \right. \\ & + \left. \left( \frac{1}{3} H_1^6 c + \frac{5}{12} H_1^7 d \right) R_1^3 \right] + \rho_2 g \left[ \left( H_2^2 a_{21} + \frac{1}{2} H_2^3 a_{22} + \frac{1}{3} H_2^4 a_{23} \right. \right. \\ & + \left. \frac{1}{4} H_2^5 a_{24} + \frac{1}{5} H_2^6 a_{25} + \frac{1}{6} H_2^7 a_{26} \right) R_2 + \left( H_2^4 a_{41} + \frac{1}{2} H_2^5 a_{42} \right. \\ & \left. \left. - \frac{1}{3} H_2^6 a_{25} - \frac{5}{12} H_2^7 a_{26} \right) R_2^3 \right] \quad (\text{A6}) \end{aligned}$$

$R_i$  ( $i=1$  to 2) is the aspect ratio,  $L/H_i$ , of the layers.

#### APPENDIX B

```

10  !"COMB86NAPW"
20  !A plotting,printing program for double-layer spreading nappe with vanishing
    shear stress at top surface;valid for initial instantaneous velocities
30  !Theory and program (HPbasic,2,1;computer HP9816s) By Hans Ramberg,Uppsala
40  !Adjustment-if any-of viscosity,layer thickness,density (lines490,600) or pen-
    velocity (line 230) must be don prior to pressing "RUN"
50  !Scale values (line 280) are generally input after start but may even be in-
    rted prior to start
60  !To start program put on the plotter and press "RUN"
70  !!
80  !The two polynomial STREAM FUNCTIONS are:
90  !Psi1=-(AY^2+BY^3+CY^4+DY^5+EY^6+FY^7)X+(CY^2+5/3DY^3+10/3EY^4+14/3FY^5)X^3-(
    EY^2+7/3FY^3)X^5
100 !Psi2=(A21+A22Y+A23Y^2+A24Y^3+A25Y^4+A26Y^5)X+(A41+A42Y-(A25+5*A61)Y^2-5/3*(
    A26+A62)Y^3)X^3+(A61+A62Y)X^5
110 !!
120 !H1,H2 are thicknesses,Rh=H1/H2,L= length,R2(INPUT item!)=R=L/H2,R1=L/H1,Ro1
    ,Ro2 are densities,Rro=Ro1/Ro2,Mu1,Mu2 are viscosities,Rm(INPUT item!)=Mu1/Mu2
130 !!
140 ! Gr=acceleration of gravity, U1,V1,U2,V2 are horizontal (U) and vertical (V)
    velocity components in layer 1 and 2
150 !!
160 !Ufree,Vfree are velocities at front face of free-slip model;X1,Y1;X2,Y2 are
    position vectors in layer 1,resp.layer 2;Mi=X/L, Ni=Y/H in lines 1470,1490 ff.
170 ! are normalized position vectors
180 !!
190 ! If hight is in cm, density in g/cm^3, Gr in cm/s^2 and viscosity in pois
    then velocity is in cm/year;with hight in m, density in kg/m^3, viscosity in
200 !Pascal s and Gr in m/s^2 then velocity is in meter per year
210 !!
220 PRINTER IS 705 !(705 is really a plotter:HP7470A)
230 PRINT "IN;IF,VS2;!"This prepares for PLOTTING, and specifies PEN VELOCITY
240 TRACE PAUSE

```

```

250 !When "PRINT SC---,---,---,---"etc. appears on screen press "EDIT, 280" fol
lowed by "EXECUTE", and line 280 will appear
260 !If scale values are inserted prior to start then press "CONTINUE" directly
when line 280 appears,else:
270 !Insert desired scale values, (considering the R2,Sym and Rm commands to be
INPUT later!) press "ENTER" followed by "RUN"
280 PRINT "SC-50,50,0,72"!This is an example
290 !!
300 !After "RUN" is pressed,"PRINT "SC---,---,---,---" again appears on screen, and
now with numbers inserted
310 !!
320 !Then press "CONTINUE" which puts"R2,Rm,Ini,Sym,Bou,Lay1,Lay2,Print,etc" on
screen; insert values for R2,Rm,etc. and press "CONTINUE" anew to start plotting
330 !!
340 ! Together with the input values for R2 and Rm the following "yes/no" or 1/
zero choices are possible:
350 !Ini =0 plots initial profile,Ini=1 plots deformed profile,Sym=-1 plots sym
metric profile,Sym=0 plots right hand half of profile
360 !!
370 !Bou=1 plots top boundary first,Bou=0 plots base first; Lay1=1,Lay2=0,plots
layer 1 only,Lay2=1,Lay1=0 plots only layer 2,Lay1=1,Lay2=1 plots both layers
380 !!
390 !!Printing of velocities follows plotting if Print is put =1 and Velfro and
Veltop are given values 0 or 1;Print=1 and Velfro=1,Veltop=0 gives the velocity
400 !at the front face of both layers;Print=1,Velfro=0,Veltop=1 gives the veloci
ty at the top boundary of both layers;Print=1 and Velfro=0,Veltop=0 prints the
410 !velocity throughout both layers. Print=0 prevents velocity to be displayed
or printed: If Lay1=Lay2 =0, Print=1 and Velfro=0 or 1,Veltop=1 or 0 then
420 !velocity is printed without activating plotting
430 !!
440 !For plotting of both upper and lower boundaries press "RUN" and "CONTINUE"
directly after the first plotting or printing ends,then make input for "R2,Rm,
450 !Ini etc", but now using the alternative command for Bou,and press CONTINUE
again
460 INPUT "R2,Rm,Ini,Sym,Bou,Lay1,Lay2","R2,Rm,Ini,Sym,Bou,Lay1,Lay2
470 INPUT "Print,Velfro,Veltop",Print,Velfro,Veltop
480 COM REAL H1,H2,R,R2,R1,Rh,Gr,Ro1,Ro2,Rro,Mu1,Mu2,Rm,Den,Epota,Epota,Estra,
Estrb,Estrab
490 H1=5*10^3!cm,change as needed befor start
500 H2=5*10^5!cm,change as needed --- "" ---
510 Rh=H1/H2
520 R=R2
530 L=R*H2
540 R1=R2/Rh
550 Gr=981!cm/s^2
560 Ro1=2.8!g/cm^3,change as needed befor start
570 Ro2=2.8!g/cm^3,change as needed --- "" ---
580 Mu2=10^22 !Pois,change as needed --- "" ---
590 Mu1=Mu2*Rm
600 Rro=Ro1/Ro2
610 CALL Energyfactors
620 !!
630 !CALCULATION OF THE COEFFICIENTS A,B,...,A41,A42 IN THE STREAM FUNCTIONS
Psi(1) AND Psi(2) FOLLOW
640 Q=Epota/Epota
650 Phi=(2*Q*Estra-Estrab)/(2*Estrb*H2-Q*Estrab*H2)
660 A=- (Epota+Epota*H2*Phi)/(Estra+Estrb*H2^2*Phi^2+Estrab*H2*Phi)
670 B=Phi*A
680 C=(A+(3+3/Rh)*H1*B)/(Den*H1^2) !"Den" is defined line 1760
690 D=- (A+(3+3/Rh)*H1*B)/(Den*(5+5/Rh)*H1^3)
700 A21=- (A*H1^2+B*H1^3+C*H1^4+D*H1^5)
710 A22=- (2*A*H1+3*B*H1^2+4*C*H1^3+5*D*H1^4)
720 A23=-Rm*(A+3*B*H1+(9-3/Rm)*C*H1^2+(15-5/Rm)*D*H1^3)
730 A24=-Rm*B+(2*Rm-6)*C*H1+(5*Rm-15)*D*H1^2
740 A25=-Rm*(C+5*D*H1)
750 A26=-Rm*D
760 A41=C*H1^2+5/3*D*H1^3
770 A42=2*C*H1+5*D*H1^2
780 IF Lay1=0 THEN 1100
790 IF Ini=0 THEN
800 PRINT "LT2,1" !Commands plot with dashed line (for initial profile)
810 ELSE
820 PRINT "LT" !Commands plot with solid line (for deformed profile)
830 END IF

```

```

840 FOR M=Sym TO 1 STEP .1 !Sym is input as 0 or -1,Sym=0 plots right hand
half profile,Sym=-1 plots full symmetric profile
850 IF M=Sym THEN
860 FOR M1=10*R2*Sym TO 10*R2 STEP R2/10 !This draws the top (if Bou=1) or b
tom (if Bou=0) boundary of layer 1
870 X1=M1*H1/R1/(10*R2)
880 Y1=H1*Bou
890 U1=((2*A*Y1+3*B*Y1^2+4*C*Y1^3+5*D*Y1^4)*X1-(2*C*Y1+5*D*Y1^2)*X1^3)*3.1*1
7*Ini
900 V1=(-(A*Y1^2+B*Y1^3+C*Y1^4+D*Y1^5)+(3*C*Y1^2+5*D*Y1^3)*X1^2)*3.1*10^7*In
910 X=M1+U1*X1
920 Y=(10*Rh+V1*10)*Bou !H2 is taken to equal 10 USERS UNITS so that H1= 10*
USERS UNITS; the velocities are multiplied by a 10-units time periode
930 PRINT "PA",X,"",Y,"";PD;SP1;"
940 NEXT M1
950 PRINT "PU;"
960 END IF
970 FOR N1=0 TO 10 STEP .2 !This draws the initially straight vertical marke
in layer 1 Because of the small Rh value the vertical scale must generally be
980 ! greatly exaggerated when plotting structures in layer 1
990 X1=R1*H1*M
1000 Y1=N1*H1/10
1010 U1=((2*A*Y1+3*B*Y1^2+4*C*Y1^3+5*D*Y1^4)*X1-(2*C*Y1+5*D*Y1^2)*X1^3)*3.1*
7*Ini
1020 V1=(-(A*Y1^2+B*Y1^3+C*Y1^4+D*Y1^5)+(3*C*Y1^2+5*D*Y1^3)*X1^2)*3.1*10^7*In
1030 X=10*R*M+U1*X1
1040 Y=N1*Rh+V1*10 !See 920
1050 PRINT "PA",X,"",Y,"";PD;SP1;"
1060 NEXT N1
1070 PRINT "PU;"
1080 NEXT M
1090 PRINT "PU;"
1100 IF Lay2=0 THEN 1420
1110 IF Ini=0 THEN
1120 PRINT "SP1;LT2,1"!See 800
1130 ELSE
1140 PRINT "SP2;LT"!See 820
1150 END IF
1160 FOR M=Sym TO 1 STEP .1 !Here starts preparation for plotting of layer
1170 IF M=Sym THEN
1180 FOR M2=10*R2*Sym TO 10*R2 STEP R2/10
1190 X2=M2*H2*R2/(10*R2)
1200 Y2=H2*Bou
1210 U2=(-(A22+2*A23*Y2+3*A24*Y2^2+4*A25*Y2^3+5*A26*Y2^4)*X2+(-A42+2*A25*Y2+
26*Y2^2)*X2^3)*3.1*10^7*Ini
1220 V2=(A21+A22*Y2+A23*Y2^2+A24*Y2^3+A25*Y2^4+A26*Y2^5+(3*A41+3*A42*Y2-3*A4
2^2-5*A26*Y2^3)*X2^2)*3.1*10^7*Ini
1230 X=M2+10*X2
1240 Y=(10+10*V2)*Bou+10*Rh ! H2 is taken to equal 10 USERS UNITS and the ve
ity is multiplied by a periode of 10 time units
1250 PRINT "PA",X,"",Y,"";PD;"
1260 NEXT M2
1270 PRINT "PU;"
1280 END IF
1290 FOR N2=0 TO 10 STEP .5 !Now follow plotting of initially straight vert
markers in layer 2
1300 X2=R2*H2*M
1310 Y2=N2*H2/10
1320 U2=(-(A22+2*A23*Y2+3*A24*Y2^2+4*A25*Y2^3+5*A26*Y2^4)*X2+(-A42+2*A25*Y2+
26*Y2^2)*X2^3)*3.1*10^7*Ini
1330 V2=(A21+A22*Y2+A23*Y2^2+A24*Y2^3+A25*Y2^4+A26*Y2^5+(3*A41+3*A42*Y2-3*A4
2^2-5*A26*Y2^3)*X2^2)*3.1*10^7*Ini
1340 X=10*R2*M+10*X2
1350 Y=10*Rh+N2+10*V2 !SEE 1240
1360 PRINT "PA",X,"",Y,"";PD;"
1370 NEXT N2
1380 PRINT "PU;"
1390 NEXT M
1400 PRINT "PU;SP0;"!Here plotting ends and printing of velocities etc star
according to the commands below
1410 !!
1420 IF Print=0 THEN 1710
1430 Epsi=Ro2*Gr*H2/(B*Mu2)

```

```

> !When "PRINT SC---,---,---,---"etc. appears on screen press "EDIT, 280" fol
led by "EXECUTE", and line 280 will appear
! If scale values are inserted prior to start then press "CONTINUE" directl
n line 280 appears, else:
! Insert desired scale values. (considering the R2, Sym and Rm commands to be
UT later!) press "ENTER" followed by "RUN"
PRINT "SC-50,50,0,72"! This is an example
!!
! After "RUN" is pressed, "PRINT "SC---,---,---,---" again appears on screen, and
with numbers inserted
!!
! Then press "CONTINUE" which puts "R2,Rm,Ini,Sym,Bou,Lay1,Lay2,Print,etc" on
screen; insert values for R2,Rm, etc. and press "CONTINUE" anew to start plotting
!!
! Together with the input values for R2 and Rm the following "yes/no" or 1/
choices are possible:
! Ini = 0 plots initial profile, Ini=1 plots deformed profile, Sym=-1 plots sym
ic profile, Sym=0 plots right hand half of profile
!!
! Bou=1 plots top boundary first, Bou=0 plots base first; Lay1=1, Lay2=0, plots
er 1 only, Lay2=1, Lay1=0 plots only layer 2, Lay1=1, Lay2=1 plots both layers
!!
! Printing of velocities follows plotting if Print is put = 1 and Velfro and
up are given values, 0 or 1. Print=1 and Velfro=1, Veltop=0 gives the velocity
at the front face of both layers; Print=1, Velfro=0, Veltop=1 gives the veloci
the top boundary of both layers; Print=1 and Velfro=0, Veltop=0 prints the veloci
velocity throughout both layers; Print=0 prevents velocity to be displayed
Printed; If Lay1=Lay2=0, Print=1 and Velfro=0 or 1, Veltop=1 or 0 then
velocity is printed without activating plotting
!!
! For plotting of both upper and lower boundaries press "RUN" and "CONTINUE"
ily after the first plotting or printing ends, then make input for "R2,Rm,
ni etc", but now using the alternative command for Bou, and press CONTINUE
NPUT "R2,Rm,Ini,Sym,Bou,Lay1,Lay2,",R2,Rm,Ini,Sym,Bou,Lay1,Lay2
NPUT "Print,Velfro,Veltop",Print,Velfro,Veltop
COM REAL H1,H2,R,R2,R1,Rh,Gr,Ro1,Ro2,Rro,Mu1,Mu2,Rm,Den,Epota,Epota,Estra,
Estrab
H1=5*10^3!cm, change as needed before start
H2=5*10^5!cm, change as needed ---- "" ----
Rh=H1/H2
R=R2
R1=R2/Rh
r=981!cm/s^2
rho1=2.8!g/cm^3, change as needed before start
rho2=2.8!g/cm^3, change as needed ---- "" ----
mu2=10^22 !Pois, change as needed ---- "" ----
mu1=Mu2*Rm
rho=Ro1/Ro2
ALL Energyfactors
!
CALCULATION OF THE COEFFICIENTS A,B,...,A41,A42 IN THE STREAM FUNCTIONS
AND Psi (2) FOLLOW
=Epota/Epota
ii=(2*Q*Estra-Estrab)/(2*Estrb*H2-Q*Estrab*H2)
i=(Epota+Epota*H2*Phi)/(Estra+Estrb*H2^2*Phi^2+Estrab*H2*Phi)
Phi*A
(A+(3+3/Rh)*H1*B)/(Den*H1^2) ! "Den" is defined line 1760
-(A+(3+3/Rh)*H1*B)/(Den*(5+5/Rh)*H1^3)
1=-(A*H1^2+B*H1^3+C*H1^4+D*H1^5)
2=-(2*A*H1+3*B*H1^2+4*C*H1^3+5*D*H1^4)
3=-Rm*(A+3*B*H1+(9-3/Rm)*C*H1^2+(15-5/Rm)*D*H1^3)
4=-Rm*B+(2*Rm-6)*C*H1+(5*Rm-15)*D*H1^2
5=-Rm*(C+5*D*H1)
6=-Rm*D
=C*H1^2+5/3*D*H1^3
=2*C*H1+5*D*H1^2
ay1=0 THEN 1100
ni=0 THEN
T "LT2,1" !Commands plot with dashed line (for initial profile)
T "LT" !Commands plot with solid line (for deformed profile)
IF

```

```

840 FOR M=Sym TO 1 STEP .1 !Sym is input as 0 or -1.Sym=0 plots right hand
half profile,Sym=-1 plots full symmetric profile
850 IF M=Sym THEN
860 FOR M1=10*R2*Sym TO 10*R2 STEP R2/10 !This draws the top (If Bou=1) or bot
tom (If Bou=0) boundary of layer 1
870 X1=M1*H1/(10*R2)
880 Y1=H1*Bou
890 U1=((2*A*Y1+3*B*Y1^2+4*C*Y1^3+5*D*Y1^4)*X1-(2*C*Y1+5*D*Y1^2)*X1^2)*3.1*10^
7*Ini
900 V1=(-(A*Y1^2+B*Y1^3+C*Y1^4+D*Y1^5)+(3*C*Y1^2+5*D*Y1^3)*X1^2)*3.1*10^7*Ini
910 X=M1+U1*10
920 Y=(10*Rh+V1*10)*Bou !H2 is taken to equal 10 USERS UNITS so that H1= 10*Rh
USERS UNITS; the velocities are multiplied by a 10-units time periode
930 PRINT "PA",X,"",Y,"";PD:SP1;"
940 NEXT M1
950 PRINT "PU;"
960 END IF
970 FOR N1=0 TO 10 STEP .2 !This draws the initially straight vertical markers
in layer 1 Because of the small Rh value the vertical scale must generally be
980 ! greatly exaggerated when plotting structures in layer 1
990 X1=R1*H1*M
1000 Y1=N1*H1/10
1010 U1=((2*A*Y1+3*B*Y1^2+4*C*Y1^3+5*D*Y1^4)*X1-(2*C*Y1+5*D*Y1^2)*X1^2)*3.1*10^
7*Ini
1020 V1=(-(A*Y1^2+B*Y1^3+C*Y1^4+D*Y1^5)+(3*C*Y1^2+5*D*Y1^3)*X1^2)*3.1*10^7*Ini
1030 X=10*R*M+U1*10
1040 Y=N1*Rh+V1*10 !See 920
1050 PRINT "PA",X,"",Y,"";PD:SP1;"
1060 NEXT N1
1070 PRINT "PU;"
1080 NEXT M
1090 PRINT "PU;"
1100 IF Lay2=0 THEN 1420
1110 IF Ini=0 THEN
1120 PRINT "SP1;LT2,1"!See 800
1130 ELSE
1140 PRINT "SP2;LT"!See 820
1150 END IF
1160 FOR M=Sym TO 1 STEP .1 !Here starts preparation for plotting of layer 2
1170 IF M=Sym THEN
1180 FOR M2=10*R2*Sym TO 10*R2 STEP R2/10
1190 X2=M2*H2/R2/(10*R2)
1200 Y2=H2*Bou
1210 U2=(-(A22+2*A23*Y2+3*A24*Y2^2+4*A25*Y2^3+5*A26*Y2^4)*X2+(-A42+2*A25*Y2+5*A
26*Y2^2)*X2^3)*3.1*10^7*Ini
1220 V2=(A21+A22*Y2+A23*Y2^2+A24*Y2^3+A25*Y2^4+A26*Y2^5+(3*A41+3*A42*Y2-3*A25*Y
2^2-5*A26*Y2^3)*X2^2)*3.1*10^7*Ini
1230 X=M2+10*U2
1240 Y=(10+10*X*V2)*Bou+10*Rh ! H2 is taken to equal 10 USERS UNITS and the veloc
ity is multiplied by a periode of 10 time units
1250 PRINT "PA",X,"",Y,"";PD;"
1260 NEXT M2
1270 PRINT "PU;"
1280 END IF
1290 FOR N2=0 TO 10 STEP .5 !Now follow plotting of initially straight vertical
markers in layer 2
1300 X2=R2*H2*M
1310 Y2=N2*H2/10
1320 U2=(-(A22+2*A23*Y2+3*A24*Y2^2+4*A25*Y2^3+5*A26*Y2^4)*X2+(-A42+2*A25*Y2+5*A
26*Y2^2)*X2^3)*3.1*10^7*Ini
1330 V2=(A21+A22*Y2+A23*Y2^2+A24*Y2^3+A25*Y2^4+A26*Y2^5+(3*A41+3*A42*Y2-3*A25*Y
2^2-5*A26*Y2^3)*X2^2)*3.1*10^7*Ini
1340 X=10*R2*M+10*U2
1350 Y=10*Rh+N2+10*V2 !SEE 1240
1360 PRINT "PA",X,"",Y,"";PD;"
1370 NEXT N2
1380 PRINT "PU;"
1390 NEXT M
1400 PRINT "PU;SP0;"!Here plotting ends and printing of velocities etc starts
according to the commands below
1410 !!
1420 IF Print=0 THEN 1710
1430 Epsi=Ro2*Gr*H2/(8*Mu2)

```

```

1440 Ufree=Epsi*H2*R2*3.1*10^7
1450 Vfree=-Epsi*H2*3.1*10^7
1460 IF Velfro=1 THEN 1490
1470 FOR Mi=1 TO 0 STEP -.1
1480 IF Veltop=1 THEN 1510
1490 FOR Ni=1 TO 0 STEP -.1
1500 IF Velfro=1 THEN Mi=1
1510 X1=Mi*R1*H1
1520 X2=Mi*R2*H2
1530 IF Veltop=1 THEN Ni=1
1540 Y1=Ni*H1
1550 Y2=Ni*H2
1560 U1=((2*A*Y1+3*B*Y1^2+4*C*Y1^3+5*D*Y1^4)*X1-(2*C*Y1+5*D*Y1^2)*X1^3)*3.1*10^7
1570 V1=(-(A*Y1^2+B*Y1^3+C*Y1^4+D*Y1^5)+(3*C*Y1^2+5*D*Y1^3)*X1^2)*3.1*10^7
1580 U2=(-(A22+2*A23*Y2+3*A24*Y2^2+4*A25*Y2^3+5*A26*Y2^4)*X2+(-A42+2*A25*Y2+5*A26*Y2^2)*X2^3)*3.1*10^7
1590 V2=(A21+A22*Y2+A23*Y2^2+A24*Y2^3+A25*Y2^4+A26*Y2^5+(3*A41+3*A42*Y2-3*A25*Y2^2-5*A26*Y2^3)*X2^2)*3.1*10^7
1600 PRINTER IS 1
1610 IF Mi=Ni THEN PRINT "COMB86NAPW: H2=";H2;"H1=";H1;"R2=";R2;"R1=";R1;"Mu2=";Mu2;"Mu1=";Mu1;"Ro1=";Ro1;"Ro2=";Ro2;"Ufree=";Ufree;"Vfree=";Vfree
1620 IF Mi=1 THEN
1630 IF Ni=1 THEN PRINT USING "5X, 12A, 14A, 14A, 8A, 2A, XX, 2A";"U1";"U2";"V1";"V2";"Mi";"Ni"
1640 END IF
1650 PRINT TAB(54);Mi;Ni
1660 PRINT USING "DD.10D";U1,U2,V1,V2
1670 NEXT Ni
1680 NEXT Mi
1690 PRINT " "
1700 PRINT " "
1710 END
1720 ! ++++++
1730 SUB Energyfactors
1740 !Den IS TERM IN FOLLOWING EXPRESSIONS ,SEE ALSO C AND D, LINES 680,690
1750 COM REAL H1,H2,R,R2,R1,Rh,Gr,Ro1,Ro2,Rro,Mu1,Mu2,Rm,Den,Epota,Epotb,Estra,Estrb,Estrab
1760 Den=6/Rh-9/Rh^2-24/(Rh*Rm)+(3+3/Rh^3-3/Rh+9/Rh^2+12/(Rh*Rm))/(1+1/Rh)
1770 Ca=1/Den
1780 Cb=(3+3/Rh)/Den
1790 Da=-Ca/(5*(1+1/Rh))
1800 Db=-Cb/(5*(1+1/Rh))
1810 A21a=-Rh^2*(1+Ca+Da)
1820 A21b=-Rh^3*(1+Cb+Db)
1830 A22a=-Rh*(2+4*Ca+5*Da)
1840 A22b=-Rh^2*(3+4*Cb+5*Db)
1850 A23a=-Rm+(3-9*Rm)*Ca+(5-15*Rm)*Da
1860 A23b=-3*Rm*Rh+(3-9*Rm)*Cb*Rh+(5-15*Rm)*Db*Rh
1870 A24a=(2*Rm-6)*Ca/Rh+(5*Rm-15)*Da/Rh
1880 A24b=-Rm+(2*Rm-6)*Cb+(5*Rm-15)*Db
1890 A25a=-Rm*(Ca+5*Da)/Rh^2
1900 A25b=-Rm*(Cb+5*Db)/Rh
1910 A26a=-Rm*Da/Rh^3
1920 A26b=-Rm*Db/Rh^2
1930 A41a=Ca+5/3*Da
1940 A41b=(Cb+5/3*Db)*Rh
1950 A42a=(2*Ca+5*Da)/Rh
1960 A42b=2*Cb+5*Db
1970 C1=64/7*R1+132/15*R1^3+72/15*R1^5+4/7*R1^7
1980 D1=100/9*R1+100/7*R1^3+12*R1^5+100/21*R1^7
1990 Ac=(64/5*R1-24/9*R1^3-8/5*R1^5)
2000 Ad=(40/3*R1-10*R1^3-4*R1^5)
2010 Bc=(16*R1+6*R1^3-12/5*R1^5)
2020 Bd=(120/7*R1-8*R1^3)
2030 Cd=20*R1+20*R1^3+12*R1^5+20*R1^7
2040 !Estrab,Estrb1 AND Estrab2 BELOW ARE FACTORS TO MULTIPLY WITH A^2*H2^4,B^2*H2^6 AND A*B*H2^5 IN STRAIN ENERGY EXPRESSION FOR LAYER 1
2050 !Epota1,Epotb1 ARE FACTORS TO MULTIPLY WITH AXH2^4 AND BXH2^5 IN POTENTIAL ENERGY EXPRESSION FOR LAYER 1
2060 Estra1=(16/3*R1+4/3*R1^3+C1*Ca^2+D1*Da^2+Ac*Ca+Ad*Da+Cd*Ca*Da)*Rh^4
2070 Estrb1=(36/5*R1+4*R1^3+C1*Cb^2+D1*Db^2+Bc*Cb+Bd*Db+Cd*Cb*Db)*Rh^6
2080 Estrab1=(12*R1+4*R1^3+2*C1*Ca*Cb+2*D1*Da*Db+Ac*Cb+Ad*Db+Bc*Ca+Bd*Da+Cd*Ca*Db+Cd*Cb*Da)*Rh^5

```

```

2090 Epota1=(-(1/3+1/5*Ca+1/6*Da)*R1+(1/3*Ca+5/12*Da)*R1^3)*Rh^4
2100 Epotb1=(-(1/4+1/5*Cb+1/6*Db)*R1+(1/3*Cb+5/12*Db)*R1^3)*Rh^5
2110 !HERE FOLLOW CALCULATIONS OF THE COEFFICIENTS IN THE ENERGY EXPRESSION FOR LAYER 2
2120 Q1=16/3*R+4/3*R^3
2130 Q2=36/5*R+4*R^3
2140 Q3=64/7*R+44/5*R^3+24/5*R^5+4/7*R^7
2150 Q4=100/9*R+100/7*R^3+12*R^5+100/21*R^7
2160 Q5=4*R^3+36/5*R^5
2170 Q6=8*(R-R^3)
2180 Q7=8*(R-5/3*R^3)
2190 Q8=12*R+4*R^3
2200 Q9=64/5*R-8/3*R^3-8/5*R^5
2210 Q10=40/3*R-10*R^3-4*R^5
2220 Q11=16*R+6*R^3-12/5*R^5
2230 Q12=120/7*R-8*R^3
2240 Q13=20*(R+R^3+3/5*R^5+1/7*R^7)
2250 Q14=-10*R^3-12*R^5
2260 Q15=-24*R^3+24/5*R^5
2270 Q16=-16*(R^3+R^5)
2280 Q17=-30*R^3+12*R^5
2290 !Estra2,Estrb2= AND Estrab2 ARE FACTORS TO MULTIPLY WITH A^2*H2^4, AND A*B*H2^5 IN THE STRAIN ENERGY EXPRESSION FOR LAYER 2.
2300 !!!
2310 Estra12=4*R*A22a^2+Q1*A23a^2+Q2*A24a^2+Q3*A25a^2+Q4*A26a^2+12*R^3*5*A42a^2+A22a*8*(A23a*R+A24a*R+Q6/8*A25a+Q7/8*A26a+A42a)*R^3
2320 Estra22=A23a*(Q8*A24a+Q9*A25a+Q10*A26a-8*R^3*A41a+4*R^3*A42a)+A24a+Q12*A26a-12*R^3*A41a)+A25a*(Q13*A26a+Q14*A42a+Q15*A41a)+12*R^3*A41a)
2330 Estra2=Estra12+Estra22+A26a*(Q16*A42a+Q17*A41a)
2340 !!!
2350 Estrb12=4*R*A22b^2+Q1*A23b^2+Q2*A24b^2+Q3*A25b^2+Q4*A26b^2+12*R^3*5*A42b^2+A22b*8*(A23b*R+A24b*R+Q6/8*A25b+Q7/8*A26b+A42b)*R^3
2360 Estrb22=A23b*(Q8*A24b+Q9*A25b+Q10*A26b-8*R^3*A41b+4*R^3*A42b)+A24b+Q12*A26b-12*R^3*A41b)+A25b*(Q13*A26b+Q14*A42b+Q15*A41b)+12*R^3*A41b)
2370 Estrb2=Estrb12+Estrb22+A26b*(Q16*A42b+Q17*A41b)
2380 !!!
2390 Estrab12=8*R*A22a*A22b+2*Q1*A23a*A23b+2*Q2*A24a*A24b+2*Q3*A25a*A25b+2*Q4*A26a*A26b+24*R^3*A41a*A41b+2*Q5*A42a*A42b+A22a*(8*A23b*R+8*A24b*R+Q6*A25a+Q7*A26a+A42a)*R^3+2*A22b*(8*A23a*R+A24a*R+Q6/8*A25b+Q7/8*A26b+A42b)*R^3
2400 Estrab22=A22a*(Q7*A26b+8*R^3*A42b)+A22b*(8*A23a*R+A24a*R+Q6/8*A25b+Q7/8*A26b+A42b)+2*A23a*(Q8*A24b+Q9*A25b+Q10*A26b-8*R^3*A41b+4*R^3*A42b)+2*A24a*(Q8*A24a+Q9*A25a+Q10*A26a-8*R^3*A41a+4*R^3*A42a)+A25a*(Q11*A25a+Q12*A26a-12*R^3*A41a)+A26a*(Q11*A25a+Q12*A26a-12*R^3*A41a)+A24b*(Q13*A26b+Q14*A42b+Q15*A41b)+A25b*(Q13*A26a+Q14*A42a)+A26a*(Q16*A42b+Q17*A41b)+A26b*(Q16*A42a+Q17*A41a)+12*R^3*A41b*A42a
2430 Estrab2=Estrab12+Estrab22+Estrab32+Estrab42+12*R^3*A41b*A42a
2440 !!!
2450 Estra=Mu1*Estra1+Mu2*Estra2
2460 Estrb=Mu1*Estrb1+Mu2*Estrb2
2470 Estrab=Mu1*Estrab1+Mu2*Estrab2
2480 !!!
2490 !BELOW FOLLOW CALCULATION OF THE FACTORS TO MULTIPLY WITH A*H2^4 AND B*H2^5 IN THE EXPRESSION FOR POTENTIAL ENERGY IN LAYER 2
2500 Epota2=(A21a+.5*A22a+1/3*A23a+1/4*A24a+1/5*A25a+1/6*A26a)*R+(A41a-1/3*A25a-5/12*A26a)*R^3
2510 Epotb2=(A21b+.5*A22b+1/3*A23b+1/4*A24b+1/5*A25b+1/6*A26b)*R+(A41b-1/3*A25b-5/12*A26b)*R^3
2520 !!!
2530 Epota=Ro2*Gr*(Epota1*Rro+Epota2)
2540 Epotb=Ro2*Gr*(Epotb1*Rro+Epotb2)
2550 SUBEND

```

## ACKNOWLEDGEMENT

Economic support from the Swedish Natural Science Research (NFR) and the Swedish Council for Technology and Development (SFB) purchase of an expensive personal computer is sincerely acknowledged. I extend my thanks to Dr H. Schmeling and Dr D. Hayashi for discus-

```

0 Ufree=Epsi*H2*R2*3.1*10^7
0 Vfree=-Epsi*H2*3.1*10^7
0 IF Velfro=1 THEN 1490
0 FOR Mi=1 TO 0 STEP -.1
0 IF Veltop=1 THEN 1510
0 FOR Ni=1 TO 0 STEP -.1
0 IF Velfro=1 THEN Mi=1
0 X1=Mi*R1*H1
0 X2=Mi*R2*H2
0 IF Veltop=1 THEN Ni=1
0 Y1=Ni*H1
0 Y2=Ni*H2
0 U1=((2*A*Y1+3*B*Y1^2+4*C*Y1^3+5*D*Y1^4)*X1-(2*C*Y1+5*D*Y1^2)*X1^3)*3.1*10^7
0 V1=(-(A*Y1^2+B*Y1^3+C*Y1^4+D*Y1^5)+(3*C*Y1^2+5*D*Y1^3)*X1^2)*3.1*10^7
0 U2=(-(A22+2*A23*Y2+3*A24*Y2^2+4*A25*Y2^3+5*A26*Y2^4)*X2+(-A42+2*A25*Y2+5*A26*Y2^3)*X2^2)*3.1*10^7
0 V2=(A21+A22*Y2+A23*Y2^2+A24*Y2^3+A25*Y2^4+A26*Y2^5+(3*A41+3*A42*Y2-3*A25*Y2^2+3*A26*Y2^3)*X2^2)*3.1*10^7
0 PRINTER IS 1
0 IF Mi=1 THEN PRINT "COMBENAPW: H2="; H2; "H1="; H1; "R2="; R2; "Mu2="; Mu2; "Mu1"; "Ro1="; Ro1; "Ro2="; Ro2; "Ufree="; Ufree; "Vfree="; Vfree
0 IF Ni=1 THEN PRINT USING "5X, 12A, 14A, 14A) 8A, 2A, XX, 2A"; "U1", "U2", "V1", "V2", "Ni"
0 END IF
0 PRINT TAB(54); Mi; Ni
0 PRINT USING "DD.10D"; U1, U2, V1, V2
0 NEXT Ni
0 NEXT Mi
0 PRINT " "
0 PRINT " "
0 END
0 ! ++++++
SUB Energyfactors
! Den IS TERM IN FOLLOWING EXPRESSIONS ,SEE ALSO C AND D, LINES 680,690
DOM REAL H1, H2, R, R2, R1, Rh, Gr, Ro1, Ro2, Rro, Mu1, Mu2, Rm, Den, Epota, Epotb, Estrab, Estrab2
Den=6/Rh-9/Rh^2-24/(Rh*Rm)+(3+3/Rh^3-3/Rh+9/Rh^2+12/(Rh*Rm))/(1+1/Rh)
Cb=(3+3/Rh)/Den
Ia=-Ca/(5*(1+1/Rh))
Ib=-Cb/(5*(1+1/Rh))
21a=-Rh^2*(1+Ca+Da)
21b=-Rh^3*(1+Cb+Db)
22a=-Rh*(2+4*Ca+5*Da)
22b=-Rh^2*(3+4*Cb+5*Db)
23a=-Rm+(3-9*Rm)*Ca+(5-15*Rm)*Da
23b=-3*Rm*Rh+(3-9*Rm)*Cb*Rh+(5-15*Rm)*Db*Rh
24a=(2*Rm-6)*Ca/Rh+(5*Rm-15)*Da/Rh
24b=-Rm+(2*Rm-6)*Cb+(5*Rm-15)*Db
25a=-Rm*(Ca+5*Da)/Rh^2
25b=-Rm*(Cb+5*Db)/Rh
26a=-Rm*Da/Rh^3
26b=-Rm*Db/Rh^2
1a=Ca+5/3*Da
1b=(Cb+5/3*Db)*Rh
2a=(2*Ca+5*Da)/Rh
2b=2*Cb+5*Db
=64/7*R1+132/15*R1^3+72/15*R1^5+4/7*R1^7
=100/9*R1+100/7*R1^3+12*R1^5+100/21*R1^7
=(64/5*R1-24/9*R1^3-8/5*R1^5)
=(40/3*R1-10*R1^3-4*R1^5)
=(16*R1+6*R1^3-12/5*R1^5)
=(120/7*R1-8*R1^5)
20*R1+20*R1^3+12*R1^5+20*R1^7
tra1, Estrab1 AND Estrab2 BELOW ARE FACTORS TO MULTIPLY WITH A^2*H2^4, B^4
D A*B*H2^5 IN STRAIN ENERGY EXPRESSION FOR LAYER 1
0 tra1, Epotb1 ARE FACTORS TO MULTIPLY WITH A*H2^4 AND B*H2^5 IN POTENTIAL EXPRESSION FOR LAYER 1
0 a1=(16/3*R1+4/3*R1^3+C1*Ca^2+D1*Da^2+Ac*Ca+Ad*Da+Cd*Ca*Da)*Rh^4
0 b1=(36/5*R1+4*R1^3+C1*Cb^2+D1*Db^2+Bc*Cb+Bd*Db+Cd*Cb*Db)*Rh^6
0 ab1=(12*R1+4*R1^3+2*C1*Ca*Cb+2*D1*Da*Db+Ac*Cb+Ad*Db+Bc*Ca+Bd*Da+Cd*Ca*
0 Ia)*Rh^5

```

```

2090 Epota1=(-(1/3+1/5*Ca+1/6*Da)*R1+(1/3*Ca+5/12*Da)*R1^3)*Rh^4
2100 Epotb1=(-(1/4+1/5*Cb+1/6*Db)*R1+(1/3*Cb+5/12*Db)*R1^3)*Rh^5
2110 !HERE FOLLOW CALCULATIONS OF THE COEFFICIENTS IN THE ENERGY EXPRESSION FOR LAYER 2
2120 Q1=16/3*R+4/3*R^3
2130 Q2=36/5*R+4*R^3
2140 Q3=64/7*R+44/5*R^3+24/5*R^5+4/7*R^7
2150 Q4=100/9*R+100/7*R^3+12*R^5+100/21*R^7
2160 Q5=4*R^3+36/5*R^5
2170 Q6=8*(R-R^3)
2180 Q7=8*(R-5/3*R^3)
2190 Q8=12*R+4*R^3
2200 Q9=64/5*R-8/3*R^3-8/5*R^5
2210 Q10=40/3*R-10*R^3-4*R^5
2220 Q11=16*R+6*R^3-12/5*R^5
2230 Q12=120/7*R-8*R^5
2240 Q13=20*(R+R^3+3/5*R^5+1/7*R^7)
2250 Q14=-10*R^3-12*R^5
2260 Q15=-24*R^3+24/5*R^5
2270 Q16=-16*(R^3+R^5)
2280 Q17=-30*R^3+12*R^5
2290 !Estrab1, Estrab2= AND Estrab2 ARE FACTORS TO MULTIPLY WITH A^2*H2^4, B^2*H2^6 AND A*B*H2^5 IN THE STRAIN ENERGY EXPRESSION FOR LAYER 2
2300 !!!
2310 Estrab12=4*R*A22a^2+Q1*A23a^2+Q2*A24a^2+Q3*A25a^2+Q4*A26a^2+12*R^3*A41a^2+Q5*A42a^2+A22a*B*(A23a*R+A24a*R+Q6/8*A25a+Q7/8*A26a+A42a)*R^3
2320 Estrab22=A23a*(Q8*A24a+Q9*A25a+Q10*A26a-8*R^3*A41a+4*R^3*A42a)+A24a*(Q11*A25a+Q12*A26a-12*R^3*A41a)+A25a*(Q13*A26a+Q14*A42a+Q15*A41a)+12*R^3*A41a*A42a
2330 Estrab2=Estrab12+Estrab22+A26a*(Q16*A42a+Q17*A41a)
2340 !!!
2350 Estrb12=4*R*A22b^2+Q1*A23b^2+Q2*A24b^2+Q3*A25b^2+Q4*A26b^2+12*R^3*A41b^2+Q5*A42b^2+A22b*B*(A23b*R+A24b*R+Q6/8*A25b+Q7/8*A26b+A42b)*R^3
2360 Estrb22=A23b*(Q8*A24b+Q9*A25b+Q10*A26b-8*R^3*A41b+4*R^3*A42b)+A24b*(Q11*A25b+Q12*A26b-12*R^3*A41b)+A25b*(Q13*A26b+Q14*A42b+Q15*A41b)+12*R^3*A41b*A42b
2370 Estrb2=Estrb12+Estrb22+A26b*(Q16*A42b+Q17*A41b)
2380 !!!
2390 Estrab12=8*R*A22a*A22b+2*Q1*A23a*A23b+2*Q2*A24a*A24b+2*Q3*A25a*A25b+2*Q4*A26a*A26b+24*R^3*A41a*A41b+2*Q5*A42a*A42b+A22a*(B*A23b*R+8*A24b*R+Q6*A25b)
2400 Estrab22=A22a*(Q7*A26b+8*R^3*A42b)+A22b*B*(A23a*R+A24a*R+Q6/8*A25a+Q7/8*A26a+R^3*A42a)+A23a*(Q8*A24b+Q9*A25b+Q10*A26b-8*R^3*A41b+4*R^3*A42b)
2410 Estrab32=A23b*(Q8*A24a+Q9*A25a+Q10*A26a-8*R^3*A41a+4*R^3*A42a)+A24a*(Q11*A25b+Q12*A26b-12*R^3*A41b)+A24b*(Q11*A25a+Q12*A26a-12*R^3*A41a)
2420 Estrab42=A25a*(Q13*A26b+Q14*A42b+Q15*A41b)+A25b*(Q13*A26a+Q14*A42a+Q15*A41a)+A26a*(Q16*A42b+Q17*A41b)+A26b*(Q16*A42a+Q17*A41a)+12*R^3*A41a*A42b
2430 Estrab2=Estrab12+Estrab22+Estrab32+Estrab42+12*R^3*A41b*A42a
2440 !!!
2450 Estrab=Mu1*Estrab1+Mu2*Estrab2
2460 Estrb=Mu1*Estrb1+Mu2*Estrb2
2470 Estrab=Mu1*Estrab1+Mu2*Estrab2
2480 !!!
2490 !BELOW FOLLOW CALCULATION OF THE FACTORS TO MULTIPLY WITH A*H2^4 AND B*H2^5 IN THE EXPRESSION FOR POTENTIAL ENERGY IN LAYER 2
2500 Epota2=(A21a+.5*A22a+1/3*A23a+1/4*A24a+1/5*A25a+1/6*A26a)*R+(A41a+1/2*A42a-1/3*A25a-5/12*A26a)*R^3
2510 Epotb2=(A21b+.5*A22b+1/3*A23b+1/4*A24b+1/5*A25b+1/6*A26b)*R+(A41b+1/2*A42b-1/3*A25b-5/12*A26b)*R^3
2520 !!!
2530 Epota=Ro2*Gr*(Epota1*Rro+Epota2)
2540 Epotb=Ro2*Gr*(Epotb1*Rro+Epotb2)
2550 SUBEND

```

ACKNOWLEDGEMENT

Economic support from the Swedish Natural Science Research Foundation (NFR) and the Swedish Council for Technology and Development (STU) for the purchase of an expensive personal computer is sincerely acknowledged. I wish to extend my thanks to Dr H. Schmeling and Dr D. Hayashi for discussions which



have been useful for writing this paper. Miss K. Gløersen deserves my best thanks for typing the manuscript.

## REFERENCES

- Artyushkov, E.V., 1971. Rheological properties of the crust and upper mantle, *J. Geophys. Res.*, 76: 1376-1390.
- Biot, M.A., 1959. The influence of gravity on the folding of a layered viscoelastic medium under compression. *J. Franklin Inst.*, 267(3): 211.
- Biot, M.A., 1961. Theory of folding of stratified viscoelastic media and its implications on tectonics and orogenesis. *Geol. Soc. Am. Bull.*, 72: 1595.
- Biot, M.A., 1963. Stability of multilayered continua under the influence of gravity and viscoelasticity. *J. Franklin Inst.*, 276: 231.
- Biot, M.A. and Ode, H., 1965. Theory of gravity instability with variable overburden and compaction. *Geophysics*, 30: 213.
- Cathles, L.M., 1975. *The Viscosity of the Earth's Mantle*. Princeton University Press, Princeton, N.J., 386 pp.
- Courant, R., 1953. *Differential and Integral Calculus, I and II*. Interscience, New York, N.Y., 1298 pp.
- Crittenden, M.O. Jr., 1963. Effective viscosity of the earth derived from isostatic loading of Pleistocene Lake Bonneville. *J. Geophys. Res.*, 68: 5517.
- Elliott, D., 1976. The motion of thrust sheets. *J. Geophys.*, 81: 949.
- Fletcher, R.C., 1977. Folding of a single viscous layer. *Tectonophysics*, 39: 593-606.
- Gyramati, F., 1970. *Non-Equilibrium Thermodynamics*. Springer, Berlin, 184 pp.
- Haskel, N.A., 1935. The motion of a viscous fluid under a surface load. *Physics*, 6: 265.
- Jaeger, J.C., 1956. *Elasticity, Fracture and Flow*. Methuen, London, 152 pp.
- Johnson, A.M., 1970. *Physical Processes in Geology*. Freeman, Cooper, San Fransisco, Calif.
- Lagrange, J.H., 1781. *Nouv. Mém. de L'Acad. de Berlin (Oeuvres, iv, 720)*.
- Lamb, H., 1932. *Hydrodynamics*. Dover, New York, (Orig. 1879), 738 pp.
- Lambe, C.G. and Tranter, C.J., 1967. *Differential Equations for Engineers and Scientists*. The English University Press, London, 3rd impression, 369 pp.
- Murata, H. and Hasimoto, B., 1984. On the application of the finite element method, etc. *Bull. Sci. Eng. Res.*, Wasada Univ.
- Mörner, N-A., 1980. *Earth Rheology, Isostasy and Eustasy*. Wiley, New York, 597 pp.
- Price, R.A., 1973. Large scale gravitational flow of supracrustal rocks. In: K.A. de Jong and R. Scholten (Editors), *Gravity and Tectonics*, Wiley, New York.
- Protter, M.H. and Morrey, C.B., 1964. *Modern Mathematical Analysis*. Addison-Wesley, Reading.
- Ramberg, H., 1968. Instability of layered systems in the field of gravity, I and II. *Phys. Earth. Planet. Inter.*, 1: 427.
- Ramberg, H., 1981. *Gravity, Deformation and the Earth's Crust*. Academic Press, London, 452 pp.
- Ramberg, H., 1985. The velocity of nappe movement: a correction. *Tectonophysics*, 111: 137-138.
- Rankin, W.J.M., 1864. On plane waterlines in two dimensions. *Philos. Trans.*, Ser. A.
- Sampson, N.M., 1891. On Stokes current function. *Philos. Trans.*, Ser. A.
- Smith, R.B., 1975. Unified theory of the onset of folding, boudinage, and mullion structures. *Geol. Soc. Am. Bull.*, 86: 1601.
- Stokes, G.G., 1842. On the steady motion of incompressible fluids. *Cambridge Trans.* vii, pap., i, 1.
- Van Nostrand's Scientific Encyclopedia, 1958, 1839 pp.
- Yefimov, N.V., 1968. *Quadratic Forms and Matrices*. Academic Press, London, New York, 164 pp.

## CRACK-SEAL MECHANISM IN A LIMESTONE: A FACTOR OF DEFORMATION IN STRIKE-SLIP FAULTING

P. GAVIGLIO

*Laboratoire de Géologie Appliquée, case 28, Université de Provence, Marseille (France)*

(Received July 10, 1985; revised version accepted April 16, 1986)

### ABSTRACT

Gaviglio, P., 1986. Crack-seal mechanism in a limestone: a factor of deformation in strike-slip. *Tectonophysics*, 131: 247-255.

A repeated crack-seal mechanism may play a major part in the deformation process in a slip fault. This paper develops a microscopic approach to the association of shear planes and tension cracks between two en échelon faults. The simultaneous development of these fractures yields a vein pattern.

The structure, discovered in a Cretaceous limestone of the Arc basin (Bouches du Rhône, France), is located between two left-stepping sinistral strike-slip faults. The horizontal displacement does not exceed a few centimeters: therefore the structure may be representative of the early stage of deformation in a brittle shear zone. Each strain increment includes both shearing and tensile fracturing. Inhomogeneous conditions of friction seem to be prevailing.

### INTRODUCTION

Faults are discontinuous fractures at all length scales (Tchalenko, 1970; Segall et al., 1976; Segall and Pollard, 1980). The existence of tension cracks is fundamental to the early stages of fault development (Beach, 1975), as well as through the deformation of the shear zone (Tchalenko and Ambraseys, 1970; Raynolds and Delair, 1978; Segall and Pollard, 1980; Gamond, 1983).

The crack-seal mechanism is a significant process of natural rock deformation (Ramsay, 1980): a tension crack forms under accumulation of elastic strain and is filled by crystallized minerals through fluid transfer; repetition of cracking and sealing forms compound veins of fibrous crystals and, possibly, inclusion bands parallel to the rock wall. Compound veins form according to various processes of fibre growth (Cox and Fyfe, 1983). Most of the described tension veins displaying evidence of this incremental strain seem to have resulted from simple shortening and stretching.